Computational Studies of the Structures, Reactions, and Energetics of Selected Cyclic and Sterically Crowded Species

CHENG Mei-Fun

A Thesis Submitted in Partial Fulfilment

of the Requirements for the Degree of

Master of Philosophy

in

Chemistry

©The Chinese University of Hong Kong

May 2003

Computational Studies of the Structures, Reactions, and Energetics of Selected Cyclic and Sterically Crowded Species

Abstract

The Gaussian-3 models of theory and other ab initio and density functional theory methods have been applied in the following investigations: (i) heats of formation for the azine series; (ii) heats of formation for some boron hydrides; (iii) the structures and thermochemistry of mono-, di-, tri- and tetra-*tert*-butylmethane; (iv) the Diels-Alder reactivity and aromaticity of acenes and (v) the charge-delocalized and -localized forms of the croconate ($C_5O_5^{2-}$) and rhodizonate ($C_6O_6^{2-}$) dianions.

Our calculated structural and energetics results generally are in good to excellent agreements with the available experimental data. Such a good agreement lends confidence and reliability to those results with no available experimental data. In addition, our mechanistic results shed light on the reaction pathways involved in the studied Diels-Alder reactions.

Most of the contents in this thesis have been written up and submitted for publication: (i) Cheng, M.-F.; Ho, H.-O.; Lam, C.-S.; Li, W.-K., Heats of formation for the azine series: a Gaussian-3 study, *J. Serb. Chem. Soc.* **2002**, *67*, 257; (ii) Cheng, M.-F.; Ho, H.-O.; Lam, C.-S.; Li, W.-K., Heats of formation for the boron hydrides: a Gaussian-3 study, *Chem. Phys. Lett.* **2002**, *356*, 109; (iii) Cheng, M.-F.; Li, W.-K., Structural and energetics studies of tri- and tetra-*tert*-butylmethane, *J. Phys. Chem. A* (accepted); (iv) Cheng, M.-F.; Li, W.-K., A computational study of the Diels-Alder reactions involving acenes: reactivity and aromaticity, *Chem. Phys. Lett.* **2003**, *368*, 630; (v) Lam, C.-K.; Cheng, M.-F.; Li, C.-L.; Li, W.-K.; Mak, T.C.W., Stabilization of D_{5h} and C_{2v} valence tautomeric forms of the croconate dianion (to be submitted); (vi) Cheng, M.-F.; Li, C.-L.; Li, W.-K., A computational study of the charge-delocalized and charge-localized forms of the croconate and rhodizonate dianions, *Chem. Phys. Lett.* (to be submitted).

Submitted by CHENG Mei-Fun

for the degree of Master of Philosophy in Chemistry

at The Chinese University of Hong Kong in (May 2003)

環狀體系化合物及空間密度聚積化合物的結構、反應性及熱力學性質的理論計算研究

論文摘要

本論文採用 Gaussian–3 (G3) 和其他從頭計算法及密度泛函理論計算法對以下的課題進行研究：(i) 連氮系列的組合熱；(ii) 一系列硼氫化合物的結構和組合熱；(iii) 四甲基甲烷，二叔丁基甲烷，三叔丁基甲烷和四叔丁基甲烷的結構及熱化學；(iv) 莘體系化合物的狄爾斯—阿德耳反應性及其芳香性和 (v) 離域化與非離域化之 $C_5O_5^{2-}$ 及 $C_6O_6^{2-}$ 離子的辨認。

與文獻列出的實驗值相比較下，我們的計算結果令人滿意。本論文的研究表明：對於某些缺乏實驗數據的反應和體系，我們可通過類似的理論取得可靠的數值結果。此外，本論文的結果對狄爾斯—阿德耳反應途徑的設計具有指導作用。

論文中部份的內容已寫成文章並已發表：(i) Cheng, M.-F.; Ho, H.-O.; Lam, C.-S.; Li, W.-K., Heats of formation for the azine series: a Gaussian-3 study, *J. Serb. Chem. Soc.* **2002**, *67*, 257; (ii) Cheng, M.-F.; Ho, H.-O.; Lam, C.-S.; Li, W.-K., Heats of formation for the boron hydrides: a Gaussian-3 study, *Chem. Phys. Lett.* **2002**, *356*, 109; (iii) Cheng, M.-F.; Li, W.-K., Structural and energetics studies of tri- and tetra-*tert*-butylmethane, *J. Phys. Chem. A* (accepted); (iv) Cheng, M.-F.; Li, W.-K., A computational study of the Diels-Alder reactions involving acenes: reactivity and aromaticity, *Chem. Phys. Lett.* **2003**, *368*, 630; (v) Lam, C.-K.; Cheng, M.-F.; Li, C.-L.; Li, W.-K.; Mak, T.C.W., Stabilization of D_{5h} and C_{2v} valence tautomeric forms of the croconate dianion (to be submitted); (vi) Cheng, M.-F.; Li, C.-L.; Li, W.-K., A computational study of the charge-delocalized and charge-localized forms of the croconate and rhodizonate dianions, *Chem. Phys. Lett.* (to be submitted).

Acknowledgments

I am very much indebted to my supervisor, Professor Wai-Kee Li, whose guidance and encouragement have made this thesis possible.

I also wish to thank: Dr. Yu-San Cheung, Mr. Kai-Chung Lau, Mr. Siu-Hung Chien, Mr. Justin, Kai-Chi Lau, Mr. Siu-Pang Chan, Mr. Chi-Kin Law and Mr. Chi-Lun Li for their invaluable advice and support on this work.

My thanks also go to Mr. Frank Ng and the High Performance Computing Support Team of Information Technology Services Center of The Chinese University of Hong Kong for their computing support.

Furthermore, I would like to thank Mr. Ho-Lam Lee and all my colleagues in Rooms 225A and 333, Science Center (North Block).

Finally, I would like to express my thankfulness to God and my family. They have provided me with indispensable support and wisdom during these two years.

Table of Contents

List of Tables

Chapter 5

Chapter 6

List of Figures

Chapter 1

Introduction

Accurate and reliable predictions of the structures and energetics for molecular systems are the main objectives in quantum chemistry. At present, for systems with 10 to 15 heavy atoms and a slightly larger number of hydrogens, quantum mechanical methods for the calculation of thermochemical data have developed beyond the reproduction of experimental results; these methods are now able to make reliable predictions where experimental data appear to be uncertain or do not exist at all. In order to achieve the goal of accurate calculation of molecular energies, several theoretical procedure have been introduced.[1-15] In the past decade or so, Pople and his co-workers proposed a series of ab initio methods, the Gaussian-n (Gn) models,[5-15] in order to achieve these objectives. Their aim is to develop a general procedure for accurate energies applicable for a variety of molecular systems. These theoretical procedures include: Gaussian-1 (G1),[5,6] Gaussian-2 (G2)[7,8] and Gaussian-3(G3)[9-11] methods, as well as their less expensive variants. Using these general theoretical procedures, the calculated energies of a variety of molecular systems with the aforementioned size are expected to have an average absolute deviation from experiment less than 10-15 kJ mol^{-1}. The Gaussian-n techniques, based on a series of additivity approximation,[13-15] consist of a sequence of well-defined calculations so as to arrive a total energy for a given molecular species.

The G1 method is the first member of this series of theoretical procedures. Compared with G2 and G3, the G1 method yields less accurate results and is more computationally demanding. In this thesis, we mainly employ the G3 and its variant G3(MP2) to study the structures and energetics of selected chemical species.

In addition to these ab initio methods, in this thesis, we have also applied the density functional theory (DFT)[16] to study the Diels-Alder reactions of acenes.

1.1 The Gaussian-3 Method

The G3 energy is an approximation of the molecular energy at the QCISD(T)/G3large level, where G3large is a modified 6-311+G(3df,2p) basis set. In the G3 model, the structure of a chemical species is optimized at the second-order

Møller-Plesset theory (MP2) using the 6-31G(d) basis set with all electrons included, i.e., at the MP2(Full)/6-31G(d) level. Based on this optimized structure, single-point calculations at QCISD(T)/6-31G(d), MP4/6-31G(d), MP4/6-31+G(d), MP4/6-31G(2df,p), and MP2(Full)/G3large levels are carried out. Also, this model requires a higher level correction (HLC) in the calculation of total electronic energies (E_e). This HLC is: $-6.386 \times 10^{-3}n_\beta - 2.977 \times 10^{-3}(n_\alpha-n_\beta)$ for molecules and $-6.219 \times 10^{-3}n_\beta - 1.185 \times 10^{-3}(n_\alpha-n_\beta)$ for atoms, in which n_α and n_β are the number of α and β electrons, respectively, with $n_\alpha \geq n_\beta$. The HF/6-31G(d) or MP2(Full)/6-31G(d) harmonic vibrational frequencies, scaled by 0.8929 or 0.9661,[17] respectively, are applied for the zero-point vibrational energy (ZPVE) correction at 0 K ($E_0 = E_e +$ ZPVE).

The G3 theory has been used to calculate molecular energies, such as atomization energies,[5-13] ionization energies,[5,14] proton affinities,[5,14] and electron affinities[5] of 125 molecules for which these quantities have been well established experimentally. The average absolute deviation of G3 theory with experiment for the 299 energies of these 125 molecules is 4.27 kJ mol^{-1}.[9] Detailed methodology of the G3 theory is given in Appendix A.

1.2 The G3 Method with Reduced Møller-Plesset Order and Basis Set

An economical variant of the G3 theory, G3(MP2), was introduced by Pople et al. recently.[10] The G3(MP2) model involves only two single-point energy calculations at the QCISD(T)/6-31G(d) and MP2/G3MP2large levels, based on the geometry optimized at the MP2(Full)/6-31G(d) level. The G3MP2large basis set is the same as the aforementioned G3large basis set, except the core polarization functions have been removed.[10] Once again, a HLC is also included to yield the E_e of the molecule, where HLC $= -9.729 \times 10^{-3}n_\beta - 4.471 \times 10^{-3}(n_\alpha-n_\beta)$ for molecules and $-9.345 \times 10^{-3}n_\beta - 2.021 \times 10^{-3}(n_\alpha-n_\beta)$ for atoms. Similar to the G3 method, the MP2(Full)/6-31G(d) vibrational frequencies, scaled by 0.9661,[17] are applied for the ZPVE correction at 0 K to give the total energy of (E_0) for the molecule.

It is noted that the G3(MP2) method is able to yield results with average absolute deviations of 5.44 kJ mol^{-1} for the aforementioned 299 energies determined by experiments.[9]

1.3 Density Functional Theory (DFT)

The basis for DFT is the proof by Hohenberg and Kohn[16] that the ground state electronic energy is determined completely by the electron density, $\rho(\mathbf{r})$. In particular, the set of self-consistent one-electron equations by Kohn and Sham[18] which include, in an approximate way, exchange and correlation effects. Substituting the mathematical expressions for the kinetic and potential energies, the total energy for N electrons (index i) and M nuclei (index α) can be written, without approximation, as:

$$E^{El} = -\frac{1}{2}\sum_{i=1}^{N}\int \varphi_i^*(r_1)\nabla^2\varphi_i(r_1)dr_1 + \sum_{\alpha=1}^{M}\int \frac{Z_\alpha}{|R_\alpha - r_1|}\rho(r_1)dr_1$$
$$+ \frac{1}{2}\iint \frac{\rho(r_1)\rho(r_2)}{r_{12}}dr_1 dr_2 + E_{XC}[\rho]$$

where the first term describes the kinetic energy of N non-interacting electrons with density $\rho(\mathbf{r})$, the second term represents Coulomb interaction between the electron and nucleus, the third term represents the Coulomb interaction between the two charge distributions, and the last term, the $E_{XC}[\rho]$ functional, accounts for the exchange-correlation energy.

1.4 Calculation of Thermodynamical Data

The heats of formation at temperature T, ΔH°_{fT}, in this work were calculated in the following manner. For molecule AB, its ΔH°_{fT} at a given theoretical level was calculated from the corresponding heat of reaction $\Delta H^\circ_{rT}(A + B \rightarrow AB)$ and the respective experimental $\Delta H^\circ_{fT}(A)$ and $\Delta H^\circ_{fT}(B)$ for elements A and B. In the calculations of ΔH°_{rT} for anions, we set the ΔH°_{rT} value of a free electron to be zero.

1.5 Remark on the Location of Transition Structures

In this thesis, all stationary points on the potential energy surface were characterized by vibrational frequency calculations. In other words, equilibrium structures have only real vibrational frequencies, while transition structures (TSs) have one and only one imaginary frequency. For each TS, the "reactant(s)" and "product(s)" were confirmed by intrinsic reaction coordinate (IRC)[19,20] calculations.

1.6 Natural Bond Orbital (NBO) Analysis

The Natural Bond Orbital (NBO) analysis has been carried out for a number of species in order to study the bonding and interactions of the acenes as well as the croconate $(C_5O_5^{2-})$ and rhodizonate $(C_6O_6^{2-})$ dianions in Chapters 5 and 6, respectively. This analysis allows us to isolate the interaction energies in low-order perturbative expressions of easily interpretable form and to relate these expressions to chemical explanations. The bond interaction in the various isomers is discussed in terms of stabilization energies, $\Delta E_{(2)}$, which is calculated by the second-order perturbation analysis of the Fock matrix obtained in the NBO analysis.[21] By this perturbational approach, the donor-acceptor interaction involving a filled orbital φ (donor) and an unfilled antibonding orbital φ^* (acceptor) can be quantitatively described. Specifically, this stabilization energy is calculated by the following expression:

$$\Delta_{\varphi\varphi^*}E_{(2)} = -2\frac{(<\varphi\,|\,F\,|\,\varphi^*>)^2}{\varepsilon_{\varphi^*} - \varepsilon_{\varphi}}$$

where F is the Fock operator and ε_{φ} and ε_{φ^*} are the NBO energies of the donor and acceptor orbitals, respectively.[22]

1.7 Scope of the Thesis

In the following chapters, the calculation results of a number of molecular systems will be discussed. The heats of formation of the azine series and boron hydrides will be discussed in Chapters 2 and 3, respectively. In Chapter 4, a structural and energetics study of tri-*tert*-butylmethane and tetra-*tert*-butylmethane will be investigated. The method employed in these three chapters were the G3 and G3(MP2) models of theory. In Chapter 5, the Diels-Alder reactivity and aromaticity of acenes are studied with the B3LYP and MP2 levels of theory. The structures of the charge-delocalized and -localized forms of the croconate and rhodizonate dianions will be discussed in Chapter 6. Finally, a conclusion will be given in Chapter 7.

Editorial Note: Each chapter of this thesis should be treated as a separate entity. In other words, it has its own numbering system for molecular species, equations, tables, figures, and references.

1.8 References

(1) Nyden, M. R.; Petersson, G. A. *J. Chem. Phys.* **1981**, *75*, 1843.

(2) Petersson, G. A.; Al-Laham, M. A. *J. Chem. Phys.* **1991**, *94*, 6081.

(3) Ochterski, J. W.; Petersson, G. A.; Montgomery, J. A. *J. Chem. Phys.* **1996**, *104*, 2598.

(4) Montgomery, J. A.; Ochterski, J. W.; Petersson, G. A. *J. Chem. Phys.* **1994**, *101*, 5900.

(5) Pople, J. A.; Head-Gordon, M.; Fox, D. J.; Raghavachari, K.; Curtiss, L. A. *J. Chem. Phys.* **1989**, *90*, 5622.

(6) Curtiss, L. A.; Jones, C.; Trucks, G. W.; Raghavachari, K.; Pople, J. A. *J. Chem. Phys.* **1990**, *93*, 2537.

(7) Curtiss, L. A.; Raghavachari, K.; Trucks, G. W.; Pople, J. A. *J. Chem. Phys.* **1991**, *94*, 7221.

(8) Curtiss, L. A.; Raghavachari, K.; Pople, J. A. *J. Chem. Phys.* **1993**, *98*, 1293.

(9) Curtiss, L. A.; Raghavachari, K.; Redfern, P. C.; Rassolov, V. R.; Pople, J. A. *J. Chem. Phys.* **1998**, *109*, 7764.

(10) Curtiss, L. A.; Raghavachari, K.; Redfern, P. C.; Rassolov, V. R.; Pople, J. A. *J. Chem. Phys.* **1999**, *110*, 4703.

(11) Curtiss, L. A.; Redfern, P. C.; Raghavachari, K.; Pople, J. A. *J. Chem. Phys.* **2001**, *114*, 108.

(12) Curtiss, L. A.; Carpenter, J. E.; Raghavachari, K.; Pople, J. A. *J. Chem. Phys.* **1992**, *96*, 9030.

(13) Curtiss, L. A.; Raghavachari, K.; Pople, J. A. *Chem. Phys. Lett.* **1993**, *214*, 183.

(14) Curtiss, L. A.; Raghavachari, K.; Redfern, P. C.; Pople, J. A. *J. Chem. Phys.* **1997**, *106*, 1063.

(15) Curtiss, L. A.; Raghavachari, K.; Redfern, P. C.; Pople, J. A. *J. Chem. Phys.* **1998**, *109*, 42.

(16) Hohenberg, P.; Kohn, W. *Phys. Rev.* **1964**, *136*, B864.

(17) Scott, A. P.; Radom, L. *J. Phy. Chem.* **1996**, *100*, 16502.

(18) Kohn, W.; Sham, L. J. *Phys. Rev. A* **1965**, *140*, 1133.

(19) Gonzalez, C.; Schlegel, H. B. *J. Chem. Phys.* **1989**, *90*, 2154.

(20) Gonzalez, C.; Schlegel, H. B. *J. Chem. Phys.* **1990**, *94*, 5523.

(21) Reed, A. E.; Curtiss, L. A.; Weinhold, F. *Chem. Rev.* **1988**, *88*, 899.

(22) Klaptke, T. M.; Schulz, A. *Quantum Chemical Methods in Main-Group Chemistry*; Wiley: Chichester, 1998.

Chapter 2

Heats of Formation for the Azine Series: A Gaussian-3 Study

Abstract

Applying the Gaussian-3 (G3) model and its variant G3(MP2), and using the atomization scheme, the heats of formation (ΔH_f) at 0 K and 298 K have been calculated for twelve monocyclic azines with the general formula $N_n(CH)_{6-n}$, n = 1, 2,..., 6. Upon comparing the calculated results with available experimental data, it is found that the calculated structural parameters agree very well with experiment. Additionally, most of the calculated ΔH_f values are well within ± 10 kJ mol^{-1} of the available experimental data. Thus, it is concluded that the unfavorable accumulation of component errors found in the Gaussian-2 methods is greatly reduced in the G3 models. Also, the calculated ΔH_f values for those azines with no experimental data should be reliable estimates.

2.1 Introduction

Azines are the six-membered heterocyclic compounds with the general formula, $N_n(CH)_{6-n}$, with n = 1, 2,..., 6. This series of compounds range from the very familiar pyridine to the heretofore unknown pentazine (N_5CH) and hexazine (N_6). In addition, members of this series exhibit interesting chemistry. For instance, the Diels-Alder reactions between unsubstituted and phenyl-substituted acetylenes and 1,2,4,5-tetrazines have been studied experimentally and computationally.[1] Furthermore, substituted dialkyl-amino 2,4-triazines constitute a family of compounds with herbicidal activity. They also inhibit photosynthetic electron flow in higher plants.[2]

In our previous works,[3,4] the heats of formation at 0 K (ΔH_{f0}) and at 298 K (ΔH_{f298}) were calculated using the Gaussian-2 (G2)[5] and Gaussian-3 (G3)[6] based methods. In the earlier report,[3] it was found that the G2 methods suffer "an unfavorable accumulation of component small errors." Furthermore, this shortcoming may be circumvented using isodesmic reactions in the computation scheme. On the other hand, in the more recent report,[4] it was found that the aforementioned error accumulation is significantly reduced in the G3 methods and

hence the ΔH_f values of molecules with the size of benzene may be calculated directly, i.e., using the atomization scheme. This result is important, as, for some compounds, the isodesmic reactions cannot always be written readily.

In the present work, the ΔH_f values of twelve azines are calculated using the G3 method, as well as a variant of this method, G3(MP2).[7] The purpose of these calculations is twofold. First, by comparing the calculated results with available experimental data, the relative merits of these G3 methods can be assessed. Second, if the G3 methods prove to be trustworthy, their ΔH_f results for those azines with no experimental data should be reliable estimates.

2.2 Methods of Calculation and Results

All calculations were carried out on various workstations using the Gaussian 98 package of programs.[8] The methods of calculation employed were G3 and G3(MP2) models of theory.

Table 1 lists the total energies at 0 K (E_0) and enthalpies at 298 K (H_{298}) for the azines calculated at the G3 and G3(MP2) levels. To convert these results into ΔH_f values for the azines using the so-called atomization scheme,[3,4,9] the experimental[10] ΔH_{f0} values of C (711.2 kJ mol^{-1}), H (216.0 kJ mol^{-1}), and N (470.8 kJ mol^{-1}), as well as the experimental[10] ΔH_{f298} values of C (716.7 kJ mol^{-1}), H (218.0 kJ mol^{-1}), and N (472.7 kJ mol^{-1}) are required. The G3 and G3(MP2) heats of reactions at 0 K and 298 K for the azines are summarized in Table 2, along with available experimental data for ready comparison.

The structural parameters of the azines, optimized at the MP2(Full)/6-31G(d) level, are tabulated in Table 3. Also included in this table are the available experimental structural data as well as those calculated at other theoretical levels. The molecular structures and labeling of atoms for the azines are shown in Figure 1.

2.3 Discussion

We first examine the structural data listed in Table 3. Five azines, pyridine (**1**), pyridazine (**2a**), pyrimidine (**2b**), pyrazine (**2c**), and 1,3,5-triazine (**3c**), have experimental structural data[11,12] available in the literature. Upon comparing these data with our calculated results, we see that the agreement ranges from good to excellent. The only relatively poor agreement occurs for the C^2C^2 bond in **2a**: 1.385 Å vs 1.375 Å. Also, it is not surprising that calculations at the

MP2/6-311G(d,p) level for **2a** yield slightly better results.[1] On the other hand, theoretical results for **3c** at the MP2/cc-pVTZ level are very similar to ours. Finally, it is noted that hexazine (**6**) was reportedly observed in a matrix about twenty years ago,[13] which inspired a number of theoretical studies.[14]

Attention is now turned to the energetics results. Examining Table 2, it is seen that only the experimental heats of formation at 298 K of some azines are available for comparison, while there are no experimental ΔH_{f0} values for azines found in the literature. Comparing the G3 and G3(MP2) ΔH_{f298} values with their experimental counterparts, it is seen that most of the agreements are well within ±10 kJ mol^{-1}, the expected error range for these two theoretical methods. The only obvious exception is the difference between the calculated and experimental ΔH_{f298} values for 1,2,4,5-tetrazine (**4b**), which is about 25 kJ mol^{-1}. Upon further checking of the literature, it is found that the "experimental" ΔH_{f298} for **4b**, 464 kJ mol^{-1} or 111 kcal mol^{-1}, was "predicted" by adding the bond ΔH_f values in the following manner:[15] 2×35.3 kcal mol^{-1} (ΔH_f for N$\cdots$N) + 4×13.5 kcal mol^{-1} (ΔH_f for C$\cdots$N) + $2\times(-6.8$ kcal mol^{-1}) (ΔH_f for C$\cdots$H). Obviously, in view of the accuracy of the G3 results for the other azines, there is no reason to believe that the value predicted for **4b** by such a simple additivity rule should be more reliable than the G3 results. Finally, for pyrazine (**2c**), the G3(MP2) and G3 ΔH_{f298} values (207.0 and 209.0 kJ mol^{-1}, respectively) may be considered as barely within 10 kJ mol^{-1} of the experimental result (196.0$\pm$1.3 kJ mol^{-1}).

2.4 Conclusion

The heats of formation of twelve monocyclic azines with the general formula $N_n(CH)_{6-n}$, n = 1, 2,..., 6, have been calculated using the G3 and G3(MP2) models of theory. Upon examining the results, it is found that the geometrical parameters optimized at the MP2(Full)/6-31G(d) level are in general in very good agreement with experiment. Also, most of the calculated ΔH_{f298} values are well within ±10 kJ mol^{-1} of the experimental data. Hence, it may once again be concluded that the unfavorable accumulation of component errors found in the G2-based methods has been markedly reduced in the G3 methods. Also, the G3 results for those azines with no experimental data should be reliable estimates. Finally, it is pointed out that G3 and G3(MP2) methods yield very comparable results for the azines, even though the more

elaborated G3 model gives slightly better results for some members of the series. Hence, if computation resource limitation is a factor, the G3(MP2) model is dependable substitute for the G3 method.

2.5 Publication Note

An article based on the results reported in this Chapter has now appeared: Cheng, M.-F.; Ho, H.-O.; Lam, C.-S.; Li, W.-K., Heats of formation for the azine series: a Gaussian-3 study, *J. Serb. Chem. Soc.* **2002**, *67*, 257.

2.6 References

(1) Cioslowski, J.; Sauer, J.; Hetzenegger, J.; Kacher, T.; Hierstetter, T. *J. Am. Chem. Soc.* **1993**, *115*, 1353.

(2) Creuzet, S.; Langlet, J. *Chem. Phys. Lett.* **1993**, *208*, 511.

(3) Cheung, Y.-S.; Wong, C.-K.; Li, W.-K. *J. Mol. Struct. (Theochem)* **1998**, *454*, 17.

(4) Cheung, T.-S.; Law, C.-K.; Li, W.-K. *J. Mol. Struct. (Theochem)* **2001**, *572*, 243.

(5) Curtiss, L. A.; Raghavachari, K.; Trucks, G. W.; Pople, J. A. *J. Chem. Phys.* **1991**, *94*, 7221.

(6) Curtiss, L. A.; Raghavachari, K.; Redfern, P. C.; Rassolov, V.; Pople, J. A. *J. Chem. Phys.* **1998**, *109*, 7764.

(7) Curtiss, L. A.; Raghavachari, K.; Redfern, P. C.; Rassolov, V.; Pople, J. A. J. Phys. Chem A **1999**, *110*, 4703.

(8) Frisch, M. J.; Trucks, G. W.; Schlegel, H. B.; Scuseria, G. E.; Robb, M. A.; Cheeseman, J. R.; Zakrzewski, V. G.; Montgogery, J. A.; Jr.; Stratmann, R.E.; Burant, J. C.; Dapprich, S.; Millam, J. M.; Daniels, A. D.; Kudin, K. N.; Strain, M. C.; Farkas, O.; Tomasi, J.; Barone, V.; Cossi, M.; Cammi, R.; Mennucci, B.; Pomelli, C.; Adamo, C.; Clifford, S.; Ochterski, J.; Petersson, G. A.; Ayala, P. Y.; Cui, Q.; Morokuma, K.; Malick, D. K.; Rabuck, A. D.; Raghavachari, K.; Foresman, J. B.; Cioslowski, J.; Ortiz, J. V.; Baboul, A. G.; Stefanov, B. B.; Liu, G.; Liashenko, A.; Piskorz, P.; Komaromi, I.; Gomperts, R.; Martin, R. L.; Fox, D. J.; Keith, T.; Al-Laham, M. A.; Peng, C. Y.; Nanayakkara, A.; Gonzalez, C.; Challacombe, M.; Gill, P. M. W.; Johnson, B.; Chen, W.; Wong, M. W.; Andres,

J. L.; Gonzalez, C.; Head-Gordon, M.; Replogle, E. S.; Pople, J. A. *GAUSSIAN 98*, Revision A.11; Gaussian, Inc., Pittsburgh PA, 1998.

(9) Nicolaides, A.; Radom, L. *Mol. Phys.* **1996**, *88*, 759.

(10) Lias, S. G.; Bartmess, J. E.; Liebman, J. F.; Holmes, J. F.; Levin, R. E.; Mallard, W. J. *J. Phys. Chem. Ref. Data* **1988**, *17*, Suppl. No.1.

(11) Eicher, T.; Hauptmann, S. The Chemistry of Heterocycles, Verlag, Stuttgart, 1995.

(12) Pai, S. V.; Chabalowski, C. F.; Rice, B. M. *J. Phys. Chem.* **1996**, *100*, 5681.

(13) Vogler, A.; Wright, R. E.; Kunkley, H. *Angew. Chem. Int. Ed. Engl.* **1980**, *19*, 717.

(14) See, for example, Engelke, R. *J. Phys. Chem.* **1992**, *96*, 10789 and references cited therein.

(15) Joshi, R. M. *J. Macromol. Sci. Chem.* **1982**, *A18*, 861.
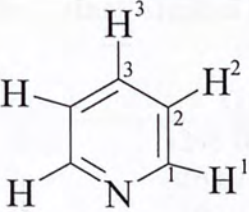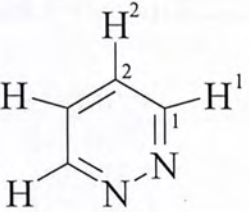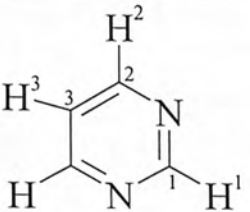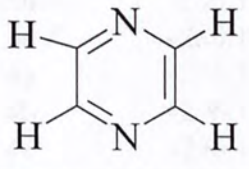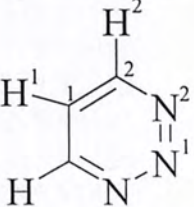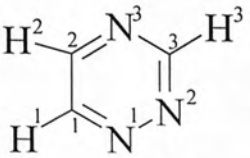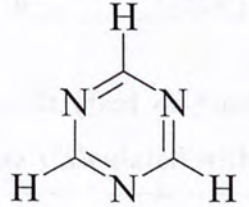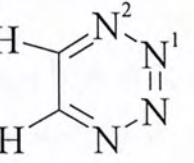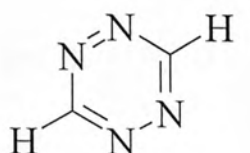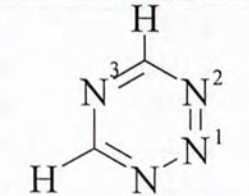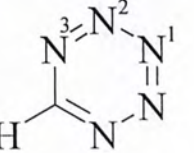
H³ — 3 — H² ⟨ring⟩ H — 2 — H — N — H¹ pyridine **1**, C_{2v}	H² ⟨ring⟩ H — 2 — H¹ — H — N — N — H pyridazine **2a**, C_{2v}	H² ⟨ring⟩ H³ — 3 — 2 — N — H — N — 1 — H¹ pyrimidine **2b**, C_{2v}
H — N — H ⟨ring⟩ H — N — H pyrazine **2c**, D_{2h}	H² ⟨ring⟩ H¹ — 1 — 2 — N² — H — N — N¹ 1,2,3-triazine **3a**, C_{2v}	H² — 2 — N³ — 3 — H³ ⟨ring⟩ H¹ — N¹ — N² 1,2,4-triazine **3b**, C_s
H ⟨ring⟩ N — N H — N — H 1,3,5-triazine **3c**, D_{3h}	H — N² — N¹ ⟨ring⟩ H — N — N 1,2,3,4-tetrazine **4a**, C_{2v}	N — N — H ⟨ring⟩ H — N — N 1,2,4,5-tetrazine **4b**, D_{2h}
H ⟨ring⟩ N³ — N² — N¹ H — N 1,2,3,5-tetrazine **4c**, C_{2v}	N³ — N² — N¹ ⟨ring⟩ H — N pentazine **5**, C_{2v}	N — N — N ⟨ring⟩ N — N — N hexazine **6**, D_{6h}

Figure 1. The molecular structures and labeling of atoms for the twelve $N_n(CH)_{6-n}$, n = 1-6, isomers studied in this work.

Table 1: Total Energies (in Hartrees) at 0 K (E_0) and Enthalpies at 298 K (H_{298}) for the Azines Studied in This Work Calculated at the G3 and G3(MP2) Levels

| Azine | E_0 | | H_{298} | |
	G3	G3(MP2)	G3	G3(MP2)
1	-248.09290	-247.86761	-248.08759	-247.86230
2a	-264.10064	-263.87320	-264.09542	-263.86798
2b	-264.13679	-263.90868	-264.13160	-263.90350
2c	-264.12963	-263.90195	-264.12446	-263.89678
3a	-280.11543	-279.88569	-280.11029	-279.88054
3b	-280.14086	-279.91089	-280.13577	-279.90580
3c	-280.18390	-279.95312	-280.17884	-279.94806
4a	-296.12560	-295.89395	-296.12050	-295.88885
4b	-296.14664	-295.91486	-296.14160	-295.90982
4c	-296.15830	-295.92601	-296.15326	-295.92096
5	-312.13765	-311.90400	-312.13253	-311.89889
6	-328.12095	-327.88608	-328.11544	-327.88057

Table 2: Heat of Formation (kJ mol⁻¹) at 0 K (ΔH_{f0}) and 298 K (ΔH_{f298}) for Azines Calculated with the G3 and G3(MP2) Methods

| Azine | ΔH_{f0}[a] | | ΔH_{f298}[b] | | |
	G3	G3(MP2)	G3	G3(MP2)	Experimental[c]
1	157.8	153.7	143.0	138.9	140±1
2a	299.7	297.1	285.3	282.6	278.3±1
2b	204.8	203.9	190.3	189.3	196.6±0.9
2c	223.6	221.6	209.0	207.0	196.0±1.3
3a	423.1	422.3	409.1	408.2	416
3b	356.3	356.1	342.2	341.9	334
3c	243.4	245.2	229.1	231.0	226±1
4a	558.6	558.6	545.1	545.0	
4b	503.4	503.7	489.7	489.9	464[d]
4c	472.8	474.4	459.1	460.7	
5	689.2	690.2	676.3	677.2	
6	895.3	895.2	884.0	883.9	

[a] To obtain these ΔH_{f0} values, in addition to the E_0 values given in Table 1, we also require the E_0 values of the constituent atoms. At the G3 level, the E_0 values for C, H and N are −37.82772, −0.50100, and −54.56434 hartrees, respectively. At the G3(MP2) level, the corresponding values are −37.78934, −0.50184, and −54.52519 hartrees.

[b] To obtain these ΔH_{f298} values, in addition to the H_{298} values listed in Table 1, we also require the H_{298} values for the constituent atoms. We can obtain these quantities by adding $E_{trans} + PV$ (= $2.5RT$ = 0.00236 hartrees at 298 K) to the atomic E_0 values.

[c] Taken from ref. 10.

[d] See discussion in text.

Table 3: Calculated Structural Parameters (in Å and Degrees) Optimized at the MP2(Full)/6-31G(d) Level of the Azines Studied in This Work

Parameter	Calculated	Expt.	Other	Parameter	Calculated	Expt.	Other
pyridine **1**				1,2,3-triazine **3a**			
NC^1	1.344	1.338 [a]		N^1N^2	1.340		
C^1C^2	1.394	1.394 [a]		N^2C^2	1.345		
C^2C^3	1.393	1.392 [a]		C^1C^2	1.387		
C^1H^1	1.088	1.083 [a]		H^1C^1	1.085		
C^2H^2	1.086	1.083 [a]		H^2C^2	1.087		
C^3H^3	1.087	1.082 [a]		$N^2N^1N^2$	121.0		
C^1NC^1	116.8	116.9 [a]		$N^1N^2C^2$	119.7		
NC^1C^2	123.8	123.8 [a]		$N^2C^2C^1$	122.2		
$C^1C^2C^3$	118.6	118.5 [a]		$C^2C^1C^2$	115.2		
$C^2C^3C^2$	118.4	118.5 [a]		$H^1C^1C^2$	122.3		
$H^1C^1C^2$	120.5			$H^2C^2N^2$	115.1		
$H^2C^2C^3$	121.1			1,2,4-triazine **3b**			
$H^3C^3C^2$	120.8			N^1N^2	1.346		
pyridazine **2a**				N^2C^3	1.340		
NN	1.347	1.330 [a]	1.340 [b]	C^3N^3	1.345		
NC^1	1.343	1.341 [a]	1.341 [b]	N^3C^2	1.335		
C^1C^2	1.396	1.393 [a]	1.398 [b]	C^1C^2	1.395		
C^2C^2	1.385	1.375 [a]	1.367 [b]	C^1N^1	1.340		
C^1H^1	1.087		1.075 [b]	H^1C^1	1.086		
C^2H^2	1.086		1.075 [b]	H^2C^2	1.087		
NNC^1	119.0	119.3 [a]		H^3C^3	1.086		
NC^1C^2	124.0	123.7 [a]		$C^1N^1N^2$	117.6		
$C^1C^2C^2$	117.0	117.1 [a]		$N^1N^2C^3$	118.0		
H^1C^1N	114.4			$N^2C^3N^3$	127.4		
$H^2C^2C^2$	122.1			$C^3N^3C^2$	114.1		
pyrimidine **2b**				$N^3C^2C^1$	120.7		
C^1N	1.340	1.340 [a]		$C^2C^1N^1$	122.2		
NC^2	1.342	1.350 [a]		$H^1C^1N^1$	115.5		
C^2C^3	1.391	1.410 [a]		$H^2C^2N^3$	117.4		
H^1C^1	1.087			$H^3C^3N^3$	117.1		
H^2C^2	1.088			1,3,5-triazine **3c**			
H^3C^3	1.085			NC	1.339	1.338 [c]	1.335 [c]
NC^1N	127.4	129.7 [a]		HC	1.087	1.084 [c]	1.082 [c]
C^1NC^2	115.6	115.0 [a]		CNC	114.0	113.2 [c]	114.1 [c]
NC^2C^3	122.3	121.3 [a]		NCN	126.0	126.8 [c]	126.0 [c]
$C^2C^3C^2$	116.8	118.6 [a]		HCN	117.0	116.6 [c]	117.0 [c]
H^1C^1N	116.3			1,2,3,4-tetrazine **4a**			
H^2C^2N	116.2			N^1N^1	1.335		
$H^3C^3C^2$	121.5			N^1N^2	1.346		
pyrazine **2c**				N^2C	1.337		
NC	1.343	1.339 [a]		CC	1.390		
CC	1.394	1.393 [a]		HC	1.086		
HC	1.088			$N^1N^1N^2$	121.6		
CNC	115.4	116.3 [a]		N^1N^2C	117.8		
NCC	122.3	121.8 [a]		N^2CC	120.6		
HCN	116.6			HCN^2	116.3		

Parameter	Calculated	Expt.	Other
1,2,4,5-tetrazine 4b			
NN	1.339		1.333 [b]
CN	1.344		1.341 [b]
HC	1.085		1.084 [b]
NNC	116.4		
NCN	127.2		
HCN	116.4		
1,2,3,5-tetrazine 4c			
N^1N^2	1.337		
N^2C	1.342		
CN^3	1.336		
HC	1.086		
$N^2N^1N^2$	119.7		
N^1N^2C	118.2		
N^2CN^3	125.6		
CN^3C	112.7		
HCN^3	118.1		
pentazine 5			
N^1N^2	1.340		
N^2N^3	1.336		
N^3C	1.338		
HC	1.085		
$N^2N^1N^2$	121.8		
$N^1N^2N^3$	119.8		
N^2N^3C	116.6		
N^3CN^3	125.4		
HCN^3	117.3		
hexazine 6			
NN	1.337 [d]		1.337 [e]

[a] Ref. 11. [b] Ref. 1. [c] Ref. 12.
[d] Parameter optimized at the HF/6-31G(d) level.
[e] Ref. 14.

Chapter 3

Heats of Formation for Some Boron Hydrides: A Gaussian-3 Study

Abstract

Applying the Gaussian-3 (G3) model, using both the isodesmic and atomization schemes, the heats of formation (ΔH_f) at 0 K and 298 K are calculated for nineteen boron hydrides with one to ten boron atoms. Upon examining the results, it is found that essentially all of the isodesmic ΔH_{f0} and ΔH_{f298} values are well within ± 10 kJ mol^{-1} of the experimental data, the only exceptions being those for $B_{10}H_{14}$. Hence, the isodesmic G3 results for those boron hydrides (studied in this work) with no experimental data should be reliable estimates. On the other hand, the atomization scheme leads to much more inferior results, even though, as shown in previous work, the same method yields very good results for the $(CH)_6$ isomers. A possible source for this deficiency of the G3 method has been suggested.

3.1 Introduction

Boron hydrides or boranes are compounds containing only the elements boron and hydrogen. Boron compounds have wide applications in many technological areas such as separation, catalysis, and radiation therapy and they are also potential high-energy fuels.[1] The study of metallaboranes is one of the most popular topics in inorganic chemistry and boranes are often the precursors of these compounds. However, due to their propensity to explode, the thermochemistry of the boron hydrides is relatively unexplored. In the present work, the heats of formation (ΔH_f) of various boranes with different sizes are calculated. These boranes include species having one to ten boron atoms: BH_3, B_2H_6, B_3H_7, B_3H_9, B_4H_8, B_4H_{10}, B_4H_{12}, B_5H_9, B_5H_{11}, B_6H_{10}, B_6H_{12}, B_6H_{14}, B_7H_{11}, B_8H_{12}, B_8H_{14}, B_9H_{15}, and $B_{10}H_{14}$.

Recently, the unusual properties of boron hydrides have stimulated a lot of theoretical studies. Early in the 1980s, McKee studied the transient species B_3H_7, B_3H_9, B_4H_8, B_4H_{12}, and $B_3H_8^-$ by ab initio theory.[2] The most stable structures of these boron hydrides were reported. Later, he also studied the five structures of B_5H_9 and the transition structures linking them,[3] as well as the bridge hydrogen scrambling in B_5H_{11} and B_6H_{10}.[4] In 1989, he attempted to estimate the ΔH_f values of the boron

16

hydrides from their ab initio energies.[5] The geometries of the boron hydrides he studied were optimized at the HF/3-21G level and the stabilities were calculated relative to BH_3 and H_2. In 1998, Feller and Dixon also obtained the ΔH_f values of simple boron compounds,[1] such as BH, BH_2, BH_3 and B_2H_6, from ab initio coupled cluster calculations by using a systematic sequence of correlation consistent Gaussian basis set.

In our previous studies on $(CH)_6$ isomers,[6,7] the heats of formation at 0 K (ΔH_{f0}) and at 298 K (ΔH_{f298}) were calculated using the Gaussian-2 (G2)[8] and Gaussian-3 (G3)[9] based methods. In the earlier report,[6] it was found that the G2 methods suffer "an unfavorable accumulation of component small errors." Furthermore, this shortcoming may be circumvented using isodesmic reactions in the computation scheme. On the other hand, in the more recent report,[7] it was found that the aforementioned error accumulation is significantly reduced in the G3 methods and hence the ΔH_f values of molecules with the size of benzene may be calculated directly, i.e., using the atomization scheme. This result is important, as, for some compounds, isodesmic reactions cannot always be written readily. More recently, the twelve monocyclic azines with the general formula $N_n(CH)_{6-n}$, n = 1, 2,..., 6, have been studied in a similar fashion[10] using the G3[9] and G3(MP2)[11] models of theory. Upon examining the results, it is found that the geometrical parameters optimized at the MP2(Full)/6-31G(d) level are in general in very good agreement with experiment. Also, most of the calculated ΔH_{f298} values are well within ±10 kJ mol^{-1} of the experimental data. Hence, it may be once again concluded that the unfavorable accumulation of component errors found in the G2-based methods has been markedly reduced in the G3 methods.

In the present work, the structures of the nineteen aforementioned boron hydrides are determined and their heats of formation ΔH_{f0} and ΔH_{f298} are calculated using the G3 method. Both the atomization[6,7,12] and isodesmic[5,13] schemes are used. The isodesmic scheme we have employed is based on one first devised for boranes by McKee.[5] In this original work, energies were calculated at the MP2/6-31G(d) level. In the present work, energies are calculated at the G3 level of theory. Furthermore, we note that the isodesmic approach for calculating ΔH_f values using G2-based methods was first proposed by Raghavachari et al. in 1997.[13] The purpose of the present calculations is twofold. First, by comparing the calculated results of

G3 atomization and the isodesmic schemes with the available experimental values, the more suitable scheme in the study of boron hydrides can be found. Second, if the calculation method proves to be trustworthy, their ΔH_f results for those boron hydrides with no experimental data should be reliable estimates.

3.2 Methods of Calculation and Results

All calculations were carried out on various workstations using the Gaussian 98 package of programs.[14] The method of calculation employed was G3 model of theory.

After calculated the total energies at 0 K (E_0) and the enthalpies at 298 K (H_{298}), the results were converted into ΔH_f values for the boron hydrides using the so-called atomization scheme[6,7,12] and McKee's isodesmic scheme.[5]

When using the atomization scheme, the experimental[15] ΔH_{f0} values of B (557.6 kJ mol^{-1}), and H (216.0 kJ mol^{-1}), as well as the experimental[15] ΔH_{f298} values of B (562.7 kJ mol^{-1}), and H (218.0 kJ mol^{-1}), are required.

In the isodesmic scheme, all the boron hydrides considered are derived from the equation: $xBH_3 \rightarrow$ boron hydride $+ yH_2$, where x and y are integer values representing the number of BH_3 and the number of H_2, respectively.[5] Based on the G3 results of the boron hydrides, the ΔH_f values (in kJ mol^{-1}) are calculated by using following equations:

$$\Delta H_{fT}(\text{boron hydride}) = \Delta H_{rxn,T} + x[\Delta H_f(BH_3)] \tag{1}$$

$$\Delta H_{rxn,0} = [E_0(\text{boron hydride at G3 level}) + yE_0(H_2) - xE_0(BH_3)] \times 2625.5 \tag{2}$$

$$\Delta H_{rxn,298} = [H_{f298}(\text{boron hydride at G3 level}) + yH_{f298}(H_2) - xH_{f298}(BH_3)] \times 2625.5 \tag{3}$$

where the quantity $\Delta H_f(BH_3)$ is set to the value that yields the experimental ΔH_f of B_5H_9 and the constant 2625.5 is the conversion factor from hartree to kJ mol^{-1}. In the original scheme designed by McKee,[5] the $\Delta H_f(BH_3)$ value is set to the value that yields the experimental ΔH_f of B_5H_{11}. The reason for this slight modification is twofold: it leads to better results and the experimental ΔH_{f0} of B_5H_{11} is not available in the literature. Also, in McKee's original work, the E_0 values were calculated at the MP2/6-31G(d) level. In any event, in order to obtain the ΔH_f of the boron hydrides by using the isodesmic scheme, we require the experimental ΔH_f values of B_5H_9 at 0 K and 298 K, also the E_0 of H_2 (−1.16738 hartrees) and H_{f298} of H_2 (−1.16407 hartrees) at the G3 level.

Table 1 lists the G3 E_0 and the ΔH_{f0} values of the boron hydrides, along with available experimental data. The G3 H_{298} and the ΔH_{f298} values for the boron hydrides are summarized in Table 2, along with available experimental data for ready comparison. Also included in this table are McKee's results obtained using his original isodesmic scheme at the theoretical level of MP2/6-31G(d).

The structural parameters of the boron hydrides, optimized at the MP2(Full)/6-31G(d) level, are tabulated in Table 3. Also included in this table are the available experimental structural data as well as those calculated at other theoretical levels. The molecular structures and labeling of atoms for the boron hydrides are shown in Figure 1.

3.3 Discussion

We first examine the structural data listed in Table 3. Ten boron hydrides, $BH_3(D_{3h}$ symmetry), $B_2H_6(D_{2h})$, $B_4H_{10}(C_{2v})$, $B_5H_9(C_{4v})$, $B_5H_{11}(C_1)$, $B_6H_{10}(C_s)$, $B_6H_{12}(C_2)$, $B_8H_{12}(C_s)$, $B_9H_{15}(C_s)$, and $B_{10}H_{14}(C_{2v})$ have experimental structural data[5,16] available in the literature. Upon comparing these data with our calculated results, we see that the agreement is good for most of the species studied. Still, poor agreements occur in the geometric parameters of $B_6H_{12}(C_2)$, where the experimental values are derived by gas-phase electron diffraction (GED) studies. It should be pointed out that, on the basis of structural, energetic, and NMR criteria, the accuracy of the molecular dimensions for B_6H_{12} derived by GED has been questioned by Bühl and Schleyer.[17] Additionally, the calculated chemical shifts for B_6H_{12} based on its MP2(Full)/6-31G(d) structure are in excellent agreement with experiment.[16] Hence Bühl and Schleyer suggested that the GED data are probably not as accurate as those calculated at the MP2(Full)/6-31G(d) level.[16] Also, the theoretical results for $B_3H_7(C_s)$, $B_3H_9(C_{3v})$, $B_4H_8(C_{2v})$, $B_4H_8(C_1)$, $B_4H_{12}(C_{2v})$, $B_6H_{14}(C_{2h})$, $B_7H_{11}a(C_s)$, and $B_7H_{11}b(C_s)$ calculated at HF/3-21G level and reported by McKee[5] probably are not as accurate as ours. In addition, the geometry optimization at the G3 level for $B_8H_{14}(C_s)$ is reported for the first time; this structure has already been proposed in the literature.[18]

Moreover, the $B_4H_8(C_{2v})$ structure is calculated to have three imaginary vibrational frequencies, while the $B_4H_8(C_1)$ structure has no imaginary frequency, at the MP2(Full)/6-31G(d) level. Therefore, we may say that the C_1 structure of B_4H_8 is more realistic than the C_{2v} structure. This conclusion is also supported by

McKee's calculations,[2] where the C_1 structure is estimated (at the MP3/6-31G(d) level) to be more stable than the C_{2v} structure by almost 24 kJ mol^{-1}. At the G3 level, the C_1 structure is more stable by 13 kJ mol^{-1} (at 298 K) to 16 kJ mol^{-1} (at 0 K). Finally, the $B_7H_{11}a(C_s)$ structure is calculated to have one imaginary frequency at MP2(Full)/6-31G(d) level, while it has two imaginary frequencies at HF/6-31G(d) level. Other structures of boron hydrides reported here have no imaginary frequencies.

Attention is now turned to the energetics results. Examining Tables 1 and 2, it is seen that the experimental ΔH_{f0} and ΔH_{f298} values of only a few of the boranes are available for comparison. Comparing the G3 isodesmic ΔH_{f0} and ΔH_{f298} values with their experimental counterparts, it is seen that most of the agreements are well within ± 10 kJ mol^{-1}, the expected error range for this theoretical method. Additionally, comparing the G3 and MP2 isodesmic results in Table 2, the G3 results are superior in most instances. The only glaring exception is the largest borane studied, $B_{10}H_{14}(C_{2v})$. The difference between the calculated isodesmic and experimental ΔH_{f0} values for this system is about 26 kJ mol^{-1}, and the difference between the calculated isodesmic and experimental ΔH_{f298} values for the same species is about 27 kJ mol^{-1}. These disagreements may be caused by the calculation method that involves the accumulation of error in the ΔH_f of BH_3, as suggested by McKee.[5] Since the ΔH_f values of BH_3 are estimated from the experimental ΔH_f values of $B_5H_9(C_{4v})$, so error of the ΔH_f values of BH_3 may be accumulated in the calculation of $B_{10}H_{14}(C_{2v})$. Therefore, it can be said that our method of calculation favors the smaller end of boron hydrides, i.e., those systems with eight or less boron atoms.

Finally, we compare the ΔH_f values calculated by the G3 atomization and the isodesmic schemes. Studying the results listed in Tables 1 and 2, we see that the atomization scheme underestimates the ΔH_f values while the isodesmic scheme yields more accurate values. Furthermore, the atomization results are not very good even for very small boranes. This trend is disturbingly dissimilar to the one obtained in our studies of the $(CH)_6$ isomer[7] and azines,[10] where G3 atomization and isodesmic results are quite close to each other. So now we are faced with a dilemma: Why does the G3 method with atomization scheme lead to very good thermochemical results for $(CH)_6$ isomers and azines, but not for the boranes? It is recalled that all the Gaussian-n methods have a term called higher level correction

(HLC) which is based on the number of alpha and beta valence electrons to correct the fact that these methods do not fully account for all of the electron correlation in a pair of electrons. Furthermore, the parameters for HLC in the G3 theory "are chosen to give the smallest average absolute deviation from experiment for the G2/97 test set." So far as we can ascertain, the G2/97 test set contains only three boron compounds: BH, BH_2, and BH_3, and they are not our typical boranes. In other words, for the boron hydrides under study, the HLC factor might not be appropriate. This may be the cause for the inferior results obtained with the atomization scheme. On the other hand, with isodesmic reactions or schemes, the HLC factor drops out, and more accurate ΔH_f values are resulted.

3.4 Conclusion

The ΔH_f values of nineteen boron hydrides have been calculated using the G3 model of theory, using both the atomization and isodesmic schemes. Upon examining the results, it is found that the geometrical parameters optimized at the MP2(Full)/6-31G(d) level are in general in good agreement with experiment. Also, most of the isodesmic ΔH_{f0} and ΔH_{f298} values are well within ± 10 kJ mol^{-1} of the experimental data, the only exceptions being those for $B_{10}H_{14}$. Hence, the isodesmic G3 results for those boron hydrides with no experimental data should be reliable estimates. However, the atomization scheme leads to much more inferior results for the boranes, even though the same method yields very good results for the $(CH)_6$ isomers and azines. A possible source for this deficiency of the G3 method has been suggested.

3.5 Publication Note

An article based on the results reported in this Chapter has now appeared: Cheng, M.-F.; Ho, H.-O.; Lam, C.-S.; Li, W.-K., Heats of formation for the boron hydrides: a Gaussian-3 study, *Chem. Phys. Lett.* **2002**, *356*, 109.

3.6 References

(1) Feller, D.; Dixon, D. A.; Peterson, K. A. *J. Phys. Chem. A* **1998**, *102*, 7053.

(2) McKee, M. L.; Lipscomb, W. N. *Inorg. Chem.* **1982**, *21*, 2846.

(3) McKee, M. L.; Lipscomb, W. N. *Inorg. Chem.* **1985**, *24*, 765.

(4) McKee, M. L. *J. Phys. Chem.* **1989**, *93*, 3426.

(5) McKee, M. L. *J. Phys. Chem.* **1990**, *94*, 435.

(6) Cheung, Y.-S.; Wong, C.-K.; Li, W.-K. *J. Mol. Struct. (Theochem)* **1998**, *454*, 17.

(7) Cheung, T.-S.; Law, C.-K.; Li, W.-K. *J. Mol. Struct. (Theochem)* **2001**, *572*, 243.

(8) Curtiss, L. A.; Raghavachari, K.; Trucks, G. W.; Pople, J. A. *J. Chem. Phys.* **1991**, *94*, 7221.

(9) Curtiss, L. A.; Raghavachari, K.; Redfern, P. C.; Rassolov, V.; Pople, J. A. *J. Chem. Phys.* **1998**, *109*, 7764.

(10) Cheng, M.-F.; Ho, H.-O.; Lam, C.-S.; Li, W.-K. *J. Serb. Chem. Soc.* **2002**, *67*, 257.

(11) Curtiss, L. A.; Raghavachari, K.; Redfern, P. C.; Rassolov, V.; Pople, J. A. *J. Phys. Chem A* **1999**, *110*, 4703.

(12) Nicolaides, A.; Radom, L. *Mol. Phys.* **1996**, *88*, 759.

(13) Raghavachari, K.; Stefanov, B. B.; Curtiss, L. A. *J. Chem. Phys.* **1997**, *106*, 6764.

(14) Frisch, M. J.; Trucks, G. W.; Schlegel, H. B.; Scuseria, G. E.; Robb, M. A.; Cheeseman, J. R.; Zakrzewski, V. G.; Montgogery, J. A.; Jr.; Stratmann, R.E.; Burant, J. C.; Dapprich, S.; Millam, J. M.; Daniels, A. D.; Kudin, K. N.; Strain, M. C.; Farkas, O.; Tomasi, J.; Barone, V.; Cossi, M.; Cammi, R.; Mennucci, B.; Pomelli, C.; Adamo, C.; Clifford, S.; Ochterski, J.; Petersson, G. A.; Ayala, P. Y.; Cui, Q.; Morokuma, K.; Malick, D. K.; Rabuck, A. D.; Raghavachari, K.; Foresman, J. B.; Cioslowski, J.; Ortiz, J. V.; Baboul, A. G.; Stefanov, B. B.; Liu, G.; Liashenko, A.; Piskorz, P.; Komaromi, I.; Gomperts, R.; Martin, R. L.; Fox, D. J.; Keith, T.; Al-Laham, M. A.; Peng, C. Y.; Nanayakkara, A.; Gonzalez, C.; Challacombe, M.; Gill, P. M. W.; Johnson, B.; Chen, W.; Wong, M. W.; Andres, J. L.; Gonzalez, C.; Head-Gordon, M.; Replogle, E. S.; Pople, J. A. *GAUSSIAN 98*, Revision A.11; Gaussian, Inc., Pittsburgh PA, 1998.

(15) Lias, S. G.; Bartmess, J. E.; Liebman, J. F.; Holmes, J. F.; Levin, R. E.; Mallard, W. J. *J. Phys. Chem. Ref. Data* **1988**, *17*, Suppl. No.1.

(16) Bühl, M.; Schleyer, P. v. R. *J. Am. Chem. Soc.* **1992**, *114*, 477.

(17) Bühl, M.; Schleyer, P. v. R. *Angew. Chem., Int. Ed. Engl.* **1990**, *29*, 886.

(18) Housecroft, C. E. Boranes and Metallaboranes, Ellis Horwood, Hemel Hempstead, 1994.

(19) Laurie, D.; Perkins, P. G. *Inorg. Chim. Acta* **1982**, *63*, 53.

Table 1: Total Energies (in Hartrees) at 0 K (E_0) and Heat of Formation (kJ mol^{-1}) at 0 K (ΔH_{f0}) for Various Boron Hydrides Calculated at G3 Level Using the Atomization and Isodesmic Schemes

		E_0 (G3)	ΔH_{f0} (G3)[a] (Atomization)	ΔH_{f0} (G3) (Isodesmic)	ΔH_{f0}[c] (Expt.)
BH_3	D_{3h}	-26.56752	97.8	103.2 [b]	
B_2H_6	D_{2h}	-53.19373	41.4	52.3	51.4
B_3H_7	C_s	-78.59990	125.6	139.7	
B_3H_9	C_{3v}	-79.77148	112.4	128.7	
B_4H_8	C_{2v}	-104.02490	160.3	177.6	
B_4H_8	C_1	-104.03092	144.5	161.8	
B_4H_{10}	C_{2v}	-105.22318	77.0	96.5	
B_4H_{12}	C_{2v}	-106.34262	200.6	222.4	
B_5H_9	C_{4v}	-129.49303	81.8	102.1	102.1
B_5H_{11}	C_1	-130.64840	111.1	133.8	
B_6H_{10}	C_s	-154.92102	108.6	132.4	
B_6H_{12}	C_2	-156.08002	128.4	154.4	
B_6H_{14}	C_{2h}	-157.22752	178.4	206.6	
B_7H_{11} a	C_s	-180.28058	315.1	342.1	
B_7H_{11} b	C_s	-180.30093	261.7	288.7	
B_8H_{12}	C_s	-205.79882	105.0	135.3	
B_8H_{14}	C_s	-206.96519	105.5	137.9	
B_9H_{15}	C_s	-232.41007	88.0	123.6	
$B_{10}H_{14}$	C_{2v}	-256.70949	15.2	51.8	78.1

[a] To obtain these ΔH_{f0} values, we require the E_0 values of the boron hydrides and the E_0 values of the constituent atoms. At the G3 level, the E_0 values for B and H are -24.64257 and -0.50100 hartrees, respectively.

[b] The $\Delta H_{f0}(BH_3)$ is set to the value that yields the experimental heat of formation ΔH_{f0} of B_5H_9.

[c] Ref. 15.

Table 2: The Enthalpies at 298 K (H_{298}) (in Hartrees) and Heat of Formation (kJ mol^{-1}) at 298 K (ΔH_{f298}) for Various Boron Hydrides Calculated at G3 Level Using the Atomization and Isodesmic Schemes

		H_{f298} (G3)	ΔH_{f298} (G3)[a] (Atomization)	ΔH_{f298} (G3) (Isodesmic)	ΔH_{f298} (MP2)[c] (Isodesmic)	ΔH_{f298} [d] (Expt.)
BH_3	D_{3h}	-26.56368	94.2	99.0 [b]	84.0	100.0
B_2H_6	D_{2h}	-53.18914	26.1	35.8	31.8	35.6
B_3H_7	C_s	-78.59443	107.3	119.9	112.1	
B_3H_9	C_{3v}	-79.76496	88.4	102.9	117.6	
B_4H_8	C_{2v}	-104.01947	136.6	152.1	163.6	
B_4H_8	C_1	-104.02463	123.1	138.6		
B_4H_{10}	C_{2v}	-105.21616	49.1	66.5	73.2	66.0
B_4H_{12}	C_{2v}	-106.33378	169.1	188.4	223.4	
B_5H_9	C_{4v}	-129.48683	54.8	73.2	82.0	73.2
B_5H_{11}	C_1	-130.64071	79.6	100.0	101.7	103.3
B_6H_{10}	C_s	-154.91394	78.7	100.0	96.7	95.0
B_6H_{12}	C_2	-156.07161	93.6	116.8	115.5	
B_6H_{14}	C_{2h}	-157.21656	141.9	167.0	168.6	
B_7H_{11} a	C_s	-180.27253	282.4	306.7	329.7	
B_7H_{11} b	C_s	-180.29176	232.0	256.2	392.5	
B_8H_{12}	C_s	-205.78997	69.2	96.4	80.3	(92.9) [e]
B_8H_{14}	C_s	-206.95536	63.8	92.9		
B_9H_{15}	C_s	-232.39963	42.6	74.7	110.9	
$B_{10}H_{14}$	C_{2v}	-256.69958	-28.5	4.5	19.2	31.6

[a] To obtain these ΔH_{f298} values, in addition to the H_{298} values listed in the table, we also require the H_{f298} values for the constituent atoms. We can obtain these quantities by adding $E_{trans} + PV$ ($= 2.5RT = 0.00236$ hartrees at 298 K) to the atomic E_0 values.

[b] The $\Delta H_{f298}(BH_3)$ is set to the value that yields the experimental heat of formation ΔH_{f298} of B_5H_9.

[c] Ref. 5.

[d] Unless otherwise indicated, experimental values are from ref. 15.

[e] Estimated value from ref. 19.

Table 3: Calculated Structural Parameters (in Å and Degrees) Optimized at the MP2(Full)/6-31G(d) Level of the Boron Hydrides Studied in This Work

Parameter	Calculated	Expt.	Other	Parameter	Calculated	Expt.	Other
BH$_3$ D_{3h}				**B$_4$H$_{12}$** C_{2v}			
H^{1}B^1	1.191	1.185[a]		H^{1}B^1	1.178		
B$_2$H$_6$ D_{2h}				H^{2}B^1	1.198		
H^{1}B^1	1.189			H^{3}B^1	1.291		1.310[c]
H^{2}B^1	1.309	1.314[b]	1.309[b]	H^{3}B^2	1.287		1.310[c]
B^{1}B^1	1.749	1.743[b]	1.749[b]	H^{4}B^2	1.182		
B$_3$H$_7$ C_s				H^{5}B^2	1.200		
H^{1}B^1	1.193			B^{1}B^2	2.167		2.471[c]
H^{2}B^1	1.187			B^{2}B^2	3.199		3.593[c]
H^{3}B^2	1.183			B^{1}B^1	2.819		3.235[c]
B^{1}B^2	1.655		1.689[c]	**B$_5$H$_9$** C_{4v}			
B^{1}B^1	1.992		2.080[c]	H^{1}B^1	1.183		
B^{1}H^{1,2}	1.381		1.426[c]	H^{2}B^2	1.186		
B^{2}H^{1,2}	1.292		1.271[c]	B^{1}B^2	1.686	1.690[b]	1.685[b]
B$_3$H$_9$ C_{3v}				B^{2}B^2	1.782	1.803[b]	1.783[b]
H^{1}B^1	1.183			B^{2}H^{2,2}	1.341	1.352[b]	1.342[b]
H^{2}B^1	1.200			**B$_5$H$_{11}$** C_1			
B^{1}B^1	1.972		2.256[c]	B^{1}B^2	1.854	1.870[b]	1.855[b]
B^{1}H^{1,1}	1.293		1.310[c]	B^{2}B^3	1.809	1.760[b]	1.810[b]
B$_4$H$_8$ C_{2v}				B^{3}B^4	1.777	1.770[b]	1.778[b]
H^{1}B^1	1.184			B^{4}B^5	1.735	1.720[b]	1.737[b]
H^{2}B^2	1.184			B^{5}B^1	1.883	1.870[b]	1.883[b]
B^{1}B^2	1.689		1.725[c]	B^{4}B^1	1.722	1.720[b]	1.724[b]
B^{1}B^1	1.668		1.666[c]	B^{3}B^1	1.737	1.760[b]	1.737[b]
B^{1}H^{1,2}	1.557		1.656[c]	B^{2}B^5	3.063		
B^{2}H^{1,2}	1.252		1.241[c]	B^{1}H^{1,2}	1.245	1.090[b]	1.245[b]
B$_4$H$_8$ C_1				B^{2}H^{1,2}	1.438	1.670[b]	1.437[b]
B^{1}B^2	1.763		1.813[c]	B^{2}H^{2,3}	1.398	1.300[b]	1.398[b]
B^{2}B^3	1.753		1.780[c]	B^{5}H^{4,5}	1.380	1.300[b]	1.380[b]
B^{3}B^4	1.715		1.795[c]	B^{3}H^{2,3}	1.262	1.220[b]	1.262[b]
B^{4}B^1	1.614		1.618[c]	B^{4}H^{4,5}	1.281	1.220[b]	1.281[b]
B^{1}B^3	1.700		1.735[c]	B^{3}H^{3,4}	1.316	1.180[b]	1.317[b]
B^{1}H^{1,4}	1.381		1.541[c]	B^{4}H^{3,4}	1.354	1.180[b]	1.354[b]
B^{4}H^{1,4}	1.302		1.261[c]	**B$_6$H$_{10}$** C_s			
B^{4}H^{3,4}	1.311		1.337[c]	B^{1}B^2	1.732	1.737[b]	1.732[b]
B^{3}H^{3,4}	1.372		1.343[c]	B^{2}B^3	1.781	1.794[b]	1.782[b]
B^{2}H^{2,3}	1.329		1.359[c]	B^{3}B^4	1.741	1.736[b]	1.741[b]
B^{3}H^{2,3}	1.341		1.305[c]	B^{2}B^4	1.748	1.753[b]	1.748[b]
B$_4$H$_{10}$ C_{2v}				B^{1}B^1	1.638	1.596[b]	1.638[b]
H^{1}B^1	1.185			B^{4}B^1	1.800	1.795[b]	1.800[b]
H^{2}B^1	1.252	1.315[b]	1.252[b]	B^{1}H^{1,2}	1.329	1.35[b]	1.329[b]
H^{2}B^2	1.410	1.484[b]	1.410[b]	B^{2}H^{1,2}	1.327	1.31[b]	1.327[b]
H^{3}B^2	1.197			B^{2}H^{2,3}	1.369	1.48[b]	1.369[b]
H^{4}B^2	1.192			B^{3}H^{2,3}	1.298	1.32[b]	1.298[b]
B^{1}B^1	1.714	1.704[b]	1.714[b]				
B^{1}B^2	1.835	1.856[b]	1.835[b]				
B^{2}B^2	2.772						

Parameter	Calculated	Expt.	Other	Parameter	Calculated	Expt.	Other
B$_6$H$_{12}$ C_2				**B$_8$H$_{12}$** C_s			
B^{1}B^2	1.786	1.699[b]	1.786[b]	B^{1}B^2	1.777	1.806[b]	1.778[b]
B^{2}B^3	1.727	1.913[b]	1.728[b]	B^{2}B^3	1.820	1.822[b]	1.821[b]
B^{3}B^4	1.898	1.778[b]	1.899[b]	B^{1}B^4	1.715	1.720[b]	1.715[b]
B^{4}B^1	1.784	1.821[b]	1.784[b]	B^{2}B^4	1.802	1.808[b]	1.802[b]
B^{2}B^4	1.714	1.777[b]	1.714[b]	B^{2}B^5	1.774	1.792[b]	1.775[b]
B^{3}H^{2,3}	1.353	1.416[b]	1.354[b]	B^{5}B^4	1.821	1.830[b]	1.821[b]
B^{2}H^{2,3}	1.295	1.200[b]	1.294[b]	B^{1}B^1	1.730	1.705[b]	1.731[b]
B^{2}H^{1,2}	1.360	1.308[b]	1.361[b]	B^{3}B^3	1.647	1.684[b]	1.647[b]
B^{1}H^{1,2}	1.289	1.308[b]	1.289[b]	B^{3}B^5	1.702	1.710[b]	1.702[b]
B$_6$H$_{14}$ C_{2h}				B^{1}H^{1,1}	1.338	1.300[b]	1.338[b]
H^{1}B^1	1.197			B^{1}H^{1,2}	1.391	1.496[b]	1.391[b]
H^{2}B^2	1.195			B^{2}H^{1,2}	1.298	1.287[b]	1.298[b]
H^{3}B^2	1.310		1.322[c]	B^{3}H^{3,3}	1.333	1.322[b]	1.333[b]
H^{3}B^3	1.312		1.316[c]	**B$_8$H$_{14}$** C_s			
H^{4}B^3	1.190			B^{1}B^1	1.906		
H^{5}B^3	1.190			B^{1}B^2	1.924		
H^{6}B^1	1.312		1.322[c]	B^{2}B^3	1.775		
B^{1}B^2	1.708		1.704[c]	B^{1}B^4	1.783		
B^{1}B^1	1.773		1.817[c]	B^{2}B^4	1.733		
B^{2}B^3	1.762		1.803[c]	B^{2}B^5	1.789		
B$_7$H$_{11}$ a C_s				B^{3}B^5	1.727		
B^{1}B^2	1.986		2.087[c]	B^{3}B^3	1.768		
B^{1}B^3	1.853		1.926[c]	B^{1}H^{1,1}	1.318		
B^{3}B^4	1.783		1.797[c]	B^{2}H^{2,3}	1.373		
B^{4}B^5	1.769		1.816[c]	B^{3}H^{2,3}	1.279		
B^{1}B^5	1.808		1.848[c]	B^{3}H^{3,3}	1.332		
B^{2}B^5	1.852		1.936[c]	**B$_9$H$_{15}$** C_s			
B^{1}B^4	1.806		1.850[c]	B^{1}B^2	1.840	1.86[c]	1.881[c]
B^{5}B^5	1.556		1.558[c]	B^{2}B^3	1.925	1.95[c]	1.973[c]
B^{1}H^{1,3}	1.581		1.395[c]	B^{3}B^4	1.783	1.84[c]	1.823[c]
B^{3}H^{1,3}	1.234		1.232[c]	B^{3}B^5	1.803		
B^{1}H^{1,2}	1.372		1.614[c]	B^{4}B^5	1.727	1.78[c]	1.753[c]
B^{2}H^{1,2}	1.306		1.314[c]	B^{2}B^6	1.739	1.76[c]	1.784[c]
B$_7$H$_{11}$ b C_s				B^{3}B^6	1.736	1.75[c]	1.746[c]
B^{1}B^2	1.700		1.665[c]	B^{5}B^6	1.771	1.77[c]	1.797[c]
B^{2}B^3	1.636		1.808[c]	B^{4}B^4	1.751	1.78[c]	1.788[c]
B^{3}B^4	1.692		1.791[c]	B^{2}B^2	1.771	1.80[c]	1.788[c]
B^{1}B^4	1.733		2.257[c]	B^{1}H^{1,2}	1.400		1.463[c]
B^{2}B^4	1.746		1.887[c]	B^{2}H^{1,2}	1.257		1.241[c]
B^{4}B^4	2.176		1.764[c]	B^{3}H^{3,4}	1.324		1.345[c]
B^{3}H^{3,4}	1.310		1.331[c]	B^{4}H^{3,4}	1.318		1.295[c]
B^{4}H^{4,3}	1.359		1.292[c]	B^{4}H^{4,4}	1.338		1.333[c]
				B$_{10}$H$_{14}$ C_{2v}			
				B^{1}B^2	1.775	1.775[c]	1.811[c]
				B^{2}B^2	1.978	1.973[c]	2.011[c]
				B^{1}B^3	1.717	1.715[c]	1.742[c]
				B^{2}B^3	1.780	1.786[c]	1.808[c]
				B^{3}B^4	1.773	1.778[c]	1.804[c]
				B^{4}B^4	1.770		
				B^{2}B^4	1.745	1.756[c]	1.770[c]
				B^{1}H^{1,2}	1.332	1.347[c]	1.326[c]
				B^{2}H^{1,2}	1.317	1.298[c]	1.322[c]

[a] Ref. 1. [b] Ref. 16. [c] Ref. 5.

BH$_3$ D_{3h}

H^{1}B^1 1.191

B$_2$H$_6$ D_{2h}

H^{1}B^1 1.189
H^{2}B^1 1.309
B^{1}B^1 1.749

B$_3$H$_7$ C_s

H^{1}B^1 1.193
H^{2}B^1 1.187
H^{3}B^2 1.183
B^{1}B^2 1.655
B^{1}B^1 1.992
B^{1}H^{1,2} 1.381
B^{2}H^{1,2} 1.292

B$_3$H$_9$ C_{3v}

H^{1}B^1 1.183
H^{2}B^1 1.200
B^{1}B^{1,1} 1.972
B^{1}H^{1,1} 1.293

B$_4$H$_8$ C_{2v}

H^{1}B^1 1.184
H^{2}B^2 1.184
B^{1}B^2 1.689
B^{1}B^1 1.668
B^{1}H^{1,2} 1.557
B^{2}H^{1,2} 1.252

B$_4$H$_8$ C_1

B^{1}B^2 1.763   B^{4}H^{1,4} 1.302
B^{2}B^3 1.753   B^{4}H^{3,4} 1.311
B^{3}B^4 1.715   B^{3}H^{3,4} 1.372
B^{4}B^1 1.614   B^{2}H^{2,3} 1.329
B^{1}B^3 1.700   B^{3}H^{2,3} 1.341
B^{1}H^{1,4} 1.381

B$_4$H$_{10}$ C_{2v}

H^{1}B^1 1.185   H^{4}B^2 1.192
H^{2}B^1 1.252   B^{1}B^1 1.714
H^{2}B^2 1.410   B^{1}B^2 1.835
H^{3}B^2 1.197   B^{2}B^2 2.772

B$_4$H$_{12}$ C_{2v}

H^{1}B^1 1.178   H^{5}B^2 1.200
H^{2}B^1 1.198   B^{1}B^2 2.167
H^{3}B^1 1.291   B^{2}B^2 3.199
H^{3}B^2 1.287   B^{1}B^1 2.819
H^{4}B^2 1.182

B$_5$H$_9$ C_{4v}

H^{1}B^1 1.183
H^{2}B^2 1.186
B^{1}B^2 1.686
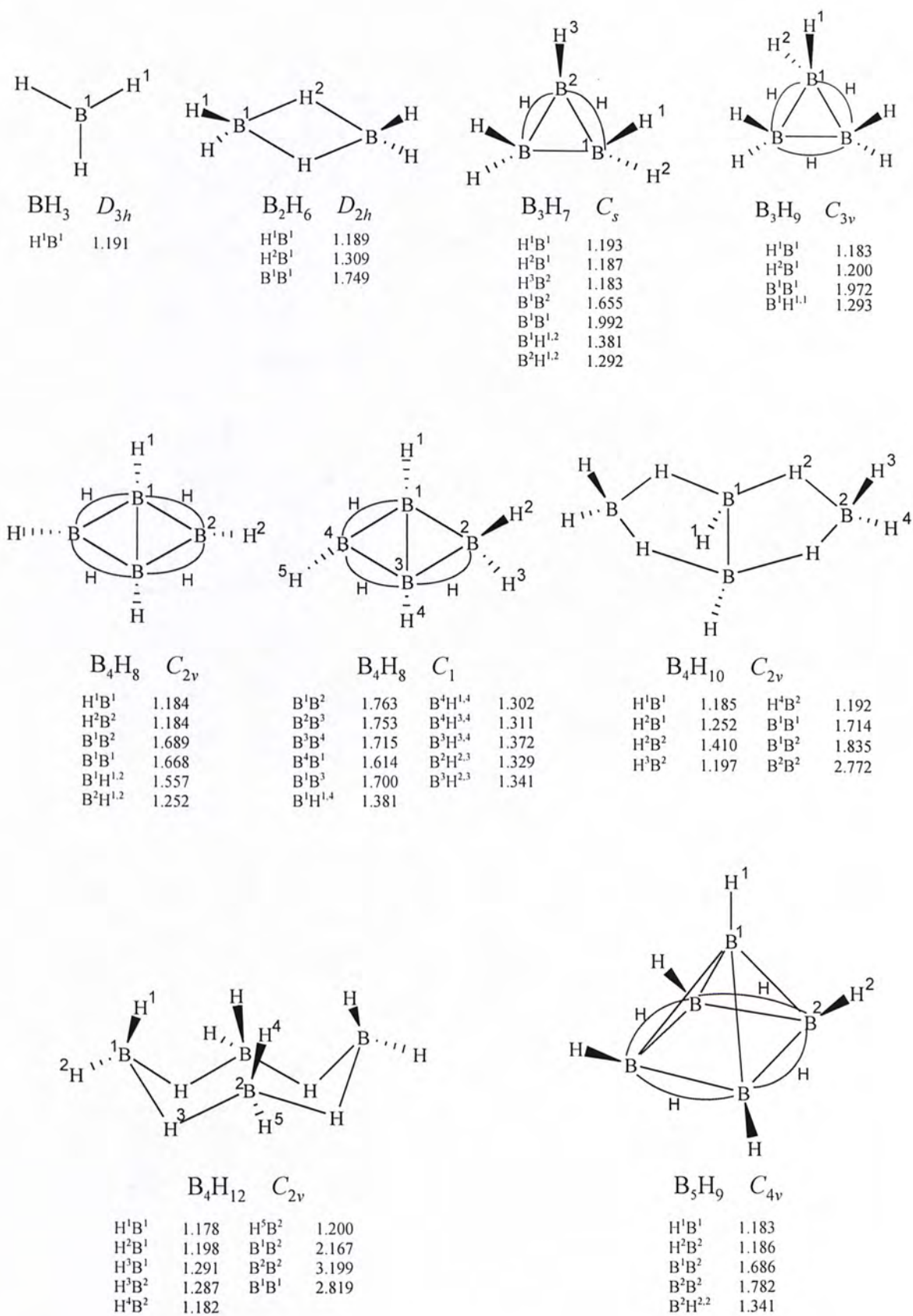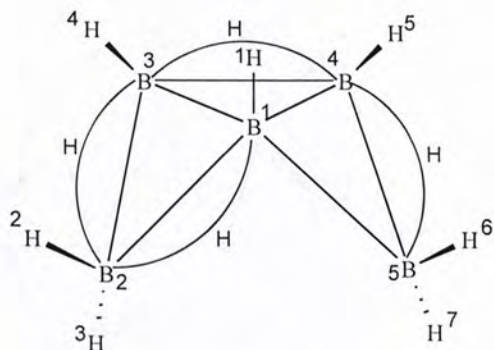B^{2}B^2 1.782
B^{2}H^{2,2} 1.341

Figure 1. The molecular structures and labeling of atoms for the nineteen boron hydrides studied in this work.

B_5H_{11} C_1

B^1B^2	1.854	$B^1H^{1,2}$	1.245
B^2B^3	1.809	$B^2H^{1,2}$	1.438
B^3B^4	1.777	$B^2H^{2,3}$	1.398
B^4B^5	1.735	$B^5H^{4,5}$	1.380
B^5B^1	1.883	$B^3H^{2,3}$	1.262
B^4B^1	1.722	$B^4H^{4,5}$	1.281
B^3B^1	1.737	$B^3H^{3,4}$	1.316
B^2B^5	3.063	$B^4H^{3,4}$	1.354

B_6H_{10} C_s
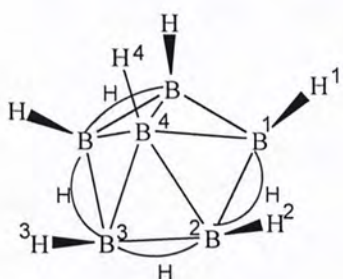
B^1B^2	1.732	B^4B^1	1.800
B^2B^3	1.781	$B^1H^{1,2}$	1.329
B^3B^4	1.741	$B^2H^{1,2}$	1.327
B^2B^4	1.748	$B^2H^{2,3}$	1.369
B^1B^1	1.638	$B^3H^{2,3}$	1.298

B_6H_{12} C_2
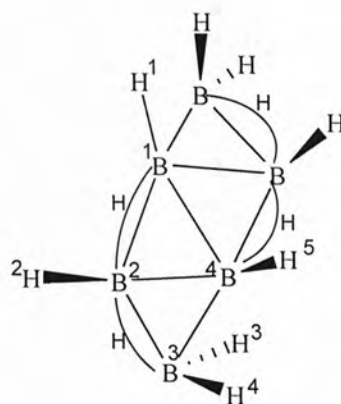
B^1B^2	1.786
B^2B^3	1.727
B^3B^4	1.898
B^4B^1	1.784
B^2B^4	1.714
$B^3H^{2,3}$	1.353
$B^2H^{2,3}$	1.295
$B^2H^{1,2}$	1.360
$B^1H^{1,2}$	1.289
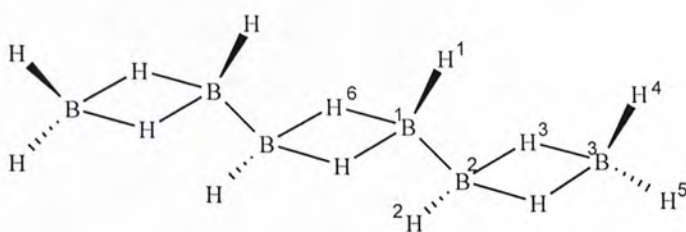
B_6H_{14} C_{2h}

H^1B^1	1.197	H^5B^3	1.190
H^2B^2	1.195	H^6B^1	1.312
H^3B^2	1.310	B^1B^2	1.708
H^3B^3	1.312	B^1B^1	1.773
H^4B^3	1.190	B^2B^3	1.762
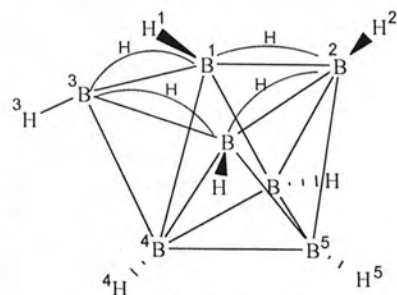
B_7H_{11} a C_s

B^1B^2	1.986	B^1B^4	1.806
B^1B^3	1.853	B^5B^5	1.556
B^3B^4	1.783	$B^1H^{1,3}$	1.581
B^4B^5	1.769	$B^3H^{1,3}$	1.234
B^1B^5	1.808	$B^1H^{1,2}$	1.372
B^2B^5	1.852	$B^2H^{1,2}$	1.306

Figure 1. (Continued).

28

B_7H_{11} b C_s

B^1B^2	1.700	B^2B^4	1.746
B^2B^3	1.636	B^4B^4	2.176
B^3B^4	1.692	$B^3H^{3,4}$	1.310
B^1B^4	1.733	$B^4H^{4,3}$	1.359

B_8H_{12} C_s

B^1B^2	1.777	B^3B^3	1.647
B^2B^3	1.820	B^3B^5	1.702
B^1B^4	1.715	$B^1H^{1,1}$	1.338
B^2B^4	1.802	$B^1H^{1,2}$	1.391
B^2B^5	1.774	$B^2H^{1,2}$	1.298
B^5B^4	1.821	$B^3H^{3,3}$	1.333
B^1B^1	1.730		

B_8H_{14} C_s

B^1B^1	1.906	B^3B^5	1.727
B^1B^2	1.924	B^3B^3	1.768
B^2B^3	1.775	$B^1H^{1,1}$	1.318
B^1B^4	1.783	$B^2H^{2,3}$	1.373
B^2B^4	1.733	$B^3H^{2,3}$	1.279
B^2B^5	1.789	$B^3H^{3,3}$	1.332

B_9H_{15} C_s

B^1B^2	1.840	B^4B^4	1.751
B^2B^3	1.925	B^2B^2	1.771
B^3B^4	1.783	$B^1H^{1,2}$	1.400
B^3B^5	1.803	$B^2H^{1,2}$	1.257
B^4B^5	1.727	$B^3H^{3,4}$	1.324
B^2B^6	1.739	$B^4H^{3,4}$	1.318
B^3B^6	1.736	$B^4H^{4,4}$	1.338
B^5B^6	1.771		

$B_{10}H_{14}$ C_{2v}

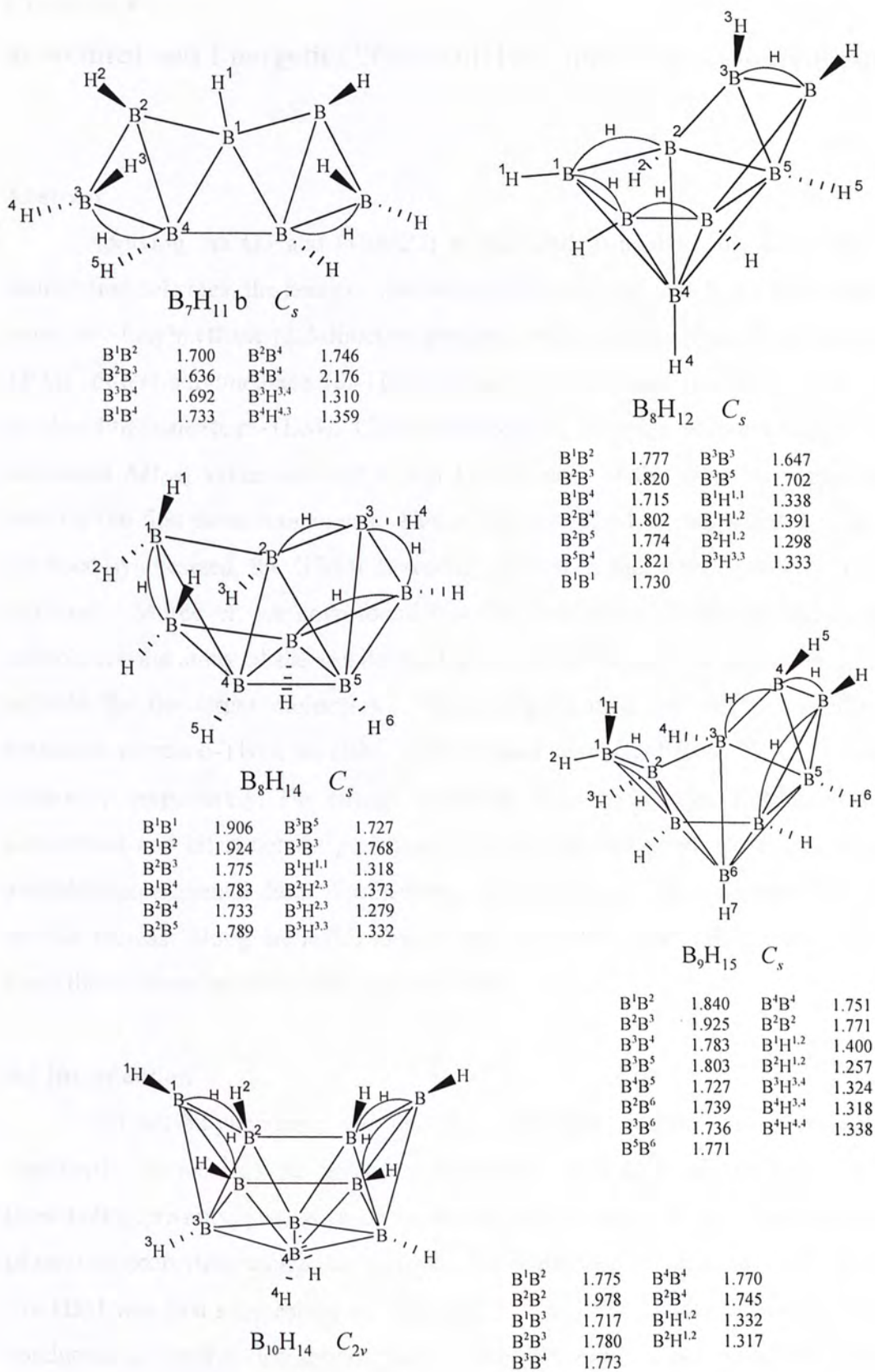|			
B^1B^2	1.775	B^4B^4	1.770
B^2B^2	1.978	B^2B^4	1.745
B^1B^3	1.717	$B^1H^{1,2}$	1.332
B^2B^3	1.780	$B^2H^{1,2}$	1.317
B^3B^4	1.773		

Figure 1. (Continued).

29

Chapter 4

Structural and Energetics Studies of Tri- and Tetra-*tert*-butylmethane

Abstract

Applying the G3 and G3(MP2) models and using both the isodesmic and atomization schemes, the heats of formation (ΔH_f) at 0 and 298 K are calculated for mono-*tert*-butylmethane (2,2-dimethyl-propane or neopentane, abbreviated as mono-TBM), di-*tert*-butylmethane (di-TBM), tri-*tert*-butylmethane (tri-TBM), and tetra-*tert*-butylmethane (tetra-TBM). Upon examining the results, it is found that all of the calculated ΔH_{f298} values are well within ±10 kJ mol^{-1} of the available experimental data for the first three compounds. Hence, for tetra-TBM, a compound that has not yet been synthesized, the G3(MP2) results reported in this work should be reliable estimates. Moreover, we have found that the atomization scheme is slightly more suitable for the study of the smaller molecules, while the isodesmic scheme is more suitable for the larger molecules. Structurally, it is found that the equilibrium structures of mono-TBM, di-TBM, tri-TBM, and tetra-TBM have T_d, C_2, C_1 and T symmetry, respectively. The energy minimized structure of each TBM molecule is determined and all structural parameters are generally in good agreement with the available experimental data. Furthermore, it is found that the innermost C–C bond lengths increase along the series mono-TBM < di-TBM < tri-TBM < tetra-TBM, a trend that is expected from steric consideration.

4.1 Introduction

Tri-*tert*-butylmethane (tri-TBM), a saturated hydrocarbon molecule, is noteworthy because of the great intramolecular congestion arising from packing three bulky *tert*-butyl groups around a tertiary carbon atom. It is a classic molecule of unusual properties, which has intrigued and challenged chemists for over 30 years. Tri-TBM was first synthesized by Stiles and Lee in 1971.[1] Later, Bartell and Burgi conducted an electron diffraction study.[2,3] They attempted to determine the structure of this highly strained molecule to illuminate its properties and explain its unusual vibrational spectra. However, due to the limited resolution of the electron diffraction data, severe approximations had to be made in the process of its structural

determination. Thus, it was assumed not only that the molecule had overall C_3 symmetry, but it was also supposed that the individual *tert*-butyl groups were constrained to (local) C_{3v} symmetry. This problem was pointed out by Bartell and Burgi in their initial paper[2] where they noted: "...this adds to the evidence that the model with local C_{3v} symmetry is too restrictive and that more, though probably quite limited, information can be extracted from the experimental data." In 1994, Hagler et al. reinterpreted the experimental structure of tri-TBM by Hartree-Fock, density functional theory and class II force field methods.[4] Afterward, in 1998, Palmo et al. also studied the structure and the vibrational frequencies of tri-TBM by a spectroscopically determined force field (SDFF).[5] However, energetics and structural studies of tri-TBM with high-level molecular orbital theory are still unavailable.

Tetra-*tert*-butylmethane (tetra-TBM), which has not been synthesized yet, is even more crowded around the central carbon atom than tri-TBM. We are interested in the structure of this molecule and are intrigued by its very long C–C bonds. We intend to compare the bond lengths of these long bonds with those found in other highly congested saturated hydrocarbon molecules.

Mono- and di-*tert*-butylmethane (denoted as mono-TBM and di-TBM, respectively) are lower homologues of tri-TBM and tetra-TBM. It is clear that di-TBM is significantly less strained than tri-TBM. Meanwhile, mono-TBM, is generally considered to be unstrained. It has been the subject of several previous electron diffraction studies.[6,7,8]

In our previous studies on $(CH)_6$ isomers,[9,10] the heats of formation at 0 K (ΔH_{f0}) and at 298 K (ΔH_{f298}) were calculated with the Gaussian-2 (G2)[11] and Gaussian-3 (G3)[12] based methods. In our first study on $(CH)_6$ isomers,[9] it was found that the G2 methods suffer "an unfavorable accumulation of component small errors."[13] Furthermore, this shortcoming may be circumvented by using isodesmic reactions in the computation scheme.[13,14] On the other hand, in our subsequent study on the $(CH)_6$ isomers,[10] it was found that the aforementioned error accumulation is significantly reduced in the G3 methods and hence the ΔH_f values of molecules with the size of benzene may be calculated directly, i.e., using the atomization scheme. This result is important, as, for some compounds, isodesmic reactions cannot always be written readily. More recently, the 12 monocyclic azines with the general formula $N_n(CH)_{6-n}$, n = 1, 2,..., 6,[15] and 19 boranes with one to ten boron atoms,[16] have been

studied in a similar fashion by using the G3[12] and G3(MP2)[17] models of theory. Upon examining the results, it is found that the geometrical parameters optimized at the MP2(Full)/6-31G(d) level are in general in very good agreement with experiment. Also, most of the calculated ΔH_{f298} values are well within ± 10 kJ mol^{-1} of the experimental data. Hence, it may be once again concluded that the unfavorable accumulation of component errors found in the G2-based methods has been markedly reduced in the G3 methods.

In the present work, the structures of the aforementioned TBM molecules are determined and their ΔH_{f0} and ΔH_{f298} values are calculated by using the G3 and G3(MP2) methods. Both the atomization[9,10,13,18] and isodesmic[13,14] schemes are used in the calculation of ΔH_f values. The purpose of the present study is twofold. First, energetically, by comparing the calculated results of G3 and G3(MP2) atomization and the isodesmic schemes with the available experimental values, the more suitable scheme in the study of the TBM molecules can be found. Additionally, if the calculation method proves to be trustworthy, the calculated ΔH_f results for tetra-TBM, an unknown compound so far, should be reliable estimates. Second, structurally, congestion around the central carbon atom increases in the series mono-TBM < di-TBM < tri-TBM < tetra-TBM. We intend to study the effect of this congestion on the structure and symmetry of tri-TBM and tetra-TBM.

4.2 Methods of Calculation and Results

All calculations were carried out on various workstations with the Gaussian 98 package of programs.[19] The methods of calculation employed were G3 and G3(MP2) models of theory.

After calculating the total energies at 0 K (E_0) and the enthalpies at 298 K (H_{298}), the results were then converted into ΔH_f values for the TBM molecules by using the atomization scheme[9,10,13,18] and the isodesmic scheme.[13,14] In the atomization scheme, the experimental[20] ΔH_{f0} values of C (711.2 kJ mol^{-1}) and H (216.0 kJ mol^{-1}), as well as the experimental[20] ΔH_{f298} values of C (716.7 kJ mol^{-1}) and H (218.0 kJ mol^{-1}), are required. We used equations similar to those given in the paper by Radom et al.[18] for the calculation of the ΔH_{f298} value of a given TBM:

$$\Delta H_{f298}[\text{TBM}] = H_{298}[\text{TBM}] - x\{H_0[C_{(g)}] + 0.00236\} - y\{H_0[H_{(g)}] + 0.00236\} +$$

$$x\Delta H_{f298}{}^{\text{exp}}[C_{(g)}] + y\Delta H_{f298}{}^{\text{exp}}[H_{(g)}] \qquad (1)$$
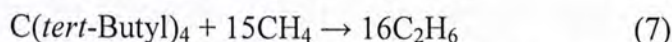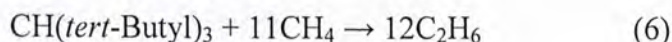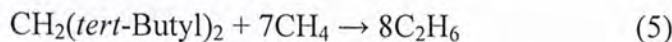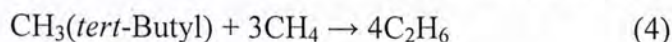
$$\Delta H_{f298}[\text{TBM}] = H_{298}[\text{TBM}] - x\{H_0[\text{C}_{(g)}] + 0.00249\} - y\{H_0[\text{H}_{(g)}] + 0.00236\} +$$

$$x\Delta H_{f298}{}^{\text{exp}}[\text{C}_{(g)}] + y\Delta H_{f298}{}^{\text{exp}}[\text{H}_{(g)}] \qquad (2)$$

$$\Delta H_{f298}[\text{TBM}] = \Delta H_{f0}[\text{TBM}] + \Delta H_{298}{}^{\text{calc}}[\text{TBM}] - x\Delta H_{298}{}^{\text{exp}}[\text{C}_{(s)}] -$$

$$(y/2)\Delta H_{298}{}^{\text{exp}}[\text{H}_{2(g)}] \qquad (3)$$

where x and y are the number of C and H atoms, respectively, in the TBM molecule. We note that eq (1) is more commonly used in the calculation of ΔH_{f298} values. In eq (2), we have replaced the calculated ΔH_{298} (which is $H_{298} - H_0$, and H_0 is simply E_0) value of $\text{C}_{(g)}$ (6.196 kJ mol^{-1}, or 0.00236 hartree) with the experimental result (6.535 kJ mol^{-1}, or 0.00249 hartree). Such a replacement was first proposed by Radom et al.[18] One other way to obtain ΔH_{f298} values is to apply eq (3), which has also been suggested by Radom et al.[18]

In the isodesmic scheme,[13,14] we combined the bond separation reactions of Raghavachari et al.[14] with the G3 and G3(MP2) models of theory. Specifically, the isodesmic bond separation reactions for our TBM molecules are:

$$\text{CH}_3(\textit{tert}\text{-Butyl}) + 3\text{CH}_4 \rightarrow 4\text{C}_2\text{H}_6 \qquad (4)$$

$$\text{CH}_2(\textit{tert}\text{-Butyl})_2 + 7\text{CH}_4 \rightarrow 8\text{C}_2\text{H}_6 \qquad (5)$$

$$\text{CH}(\textit{tert}\text{-Butyl})_3 + 11\text{CH}_4 \rightarrow 12\text{C}_2\text{H}_6 \qquad (6)$$

$$\text{C}(\textit{tert}\text{-Butyl})_4 + 15\text{CH}_4 \rightarrow 16\text{C}_2\text{H}_6 \qquad (7)$$

In order to obtain the G3 ΔH_f of the TBM molecules by using the isodesmic scheme, we require the experimental[20] ΔH_{f0} values (in kJ mol^{-1}) of CH$_4$ (−66.8) and C$_2$H$_6$ (−68.4) and the ΔH_{f298} values (in kJ mol^{-1}) of CH$_4$ (−74.5) and C$_2$H$_6$ (−84.0). Moreover, we also require the E_0 and H_{298} values of CH$_4$ and C$_2$H$_6$ calculated at the G3 and G3(MP2) levels, and these values are included in the footnotes of Tables 2 and 3.

Table 1 lists the electronic energy (E_e) of the TBM molecules calculated with different symmetry constraints. In Table 2, the G3 and G3(MP2) E_0 and the ΔH_{f0} values of the TBM molecules are shown. The G3 and G3(MP2) H_{298} and the ΔH_{f298} values for the molecules are summarized in Table 3, along with available experimental data for ready comparison.

The structural parameters of the TBM molecules, optimized at the MP2(Full)/6-31G(d) level, are tabulated in Table 4. Also included in this table are the available experimental structural data as well as those calculated at other

theoretical levels. The molecular structures and the labeling of the atoms for the TBM molecules are shown in Figure 1.

4.3 Discussion

In this section we discuss the calculated results of the four TBM molecules. Where possible, we compare the G3 or G3(MP2) structural and energetics results with the available experimental data.

Before proceeding to discussing each TBM molecule in turn, we note here there is an inherent difference between the "mean" bond lengths obtained by electron diffraction and the "equilibrium" bond lengths obtained by calculation.[21] The "mean" lengths exceed the "equilibrium" ones because of the anharmonic vibrations related to the asymmetry in the Morse-like covalent bond potentials. So, for example, taking into account zero-point vibrations, a typical C–C "mean" length is about 0.008 Å longer than the "equilibrium." In the case of C–H bonds, the typical difference of about 0.02 Å is greater because of the much larger zero-point vibrational amplitudes characteristic of the light hydrogen atoms. As we shall see, our calculated structural parameters are already in very good agreement with those obtained by electron diffraction. When the aforementioned corrections are taken into account, the agreement becomes even better.

4.3.1 Mono-tert-butylmethane (Mono-TBM)

Mono-TBM, also known as neopentane, is generally considered to be unstrained. From our study, we found that mono-TBM is a highly symmetrical molecule with T_d geometry. In Table 4, we see that the optimized bond lengths for C_t–C_m (1.528 Å) and C_m–H_m bond (1.095 Å) are in good agreement with the vapor-phase electron diffraction average:[8] 1.537 ± 0.003 and 1.114 ± 0.008 Å, respectively. Moreover, the calculated $C_t C_m H_m$ angle (110.9°) is also in excellent accord with the experimental results, $112.2 \pm 2.8°$.[8] The C_t–C_m bond (1.528 Å) of mono-TBM is the shortest innermost C–C bond found in the TBM molecules studied in this work.

We now turn our attention to the calculated ΔH_f values. In Table 3, it is seen that the ΔH_{f298} values of mono-TBM are −168.3, −170.0, and −170.6 kJ mol^{-1}, using the three slightly different atomization schemes at the G3 level, while the corresponding ΔH_{f298} values at the G3(MP2) level are −167.0, −168.7, and −169.3 kJ mol^{-1}. These two sets of values are in excellent agreement with the experimental

result,[22] -167.9 ± 0.63 kJ mol^{-1}. The corresponding ΔH_{f298} values of mono-TBM from the isodesmic scheme are -169.3 and -169.0 kJ mol^{-1}, also in excellent agreement with experiment. From these comparisons, it is seen that there is no accumulation of systematic errors[13] in the atomization scheme for this molecule, which is not unexpected for molecules of this size. In any event, both G3 and G3(MP2), coupled with either the atomization or isodesmic scheme, yield excellent results for mono-TBM.

Before proceeding further, we briefly comment on the results obtained by the three different atomization schemes, i.e., eqs (1) to (3). First, the results of these three methods, for all four TBM molecules, are in accord with each other to well within ± 10 kJ mol^{-1}, the generally accepted error range of the G3 methods. In other words, these three methods yield results of very similar quality. Furthermore, the ΔH_{f298} values generated from eqs (2) and (3) of the atomization scheme are very close to that obtained with the isodesmic scheme.

4.3.2 Di-tert-butylmethane (Di-TBM)

Di-TBM is slightly more strained than mono-TBM. Both the C_2 and C_{2v} structures of di-TBM have been studied. In Table 1, we can see that the C_2 structure is an energy-minimized structure, while the C_{2v} structure is a transition structure (TS) with one imaginary vibrational frequency. Upon intrinsic reaction coordinate analysis,[23,24] it is found that the C_{2v} structure is the TS connecting two C_2 structures, which are mirror images of each other. At the MP2(Full)/6-31G(d) level, the barrier of this rearrangement is 2.3 kJ mol^{-1}. At the G3 and G3(MP2) levels, this barrier is reduced to about 0.4 kJ mol^{-1}. Clearly, this molecule is not very rigid. This finding is consistent with the conclusion of Bartell and Bradford[8] that di-TBM "exhibits striking steric deformations due to its pair of inescapable GG' (gauche-gauche') conformations." Examining the structure of the TS more closely, it is found that the two adjacent tert-butyl groups of the TS respond to the steric stress by undergoing torsional displacements of 12° to form the minimum C_2 structure.

In Table 4, we see that the optimized bond lengths for the central C_t-C_q bonds (1.547 Å) and the C_t-H_t bond (1.100 Å) are in very good agreement with the vapor-phase electron diffraction average:[8] 1.545 ± 0.005 and 1.122 ± 0.015 Å, respectively. Also, the calculated $C_qC_tC_q$ angle (124.6°) is in excellent accord with the experimental results, 125-128°.[8] Furthermore, our results are also in agreement with those obtained

by MM3 and lower level ab initio methods.[25] It is also noted here that the C_t–C_q bond (1.547 Å) of di-TBM is longer than the C_t–C_m bond (1.528 Å) of mono-TBM. The lengthening of the innermost C–C bonds indicates the increase of strain from mono-TBM to di-TBM.

In the work of Bartell and Bradford,[8] the authors noted that the two adjacent *tert*-butyl groups of di-TBM undergo torsional displacements, tilting away from each other and opening up the central $C_qC_tC_q$ bond angle to 125-128° to release the steric stress of the molecule. It should be pointed out that the central $C_qC_tC_q$ bond angle in di-TBM is extremely large for a tetrahedrally coordinated central atom; the "unstrained" CCC bond angles about secondary carbons are usually found to be 113-114°. As pointed out by Mislow,[26] any departure from the tetrahedral angle disturbs the σ character of the bonds and leads to the formation of bent bonds. He also postulated that, with increasing angle bending, there is a corresponding change in hybridization.

Referring to the thermochemical data reported in Table 3, it is seen that the G3 and G3(MP2) ΔH_{f298} values of di-TBM are –245.2 and –243.9 kJ mol^{-1}, respectively, using eq (1) of the atomization scheme. These two values are in excellent agreement with the experimental result,[27] –241.5 ± 1.5 kJ mol^{-1}. The corresponding ΔH_{f298} values of di-TBM using the isodesmic scheme are –248.3 and –247.6 kJ mol^{-1}, also in very good agreement with experiment. From these comparisons, it is again seen that, as in the case of mono-TBM, there is hardly any accumulation of systematic errors[13] in the atomization scheme for this molecule. Indeed, with eq (1), for both mono-TBM and di-TBM, the atomization scheme leads to slightly better results.

For mono-TBM and di-TBM, both the G3 and G3(MP2) methods yield accurate ΔH_{f298} results. Indeed for di-TBM, the lower level G3(MP2) method yields even marginally better ΔH_{f298} values. For the larger molecules of tri-TBM and tetra-TBM, the resource requirement of G3 calculations would be prohibitively high. Hence we will only employ the G3(MP2) method for these larger systems. Based on our experience with mono-TBM and di-TBM, the G3(MP2) results for tri-TBM and tetra-TBM should still be reliable.

4.3.3 Tri-tert-butylmethane (Tri-TBM)

Tri-TBM is a highly crowded and strained molecule. In this work, both the C_3 and C_1 structures of tri-TBM have been studied. At the HF/6-31G(d) level, the C_3 structure, with all real vibrational frequencies, represents an energy minimum. However, at the MP2(Full)/6-31G(d) level, the C_3 structure has three imaginary vibrational frequencies with A and E symmetries. The vibrations with E symmetry will lower the symmetry of the system from C_3 to C_1. Hence, the C_3 structure cannot be an equilibrium structure. Instead, we now have the C_1 structure representing the energy minimum. As we shall see below, employing this C_1 structure to calculate the G3(MP2) ΔH_f values for tri-TBM yields results that are in very good agreement with experiment. Hence, we may conclude that the equilibrium structure of tri-TBM has C_1 symmetry.

In Table 4, we see that the optimized bond lengths for the central $C_t–C_q$ bonds (1.600 Å, within three decimal places) and the $C_t–H_t$ bond (1.102 Å) of the C_1 structure are in very good agreement with the gas-phase electron diffraction average:[3] 1.611 ± 0.005 and 1.111 ± 0.003 Å, respectively. It is noted that, in this experimental study, C_3 symmetry was assumed throughout. Moreover, the calculated $C_qC_tC_q$ angle (115.2°) is also in excellent accord with the experimental result, $116.0 \pm 0.4°$.[3] Furthermore, our results are also in agreement with those obtained by a spectroscopically determined force field (SDFF) and lower level ab initio methods.[5] It is of interest to note here that the innermost $C_t–C_q$ bond (1.600 Å) of the tri-TBM is significantly longer than the $C_t–C_q$ bond (1.547 Å) of di-TBM and the $C_t–C_m$ bond (1.528 Å) of mono-TBM. The lengthening of the innermost C–C bonds indicates the increase of strain from mono-TBM < di-TBM < tri-TBM. Also, the central $C_t–C_q$ bond of the C_3 structure is 1.622 Å, longer than that of the C_1 structure (1.600 Å). This is due to the large steric strain between the three bulky *tert*-butyl groups in the C_3 structure. This steric strain is reduced in the C_1 structure as the three *tert*-butyl groups undergo torsional displacements of 18° against each other.

Referring to the thermochemical data reported in Table 3, it is seen that the G3(MP2) ΔH_{f298} values of tri-TBM using eq (1) and isodesmic schemes are –226.0 and –231.4 kJ mol^{-1}, respectively. These two values are in good agreement with the experimental value,[28] -235.2 ± 4.3 kJ mol^{-1}, with the isodesmic scheme yielding a better result. From this comparison, it is seen that, there is a small accumulation of systematic errors (about 5 kJ mol^{-1}) in this atomization scheme for this molecule.

Therefore, eqs (2) or (3) should be used in order to reduce the systematic errors. The two values generated by these two equations are −230.4 and −231.6 kJ mol^{-1}, respectively, which are nearly the same as that of the isodesmic scheme.

Before proceeding to tetra-TBM, it is pointed out that, as may be seen from Table 3, if we used the C_3 structure of tri-TBM to calculate its thermochemical data, the ΔH_{f298} values would be in the range 170-175 kJ mol^{-1}, very different from the experimental data. This piece of calculated energetics data is an additional evidence that supports the C_1 structure for tri-TBM.

4.3.4 Tetra-tert-butylmethane (Tetra-TBM)

Tetra-TBM, a compound that has not yet been synthesized, is even more crowded around the central carbon atom than tri-TBM. In this work, both the T and T_d structures of tetra-TBM have been studied. The T_d structure is calculated to have 10 and 13 imaginary vibrational frequencies at the HF/6-31G(d) and MP2(Full)/6-31G(d) levels, respectively, while the T structure has all real vibrational frequencies at both of these two levels. Therefore, it may be concluded that the equilibrium structure of tetra-TBM has T symmetry. In Table 4, we compare the optimized bond lengths for the central C_t–C_q bonds (1.661 Å), the C_m–H_m bond (1.087 Å), and the $C_tC_qC_m$ angle (115.7°) of the optimized T structure at the MP2(Full)/6-31G(d) level with the spectroscopically determined force field (SDFF) results (1.683 Å, 1.074-1.088 Å, and 115.9°, respectively).[5] It is found that our results are in good agreement with the SDFF results except for the bond length of the C_t–C_q bond. It should be noted that the SDFF results were derived from the rather crude HF/6-31G level. Therefore, it is believed that our calculated central C_t–C_q bond (1.661 Å) should be more reliable than the SDFF result. Moreover, the C_t–C_q bond (1.661 Å) of tetra-TBM is the longest C–C bond found in the TBM molecules studied in this work. The lengthening of the innermost C–C bonds indicates the increase of strain from mono-TBM < di-TBM < tri-TBM < tetra-TBM. We also believe that tetra-TBM should have the longest C–C bond among the saturated hydrocarbon molecules.

Upon examining the structural data of unsaturated hydrocarbon compounds in the literature, it is found that the longest C–C bond length is 2.827 Å, found in [Et$_4$N]$_2$[TCNE]$_2$ (TCNE = tetracyanoethylene).[29] Less spectacularly, there are the long C–C bonds in 1,1,2,2-tetraphenyl-3,8-dibromobuta[b]naphthalene (1.712 Å), 1,1,2,2-tetraphenyl-3,8-diiodobuta[b]naphthalene (1.734 Å), and 1,1,2,2-(2,2'-

biphenyl)-3,8-diiodobuta[b]naphthalene (1.724 Å).[30] There are also other examples with slightly shorter C–C bonds such as those with lengths of 1.652, 1.653, and 1.688 Å found in *trans*-1,2-dihydroxy-1,2-bis(*p*-tolyl)-acenaphthene,[31] (4*R*,*S*,5*RS*)-4-chloro-3-phenyl-1,7-dioxa-2-azaspiro(4.4)non-2-en-6-one,[32] and hexahydro-1,2-dimethyl-3,6-pyridazinedione,[33] respectively. The last cited examples have bond lengths that are comparable to the longest C–C bonds found in the present work, 1.661 Å in tetra-TBM.

Examining the geometry of the T structure of tetra-TBM more closely, we have found that the inner five carbon atoms retain the idealized T_d structure. However, inclusion of the outer 12 methyl carbon atoms (but NOT the hydrogens) already reduces the symmetry of the aggregate to T. It is interesting to note that the central C_t–C_q bond of the T_d structure of tetra-TBM is 1.723 Å, which is longer than that of the T structure (1.661 Å). This difference is due to the large steric strain among the four bulky *tert*-butyl groups in the T_d structure of tetra-TBM. This steric strain is reduced in the T structure as the four *tert*-butyl groups undergo torsional displacements of 16° against each other.

Referring to the thermochemical data reported in Table 3, it is seen that the G3(MP2) ΔH_{f298} values of tetra-TBM using eq (1) and isodesmic schemes are –133.7 and –140.9 kJ mol^{-1}, respectively. From the experience of our study of tri-TBM, we believe the isodesmic result should be more reliable. In any event, the accumulated systematic error is still relatively small, about 7 kJ mol^{-1}, and, based on the accuracy of the calculated results for mono-TBM, di-TBM, and tri-TBM, the error range for the isodesmic ΔH_{f298} for tetra-TBM should be within ±10 kJ mol^{-1}. The two values generated from eqs (2) and (3) are –139.5 and –141.1 kJ mol^{-1}, respectively. Once again, these two values are essentially the same as the result obtained by the isodesmic scheme.

4.4 Conclusion

Employing both the isodesmic and atomization schemes, the ΔH_{f0} and ΔH_{f298} for mono-TBM, di-TBM, tri-TBM, and tetra-TBM have been calculated by using the G3 and G3(MP2) models of theory. Upon examining the results, it is found that all of the calculated ΔH_{f298} values are well within ±10 kJ mol^{-1} of the available experimental data for the first three compounds. Hence, for tetra-TBM, for which no experimental thermochemical data are available, the (isodesmic) G3(MP2) results reported in this

work should be reliable estimates. Moreover, we found that the atomization scheme is marginally more suitable for the study of small molecules, while the isodesmic scheme is more suitable for the larger ones. Structurally, it is found that the equilibrium structures of mono-TBM, di-TBM, tri-TBM, and tetra-TBM have T_d, C_2, C_1, and T symmetry, respectively. In addition, the energy-minimized structure of each molecule is determined and all structural parameters are generally in good agreement with the available experimental data. Finally, the innermost C–C bond lengths increase along the series mono-TBM < di-TBM < tri-TBM < tetra-TBM, a trend expected by considering the steric effect in these molecules.

4.5 Publication Note

An article based on the results reported in this Chapter has been written up and submitted for publication: Cheng, M.-F.; Li, W.-K., Structural and energetics studies of tri- and tetra-*tert*-butylmethane, *J. Phys. Chem. A* (accepted).

4.6 References

(1) Lee, H.-H. Thesis, The University of Michigan, 1971.

(2) Burgi, H. B.; Bartell, L. S. *J. Am. Chem. Soc.* **1972**, *94*, 5236.

(3) Bartell, L. S.; Burgi, H. B. *J. Am. Chem. Soc.* **1972**, *94*, 5239.

(4) Hagler, A. T.; Sharon, R.; Hwang, M.-J. *J. Am. Chem. Soc.* **1996**, *118*, 3759.

(5) Palmo, K.; Mirkin, N. G.; Krimm, S. *J. Phys. Chem. A* **1998**, *102*, 6448.

(6) Pauling, L.; Brockway, L. O. *J. Am. Chem. Soc.* **1937**, *59*, 1223.

(7) Beagley, B.; Brown, D. P.; Monaghan, J. J. *J. Mol. Struct.* **1969**, *4*, 233.

(8) Bartell, L. S.; Bradford, W. F. *J. Mol. Struct.* **1977**, *37*, 113.

(9) Cheung, Y.-S.; Wong, C.-K.; Li, W.-K. *J. Mol. Struct. (Theochem)* **1998**, *454*, 17.

(10) Cheung, T.-S.; Law, C.-K.; Li, W.-K. *J. Mol. Struct. (Theochem)* **2001**, *572*, 243.

(11) Curtiss, L. A.; Raghavachari, K.; Trucks, G. W.; Pople, J. A. *J. Chem. Phys.* **1991**, *94*, 7221.

(12) Curtiss, L. A.; Raghavachari, K.; Redfern, P. C.; Rassolov, V.; Pople, J. A. *J. Chem. Phys.* **1998**, *109*, 7764.

(13) Nicolaides, A.; Radom, L. *Mol. Phys.* **1996**, *88*, 759.

(14) Raghavachari, K.; Stefanov, B. B.; Curtiss, L. A. *J. Chem. Phys.* **1997**, *106*, 6764.

(15) Cheng, M.-F.; Ho, H.-O.; Lam, C.-S.; Li, W.-K. *J. Serb. Chem. Soc.* **2002**, *67*, 257.

(16) Cheng, M.-F.; Ho, H.-O.; Lam, C.-S.; Li, W.-K. *Chem. Phys. Lett.* **2002**, *356*, 109.

(17) Curtiss, L. A.; Raghavachari, K.; Redfern, P. C.; Rassolov, V.; Pople, J. A. *J. Phys. Chem. A* **1999**, *110*, 4703.

(18) Nicolaides, A.; Rauk, A.; Glukhovtsev, M. N.; Radom, L. *J. Phys. Chem.* **1996**, *100*, 17460.

(19) Frisch, M. J.; Trucks, G. W.; Schlegel, H. B.; Scuseria, G. E.; Robb, M. A.; Cheeseman, J. R.; Zakrzewski, V. G.; Montgogery, J. A.; Jr.; Stratmann, R.E.; Burant, J. C.; Dapprich, S.; Millam, J. M.; Daniels, A. D.; Kudin, K. N.; Strain, M. C.; Farkas, O.; Tomasi, J.; Barone, V.; Cossi, M.; Cammi, R.; Mennucci, B.; Pomelli, C.; Adamo, C.; Clifford, S.; Ochterski, J.; Petersson, G. A.; Ayala, P. Y.; Cui, Q.; Morokuma, K.; Malick, D. K.; Rabuck, A. D.; Raghavachari, K.; Foresman, J. B.; Cioslowski, J.; Ortiz, J. V.; Baboul, A. G.; Stefanov, B. B.; Liu, G.; Liashenko, A.; Piskorz, P.; Komaromi, I.; Gomperts, R.; Martin, R. L.; Fox, D. J.; Keith, T.; Al-Laham, M. A.; Peng, C. Y.; Nanayakkara, A.; Gonzalez, C.; Challacombe, M.; Gill, P. M. W.; Johnson, B.; Chen, W.; Wong, M. W.; Andres, J. L.; Gonzalez, C.; Head-Gordon, M.; Replogle, E. S.; Pople, J. A. *GAUSSIAN 98*, Revision A.11; Gaussian, Inc., Pittsburgh PA, 1998.

(20) Lias, S. G.; Bartmess, J. E.; Liebman, J. F.; Holmes, J. L.; Levin, R. D.; Mallard, W. G. *J. Phys. Chem. Ref. Data* **1988**, *17*, Suppl. No.1.

(21) Bartell, L.S. *J. Chem. Phys.* **1955**, *23*, 1219.

(22) Good, W. D. *J. Chem. Thermodyn.* **1970**, *2*, 237.

(23) Gonzalez, C.; Schlegel, H. B. *J. Chem. Phys.* **1989**, *90*, 2154.

(24) Gonzalez, C.; Schlegel, H. B. *J. Phys. Chem.* **1990**, *94*, 5523.

(25) Liedle, S.; Oberhammer, H.; Allinger, N. L. *J. Mol. Struct.* **1994**, *317*, 69.

(26) Mislow, K. *Tetrahedron Lett.* **1964**, *22*, 1415.

(27) Fuchs, R.; Peacock, L. A. *Can. J. Chem.* **1979**, *57*, 2302.

(28) Verevkin, S. P.; Nolke, M.; Beckhaus, H. D.; Ruchardt, C. *J. Org. Chem.* **1997**, *62*, 4683.

(29) Sesto, R. E. D.; Sommer, R. D.; Miller, J. S. *Cryst. Eng. Comm.* **2001**, *47*, 222.

(30) Tanaka, K.; Takamoto, N.; Tezuka, Y.; Kato, M.; Toda, F. *Tetrahedron* **2001**, *57*, 3761.

(31) Gatilov, Y. V.; Nagi, S. M.; Rybalova, T. V.; Borodkin, G. I. *Zh. Strukt. Khim.* **1984**, *25*, 142.

(32) Stverkova, S.; Zak, Z. Jonas, J. *Liebigs Ann. Chem.* **1993**, 1169.

(33) Ottersen, T.; Sorensen, U. *Acta Chem. Scand. Ser. A* **1977**, *31*, 808.

Table 1: The Electronic Energy (E_e) (in Hartrees) for Mono-TBM, Di-TBM, Tri-TBM, and Tetra-TBM

			E_e at HF/6-31G(d)[a]	E_e at MP2(Full)/6-31G(d)[a]
Mono-TBM	C_5H_{12}	T_d	-196.33382 (0)	-197.02325 (0)
Di-TBM	C_9H_{20}	C_2	-352.45511 (0)	-353.70094 (0)
Di-TBM	C_9H_{20}	C_{2v}	-352.45440 (1)	-353.70006 (1)
Tri-TBM	$C_{13}H_{28}$	C_1	-508.52125 (0)[b]	-510.33783 (0)
Tri-TBM	$C_{13}H_{28}$	C_3	-508.52125 (0)	-510.31558 (3)
Tetra-TBM	$C_{17}H_{36}$	T	-664.54128 (0)	-666.94137 (0)
Tetra-TBM	$C_{17}H_{36}$	T_d	-664.46634 (10)	-666.86325 (13)

[a] The number of imaginary frequencies calculated of each molecule is given in brackets.

[b] The optimized geometry has C_3 symmetry, even though no symmetry constraint was imposed initially.

Table 2: The Total Energies (in Hartrees) at 0 K (E_0) and the Heats of Formation (kJ mol^{-1}) at 0 K (ΔH_{f0}) for Mono-TBM, Di-TBM, Tri-TBM, and Tetra-TBM Calculated at the G3 and G3(MP2) Levels Using the Atomization and Isodesmic Schemes

		E_0 G3	E_0 G3(MP2)	ΔH_{f0}[a] G3 (Atomization)	ΔH_{f0}[b] G3 (Isodesmic)	ΔH_{f0}[a] G3(MP2) (Atomization)	ΔH_{f0}[b] G3(MP2) (Isodesmic)
Mono-TBM	T_d	-197.54392	-197.36164	-135.7	-134.2	-134.5	-133.9
Di-TBM	C_2	-354.62505	-354.29595	-189.6	-187.9	-188.4	-187.3
Di-TBM	C_{2v}	-354.62411	-354.29501	-187.2	-185.5	-185.9	-184.8
Tri-TBM	C_1		-511.19400			-147.1	-145.5
Tri-TBM	C_3		-511.17276			-91.4	-89.7
Tetra-TBM	T		-668.06250			-28.3	-26.1
Tetra-TBM	T_d		-667.99310			153.9	156.1

[a] To obtain these ΔH_{f0} values, we require the E_0 values of the TBM molecules and the E_0 values of the constituent atoms. At the G3 level, the E_0 values for C and H are -37.82772 and -0.50100 hartrees, respectively. At the G3(MP2) level, the corresponding values are -37.78934 and -0.50184 hartrees.

[b] To obtain these ΔH_{f0} values, we require the E_0 values of CH_4 (-40.45762 hartrees) and C_2H_6 (-79.72339 hartrees) at the G3 level. At the G3(MP2) level, the corresponding values are -40.42210 and -79.65120 hartrees.

Table 3: The Enthalpies at 298 K (H_{298}) and the Heats of Formation (kJ mol^{-1}) at 298 K (ΔH_{f298}) for Mono-TBM, Di-TBM, Tri-TBM, and Tetra-TBM calculated at the G3 and G3(MP2) Levels Using the Atomization and Isodesmic Schemes

		H_{298} G3	H_{298} G3(MP2)	$\Delta H_{f298}{}^{a}$ G3 (Atomization)	$\Delta H_{f298}{}^{b}$ G3 (Isodesmic)	$\Delta H_{f298}{}^{a}$ G3(MP2) (Atomization)	$\Delta H_{f298}{}^{b}$ G3(MP2) (Isodesmic)	ΔH_{f298} (Expt.)
Mono-TBM	T_d	-197.53585	-197.35354	-168.3 **-170.0** *-170.6*	-169.3	-167.0 **-168.7** *-169.3*	-169.0	-167.9 ± 0.63[c]
Di-TBM	C_2	-354.61186	-354.28276	-245.2 **-248.3** *-249.1*	-248.3	-243.9 **-247.0** *-247.9*	-247.6	-241.5 ± 1.5[d]
Di-TBM	C_{2v}	-354.61169	-354.28259	-244.8 **-247.8** *-248.7*	-247.9	-243.5 **-246.6** *-247.4*	-247.2	
Tri-TBM	C_1		-511.17585			-226.0 **-230.4** *-231.6*	-231.4	-235.2 ± 4.3[e]
Tri-TBM	C_3		-511.15462			-170.3 **-174.7** *-176.0*	-175.7	
Tetra-TBM	T		-668.04061			-133.7 **-139.5** *-141.1*	-140.9	
Tetra-TBM	T_d		-667.95964			78.9 **73.1** *71.5*	71.7	

[a] We use equations (1), (2) and (3) of the atomization scheme to obtain the ΔH_{f298} values shown in normal font, bold font and italic font, respectively. For the calculation of these values, we need the H_{298} values listed in the table and also the H_{f298} values for the constituent atoms.

[b] To obtain these ΔH_{f298} values, we require the H_{298} values of CH_4 (−40.45381 hartrees) and C_2H_6 (−79.71891 hartrees) at the G3 level. At the G3(MP2) level, the corresponding values are −40.41828 and −79.64672 hartrees.

[c] Ref. 22.

[d] Ref. 27.

[e] Ref. 28.

Table 4: Structural Parameters (in Å and Degrees) of Mono-TBM, Di-TBM, Tri-TBM, and Tetra-TBM Optimized at the MP2(Full)/6-31G(d) Level

Parameter	Calculated	Calculated	Experimental[a]	Other[b]
Mono-*tert*-butylmethane T_d				
$C_t–C_m$	1.528		1.537±0.003	
$C_m–H_m$	1.095		1.114±0.008	
$C_mC_tC_m$	109.5			
$C_tC_mH_m$	110.9		112.2±2.8	
$H_mC_mH_m$	108.0			
Di-*tert*-butylmethane				
	C_2	C_{2v}		
$C_t–C_q$[c]	1.547	1.546	1.545 ave	1.552
$C_q–C_m$[d]	1.534	1.535	1.545 ave	1.537
	1.532	1.530		
	1.528			
$C_t–H_t$	1.100	1.101	1.122 ave	1.100 ave
$C_m–H_m$	1.095	1.095	1.122 ave	1.100 ave
	1.095	1.095		
	1.095	1.095		
	1.096	1.096		
	1.095	1.095		
	1.093	1.091		
	1.096			
	1.096			
	1.090			
$H_tC_tH_t$	105.3	105.4	105.0	
$C_qC_tC_q$	124.6	126.0	125-128	
$C_tC_qC_m$	106.0	105.4	106.4	105.6
	112.1	113.3	112.6	114.9
	113.8		115.2	112.0
$C_qC_mH_m$	110.7	110.6		
	110.8	111.2		
	111.3			
$C_qC_tC_qC_m$	167.6	180.0		

Parameter	Calculated	Calculated	Experimental[e]	Other[b]
	Tri-*tert*-butylmethane			
	C_1	C_3		
$C_t–C_q{}^c$	1.600	1.622	1.611±0.005	1.618
	1.600			
	1.600			
$C_q–C_m{}^d$	1.537	1.535	1.548 ave	1.544
	1.543	1.548		1.553
	1.548			1.565
$C_t–H_t$	1.102	1.105	1.111 ave	1.088
$C_m–H_m$	1.084	1.084	1.111 ave	1.077-1.087
	1.095	1.093		
	1.096	1.089		
	1.095	1.096		
	1.093			
	1.087			
	1.091			
	1.089			
	1.096			
$C_qC_tC_q$	115.2	115.7	116.0±0.4	115.5
$C_tC_qC_m$	110.9	113.2	113.0 ave	110.6
	114.7	116.2		114.1
	114.1			114.8
$C_mC_qC_m$	108.8	105.7	105.8 ave	101.8
	101.7	101.6		105.9
	105.7			108.8
$C_qC_mH_m$	111.7	112.5	114.2 ave	108.7
	107.7	108.3		109.1
	114.3	113.6		109.6
	114.9	112.9		111.4
	109.0	108.3		112.0
	110.6			112.1
	113.3			114.0
	112.1			114.3
	108.8			115.4
$C_qC_tH_t$	102.9	102.1	101.6	102.4
$H_mC_mH_m$	107.1	107.2		104.5
	109.1	109.2		105.1
	106.5	105.6		106.6
	106.5	108.4		106.7
	108.3	107.0		107.1
	107.3			107.2
	107.9			107.4
	107.0			108.3
	107.4			109.5
$C_mC_qC_tH_t$	39.1	57.5		

Table 4: (continued)

Parameter	Calculated	Calculated	Experimental	Other[b]
	Tetra-*tert*-butylmethane			
	T	*T$_d$*		
C_t–C_q [c]	1.661	1.723		1.683
C_q–C_m [d]	1.553	1.554		1.565
C_m–H_m	1.087	1.081		1.074-1.088
	1.095	1.093		
	1.084			
$C_q C_t C_q$	109.4	109.4		
$C_t C_q C_m$	115.7	117.0		115.9
$C_m C_q C_m$	102.6	100.9		102.4
$C_q C_m H_m$	107.1	106.5		107.6
	113.5	114.6		114.0
	114.5			116.2
$H_m C_m H_m$	106.1	105.5		105.2
	106.5	108.8		105.4
	108.5			107.5
$H_m C_m C_q H_m$	116.7	116.5		
	117.8			
$C_m C_q C_t C_q$	75.9	60.0		

[a] Ref. 8.

[b] Data for mono- and di-TBM are experimental results taken from ref. 24. Data for tri- and tetra-TBM are spectroscopically determined force field (SDFF) results taken from ref. 5.
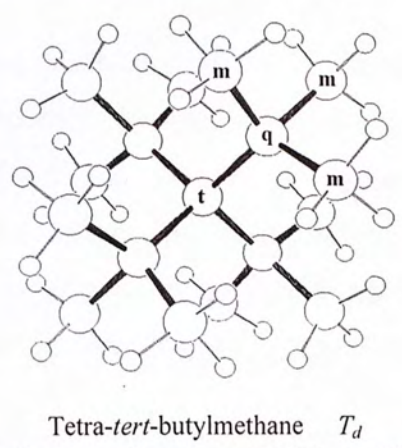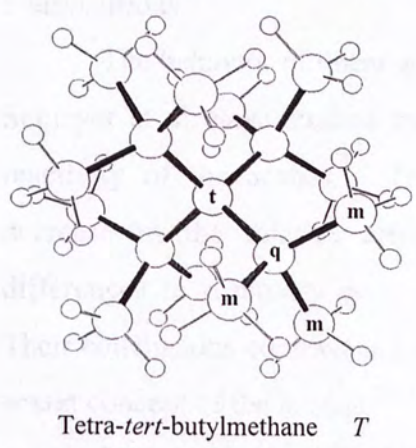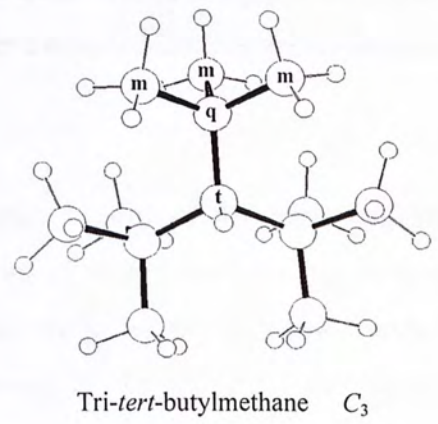
[c] t = tertiary, q = quaternary.

[d] m = methyl.

[e] Ref. 3.

Mono-*tert*-butylmethane T_d

Di-*tert*-butylmethane C_2

Di-*tert*-butylmethane C_{2v}

Tri-*tert*-butylmethane C_1

Tri-*tert*-butylmethane C_3

Tetra-*tert*-butylmethane T
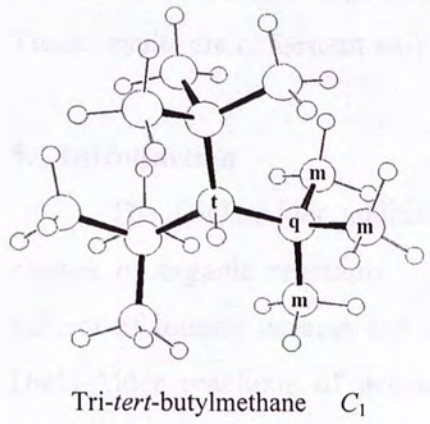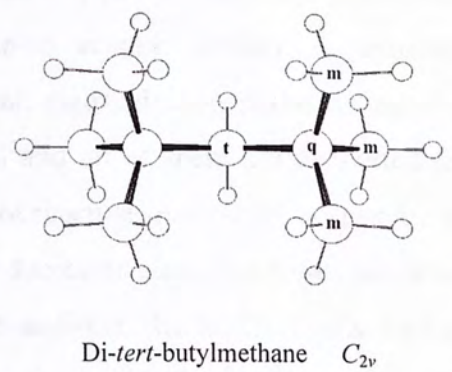
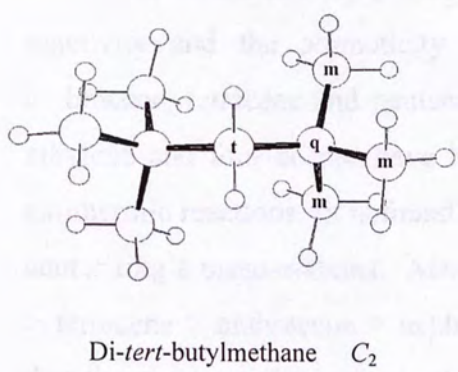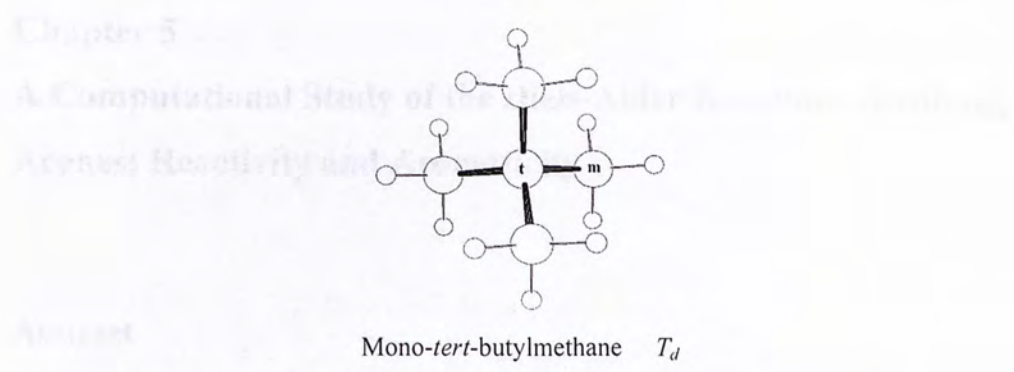Tetra-*tert*-butylmethane T_d

Figure 1. The molecular structures and labeling of atoms for mono-TBM, di-TBM, tri-TBM, and tetra-TBM.

Chapter 5

A Computational Study of the Diels-Alder Reactions Involving Acenes: Reactivity and Aromaticity

Abstract

Ab initio and DFT methods have been used to study the Diels-Alder reactivity and the aromaticity of four linear acenes, namely, naphthalene, anthracene, tetracene and pentacene. In total, eight addition pathways between ethylene and four acenes have been studied and all of them are concerted and exothermic reactions. It is found that the most reactive sites on the acenes are the center ring's meso-carbons. Also, reactivity decreases along the series pentacene > tetracene > anthracene > naphthalene. In addition, the NICS results indicate that the most reactive rings in the acenes are those with the highest aromaticity. These results are consistent with those of other theoretical studies and experiment.

5.1 Introduction

The Diels-Alder addition reactions may be one of the most important classes of organic reactions. The mechanism of these reactions has been the subject of intense interest and debate. In this work, we are concerned with the Diels-Alder reactions of acenes, which belong to the group of the aromatic hydrocarbons.

The behavior of linear acenes poses many unsolved problems.[1-7] Recently, Schleyer et al. have studied the relationship between aromatic stabilization and reactivity of the acenes.[8] Their results indicate that there is no significant decrease in the relative aromatic stabilization along the acene series: the differences in reactivity depend on the change of aromaticity during reaction. Their conclusions contravened several early MO treatments and Clar's qualitative sextet concept of the acenes.[1,2,9]

In the present work, the Diels-Alder reactivity and the aromaticity of four linear acenes, naphthalene, anthracene, tetracene and pentacene, are studied. The total energies of stationary points for the reactions between the acenes and ethylene are calculated at the MP2(Full)/6-31G(d) level.[10] In addition, we also

49

study the Diels-Alder reactivity and aromaticity of acenes by means of the reaction energetics and the NICS index.[11] The NICS (Nucleus Independent Chemical Shifts) index is a descriptor of aromaticity from the magnetic point of view. Our calculated results are in general accord with those of Schleyer's work.

5.2 Methods of Calculation and Results

All calculations were carried out on various workstations using the Gaussian 98 package of programs.[12] The structures of all the species studied in this work were optimized at the B3LYP/6-31G(d)[13,14] and MP2(Full)/6-31G(d) levels, while vibrational frequencies were calculated at the B3LYP/6-31G(d) level. The frequency calculations were used to characterize the stationary points. In addition, the transition structures (TSs) of the eight reactions were also confirmed by intrinsic reaction coordinate[15,16] calculations.

The NICS calculations were carried out in order to study the aromaticity of individual rings of the four acenes and the eight acene adducts. The NICS – defined as a negative value of the absolute shielding – was computed at the ring centers at the HF/6-31+G(d) level of theory using the GIAO[17] method, based on the structure optimized at the B3LYP/6-31G(d) level. The aromatic rings are those rings with negative NICS values: the more negative the index, the more aromatic the system. It is known that NICS values are not very sensitive to the basis set and the use of 6-31+G(d) is recommended.[11]

Figure 1 shows the structures of ethylene (**1**), naphthalene (**2**), anthracene (**3**), tetracene (**4**), pentacene (**5**) and the eight acene adducts. Also, the rings of the acenes and their adducts are labeled. In Figure 2, the eight acene addition reaction pathways studied in this work are shown. The optimized products and TSs of the Diels-Alder reactions between the acenes and ethylene with selected structural parameters (in Å and degrees) are displayed in Figure 3.

Table 1 lists the total energies for the stationary points for the Diels-Alder reactions between the acenes and ethylene. In Table 2, the barriers and the exothermicities of the eight reactions, calculated at the MP2(Full)/6-31G(d) level, are listed. The NICS values of the acenes and their adducts are tabulated in Table 3.

5.3 Discussion

In Table 3, we see that the aromaticity of the rings in acenes **2, 3, 4** and **5** increases along the series A < B < C. In other words, the center ring is always the most aromatic one. In addition, the aromaticity of the center ring increases when the ring number of the acene increases. The NICS values presented here are in agreement with other theoretical calculations.[11,18] After the addition of ethylene into the four acenes, the aromaticity of the ring with ethylene decreases sharply, as expected. The aromaticity of the ring next to the reacted ring may increase or decrease, depending on whether it is the outermost ring or not. If it is the outermost ring, the aromaticity will increase. For example, ring A in **3b** has a NICS value of −10.1, compared to −8.3 in **3**. On the other hand, if the neighboring ring is not the outermost one, the aromaticity will decrease or remain unchanged. For example, ring B in **3a** has a NICS value of −10.0, compared to −13.3 in **3**. The loss of aromaticity of the reacted ring has also been pointed out by Manoharan et al.[19] However, Clar's sextet theory,[1,2] which says that the increasing reactivity going from anthracene to hexacene is due to a gradual loss of benzenoid character of the acenes. Based on our calculations, we can see that the benzenoid character does not decrease from naphthalene (**2**) to pentacene (**5**). Instead, the benzenoid character shifts to the inner ring from the outer ring of acenes, i.e., the inner ring is more aromatic than the outer rings. These results are in agreement with Schleyer's work.[8]

All the additions studied in this work are exothermic and concerted reactions. The TSs shown in Fig. 3 indicate that the two new C–C bonds in each reaction are formed synchronously. In the TSs, the C⋯C distances for the bonds about to be formed are in the range between 2.177 and 2.342 Å, with the longest distance being found in **5c-TS**, which is 2.342 Å. This implies that reaction **5c** (addition of ethylene to the center ring of pentacene) has the earliest TS. On the other hand, reaction **2a** (addition of ethylene into naphthalene) has the latest TS, the corresponding C⋯C distance in **2a-TS** is 2.177 Å. For other TSs, the respective C⋯C distances are: 2.197 Å in **3a-TS**, 2.269 Å in **3b-TS**, 2.205 Å in **4a-TS**, 2.302 Å in **4b-TS**, 2.208 Å in **5a-TS** and 2.315 Å in **5b-TS**. We see that these C⋯C distances in the TSs correlate well with the aromaticity of the acenes: the more aromatic the ring of the acenes, the longer the C⋯C distances in the TSs.

Examining Table 2, it is found that the reaction with the largest exothermicity and the smallest barrier among the eight reactions studied is **5c**, with the ethylene molecule attacking the center ring of pentacene. This implies that this reaction is most favored energetically. When we compare the reactions of **3a** and **3b**, we find that **3b** is more favored. In other words, among the five rings in pentacene, the most aromatic (center) ring is also the most reactive. At the same time, its neighboring rings are less reactive, and the outer rings are least reactive. For tetracene, again the two center rings are more reactive than the outer rings. For anthracene, the center ring is also more reactive than the outer rings. On comparing the reactivity of the acenes, we find that reactivity decreases along the series pentacene > tetracene > anthracene > naphthalene. Interestingly, we find that the reactivity of acenes is related to their aromaticity. When the aromaticity of an individual ring is high, its Diels-Alder reaction will have a larger exothermicity and smaller barrier. Therefore, the most reactive rings in the acenes are those with the highest aromaticity.

In a complementary study, an Natural Bond Orbital (NBO)[20] analysis shows that the acenes studied in this work have strongly delocalized structures and the four carbon atoms next to the meso-carbons of the inner ring have the smallest natural charges. These results imply that these four carbons in the inner ring are electron-deficient. Therefore the addition of ethylene at the meso-carbons of the inner ring stabilizes the ring and reduces the electron-deficiency of the four carbon atoms. These results are in accord with the findings of Schleyer et al.[8] that the coefficients of the HOMOs are "consistent with the regioselectivity of Diels-Alder reactions that prefer the middle rings (despite their greater aromaticity)."

Finally, we compare our calculated results with experiments. Aromatic systems such as benzene and naphthalene are relatively unreactive when normal dienophiles are used, but with the highly reactive dicyanoacetylene they give [4+2] cycloadducts.[21] In 1979, Biermann and Schmidt[5] studied the Diels-Alder reactivity of polycyclic aromatic hydrocarbons. They measured the rates of reaction of 21 acene-type hydrocarbons with excess maleic anhydride at 91.5 °C in 1,2,4-trichlorobenzene. They found that anthracene, tetracene and pentacene, among others, react cleanly under these conditions, while benzene and naphthalene show no noticeable Diels-Alder reactivity. The measured second-

order rate constants (in L M^{-1} s^{-1}) of the reactions involving anthracene, tetracene and pentacene are 2.27×10^{-3}, 9.42×10^{-2} and 1.64, respectively. Additionally, they found that the most reactive positions of the linear acenes are the meso-carbons of the inner ring in each acene. These experimental outcomes are in total accord with the computational results reported here.

5.4 Conclusion

In this work, we study the reactivity and aromaticity of four linear acenes and eight acene adducts. It is found that all eight reactions are concerted and exothermic. The most favorable reaction pathway is **5c**, with ethylene adding to the center ring of pentacene. Also, the reactivity of an acene increases with the number of rings in the molecule. For each acene, the most reactive sites of reaction are the center ring's meso-carbons.

In addition, the NICS method is used to study the aromaticity of the acenes. It is found that the aromaticity of these systems increases with the increase in the number of rings. The NICS values show that the center rings in linear acenes are more aromatic than the outer ones, i.e, the most reactive ring in each acene is also the most aromatic one. Furthermore, the aromaticity of the outer rings decreases rapidly with increasing number of rings. Additionally, the aromaticity of the acene Diels-Alder adducts is also studied. The results reported here are in accord with those of Schleyer et al.[8] They are also consistent with the results of the experimental studies involving acenes and maleic anhydride.

5.5 Publication Note

An article based on the results reported in this Chapter has now appeared: Cheng, M.-F.; Li, W.-K., A computational study of the Diels-Alder reactions involving acenes: reactivity and aromaticity, *Chem. Phys. Lett.* **2003**, *368*, 630.

5.6 References

(1) Clar, E. Polycyclic Hydrocarbons, Academic Press, London, 1964.

(2) Clar, E. The Aromatic Sextet, Wiley, London, 1972.

(3) Bjorseth, A. Ed. Handbook of Polycyclic Aromatic Hydrocarbons, Dekker, New York, 1983.

(4) Cooke, M.; Dennis, A. J. Eds. Polynuclear Aromatic Hydrocarbons: A Decade of Progress, Battelle Press, Columbus, 1988.

(5) Biermann, D.; Schmidt, W. J. *J. Am. Chem. Soc.* **1980**, *102*, 3163.

(6) Biermann, D.; Schmidt, W. J. *J. Am. Chem. Soc.* **1980**, *102*, 3173.

(7) Harvey, R. G. Polycyclic Aromatic Hydrocarbons, Wiley-VCH, New York, 1997.

(8) Schleyer, P. v. R.; Manoharan, M.; Jiao, H.; Stahl, F. *Org. Lett.* **2001**, *3*, 3643.

(9) Suresh, C. H.; Gadre, S. R. *J. Org. Chem.* **1999**, *64*, 2505.

(10) Hehre, W. J.; Radom, L.; Schleyer, P. v. R.; Pople, J.A. Ab Initio Molecular Orbital Theory, Wiley, New York, 1986.

(11) Schleyer, P. v. R.; Maerker, C.; Dransfeld, A.; Jiao, H.; Hommes, N. J. R. v. E. *J. Am. Chem. Soc.* **1996**, *118*, 6317.

(12) Frisch, M. J.; Trucks, G. W.; Schlegel, H. B.; Scuseria, G. E.; Robb, M. A.; Cheeseman, J. R.; Zakrzewski, V. G.; Montgogery, J. A.; Jr.; Stratmann, R.E.; Burant, J. C.; Dapprich, S.; Millam, J. M.; Daniels, A. D.; Kudin, K. N.; Strain, M. C.; Farkas, O.; Tomasi, J.; Barone, V.; Cossi, M.; Cammi, R.; Mennucci, B.; Pomelli, C.; Adamo, C.; Clifford, S.; Ochterski, J.; Petersson, G. A.; Ayala, P. Y.; Cui, Q.; Morokuma, K.; Malick, D. K.; Rabuck, A. D.; Raghavachari, K.; Foresman, J. B.; Cioslowski, J.; Ortiz, J. V.; Baboul, A. G.; Stefanov, B. B.; Liu, G.; Liashenko, A.; Piskorz, P.; Komaromi, I.; Gomperts, R.; Martin, R. L.; Fox, D. J.; Keith, T.; Al-Laham, M. A.; Peng, C. Y.; Nanayakkara, A.; Gonzalez, C.; Challacombe, M.; Gill, P. M. W.; Johnson, B.; Chen, W.; Wong, M. W.; Andres, J. L.; Gonzalez, C.; Head-Gordon, M.; Replogle, E. S.; Pople, J. A. *GAUSSIAN 98*, Revision A.11; Gaussian, Inc., Pittsburgh PA, 1998.

(13) Becke, A. D. *J. Chem. Phys.* **1993**, *98*, 5648.

(14) Lee, C.; Yang, W.; Parr, R. G. *Phys. Rev. B* **1988**, *37*, 785.

(15) Gonzalez, C.; Schlegel, H. B. *J. Chem. Phys.* **1989**, *90*, 2154.

(16) Gonzalez, C.; Schlegel, H. B. *J. Phys. Chem.* **1990**, *94*, 5523.

(17) Wolinski, K.; Hinton, J. F.; Pulay, P. *J. Am. Chem. Soc.* **1990**, *112*, 8251.

(18) Cyrański, M. K.; Stępień B. T.; Krygowski, T. M. *Tetrahedron* **2000**, *56*, 9663.

(19) Manoharan, M.; Proft, F. D.; Geerlings, P. *Perkin Trans. 2* **2000**, 1767.

(20) Reed, A. E.; Curtiss, L. A.; Weinhold, F. *Chem. Rev.* **1988**, *88*, 899.

(21) Ciganek, E. *Tetrahedron Lett.* **1967**, *34*, 3321.

Table 1: Total Energies for Stationary Points for the Diels-Alder Reactions between the Acenes and Ethylene

Species	Point Group	Total Energy (Hartree) B3LYP/6-31G(d)	Total Energy (Hartree) MP2(Full)/6-31G(d)
Reactant:			
1	D_{2h}	-78.58746	-78.29429
2	D_{2h}	-385.89273	-384.66460
3	D_{2h}	-539.53052	-537.83601
4	D_{2h}	-693.16581	-691.00509
5	D_{2h}	-846.79994	-844.17329
Product:			
2a	C_s	-464.48414	-462.98954
3a	C_s	-618.12931	-616.16875
3b	C_{2v}	-618.14900	-616.19293
4a	C_s	-771.76772	-769.34073
4b	C_s	-771.79391	-769.37225
5a	C_s	-925.40335	-922.51003
5b	C_s	-925.43221	-922.54428
5c	C_{2v}	-925.43876	-922.55169
Transition State:			
2a-TS	C_s	-464.42590	-462.92508
3a-TS	C_s	-618.06710	-616.10004
3b-TS	C_{2v}	-618.07602	-616.11135
4a-TS	C_s	-771.70382	-769.27036
4b-TS	C_s	-771.71528	-769.28431
5a-TS	C_s	-925.33864	-922.43901
5b-TS	C_s	-925.35126	-922.45410
5c-TS	C_{2v}	-925.35414	-922.45758
Reactants:			
2 + 1		-464.48019	-462.95889
3 + 1		-618.11798	-616.13030
4 + 1		-771.75327	-769.29938
5 + 1		-925.38740	-922.46758

Table 2: Barriers and Exothermicities of the Diels-Alder Reactions between the Acenes and Ethylene Calculated at the MP2(Full)/6-31G(d) Level

Reaction	Barrier (kJ mol^{-1})	Exothermicity (kJ mol^{-1})
2a	88.8	-80.5
3a	79.4	-101.0
3b	49.8	-164.4
4a	76.2	-108.6
4b	39.6	-191.3
5a	75.0	-111.5
5b	35.4	-201.4
5c	26.3	-220.8

Table 3: GIAO-SCF Calculated NICSs (ppm) for the Acenes and Acene Adducts

Species		Ring	Point group	NICS 6-31+G(d)[a]	NICS 6-31+G(d)[b]	NICS 6-31+G(d)[c]
Benzene			D_{6h}	-9.7	-9.7	
Naphthalene **2**		A	D_{2h}	-10.0	-9.9	
2a,	ring with C_2H_4	A	C_s	-2.5		
	ring without C_2H_4	B		-10.2		
Anthracene **3**,	outer ring	A	D_{2h}	-8.3	-8.2	
	central ring	B		-13.3	-13.3	
3a,	ring with C_2H_4	A	C_s	-1.9		
	central ring	B		-10.0		
	outer ring	C		-10.2		
3b,	outer ring	A	C_{2v}	-10.1		
	ring with C_2H_4	B		-1.0		
Tetracene **4**,	outer ring	A	D_{2h}	-6.8		-7.1
	central ring	B		-13.1		-13.4 .
4a,	ring with C_2H_4	A	C_s	-1.7		
	central ring	B		-8.2		
	central ring	C		-13.1		
	outer ring	D		-8.6		
4b,	outer ring	A	C_s	-10.0		
	ring with C_2H_4	B		-0.4		
	central ring	C		-9.8		
	outer ring	D		-10.1		
Pentacene **5**,	outer ring	A	D_{2h}	-5.5		-5.8
	middle ring	B		-12.0		-12.4
	central ring	C		-14.3		-14.6
5a,	ring with C_2H_4	A	C_s	-1.7		
	middle ring	B		-6.6		
	central ring	C		-12.6		
	middle ring	D		-13.2		
	outer ring	E		-6.9		
5b,	outer ring	A	C_s	-10.0		
	ring with C_2H_4	B		-0.3		
	central ring	C		-8.0		
	middle ring	D		-13.0		
	outer ring	E		-8.5		
5c,	outer ring	A	C_{2v}	-10.1		
	middle ring	B		-9.8		
	ring with C_2H_4	C		0.1		

[a] HF/6-31+G(d) NICS calculations based on the B3LYP/6-31G(d) structures.
[b] Values taken from ref. 11.
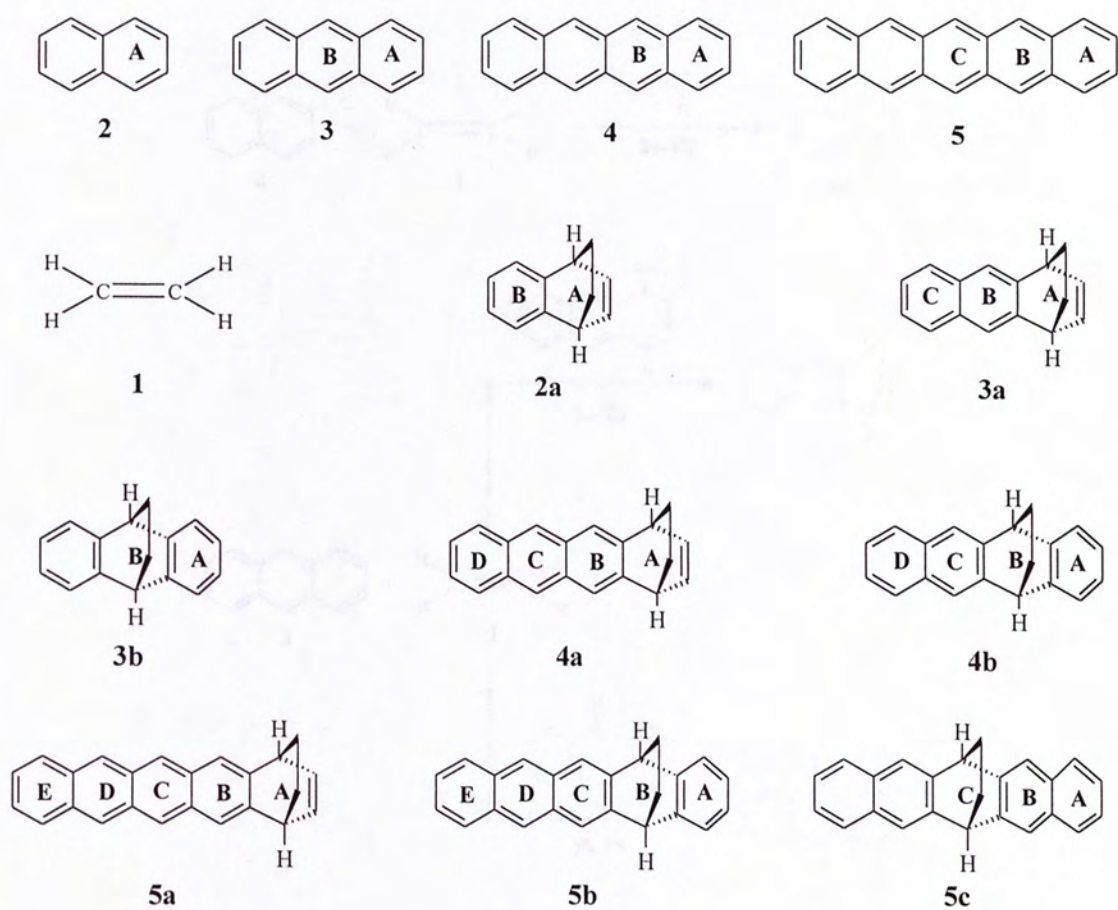[c] Values taken from ref. 18.

Figure 1. Labeling of the rings in the acenes and acene adducts studied in this work.
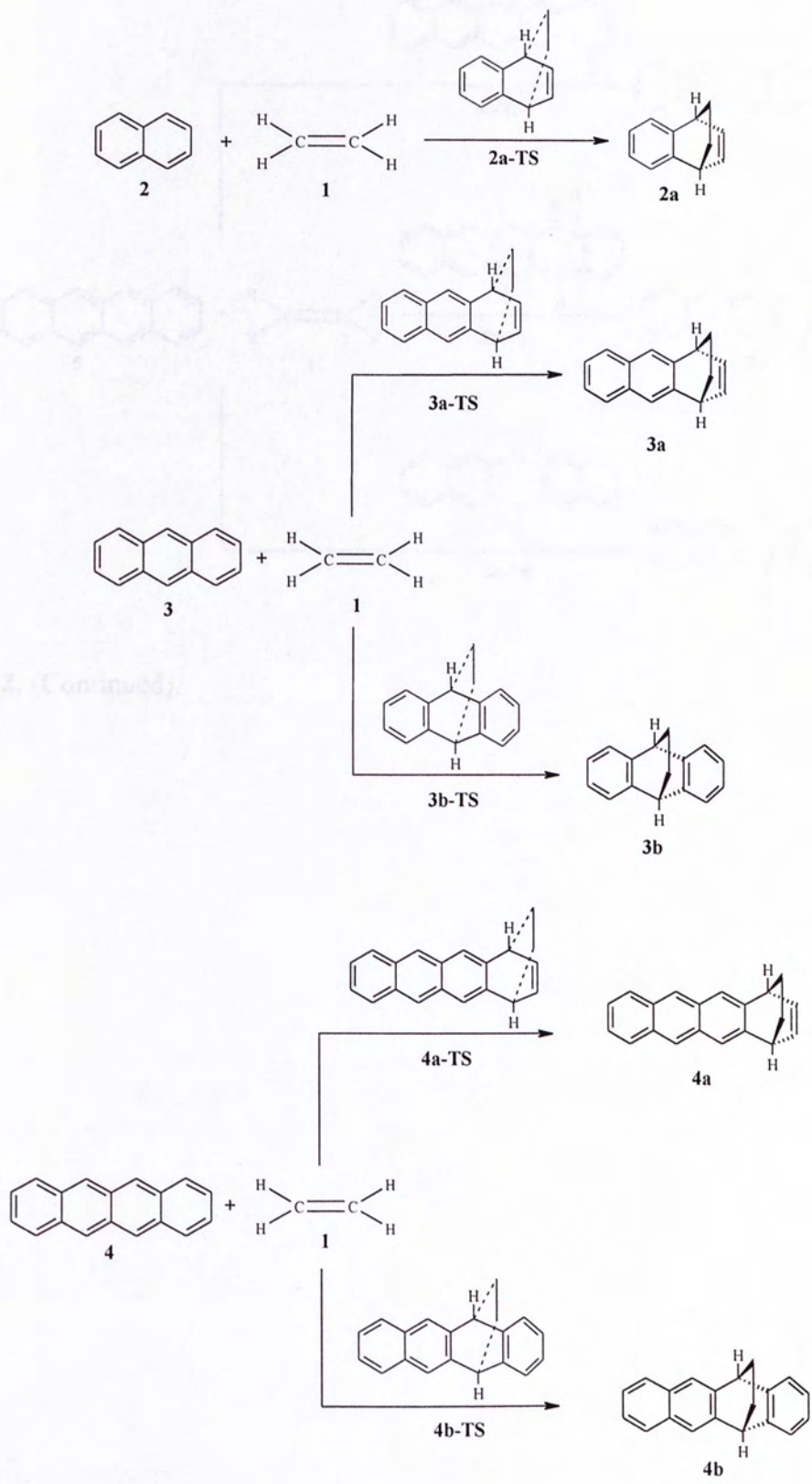
Figure 2. The reaction pathways between the acenes and ethylene studied in this work.
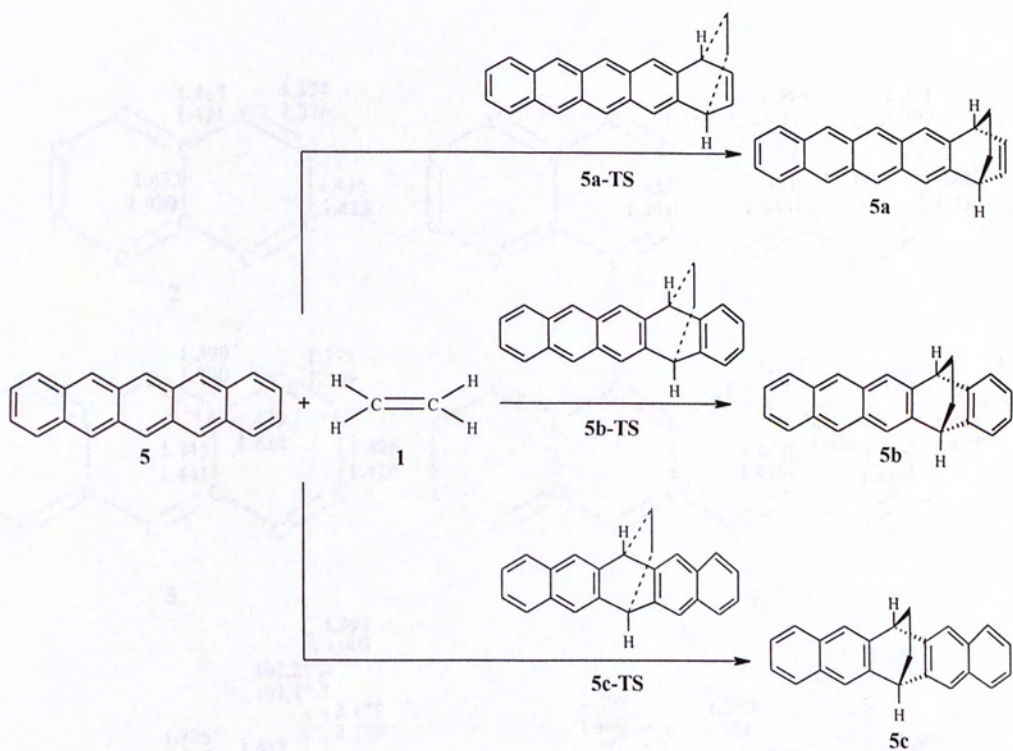
Figure 2. (Continued).

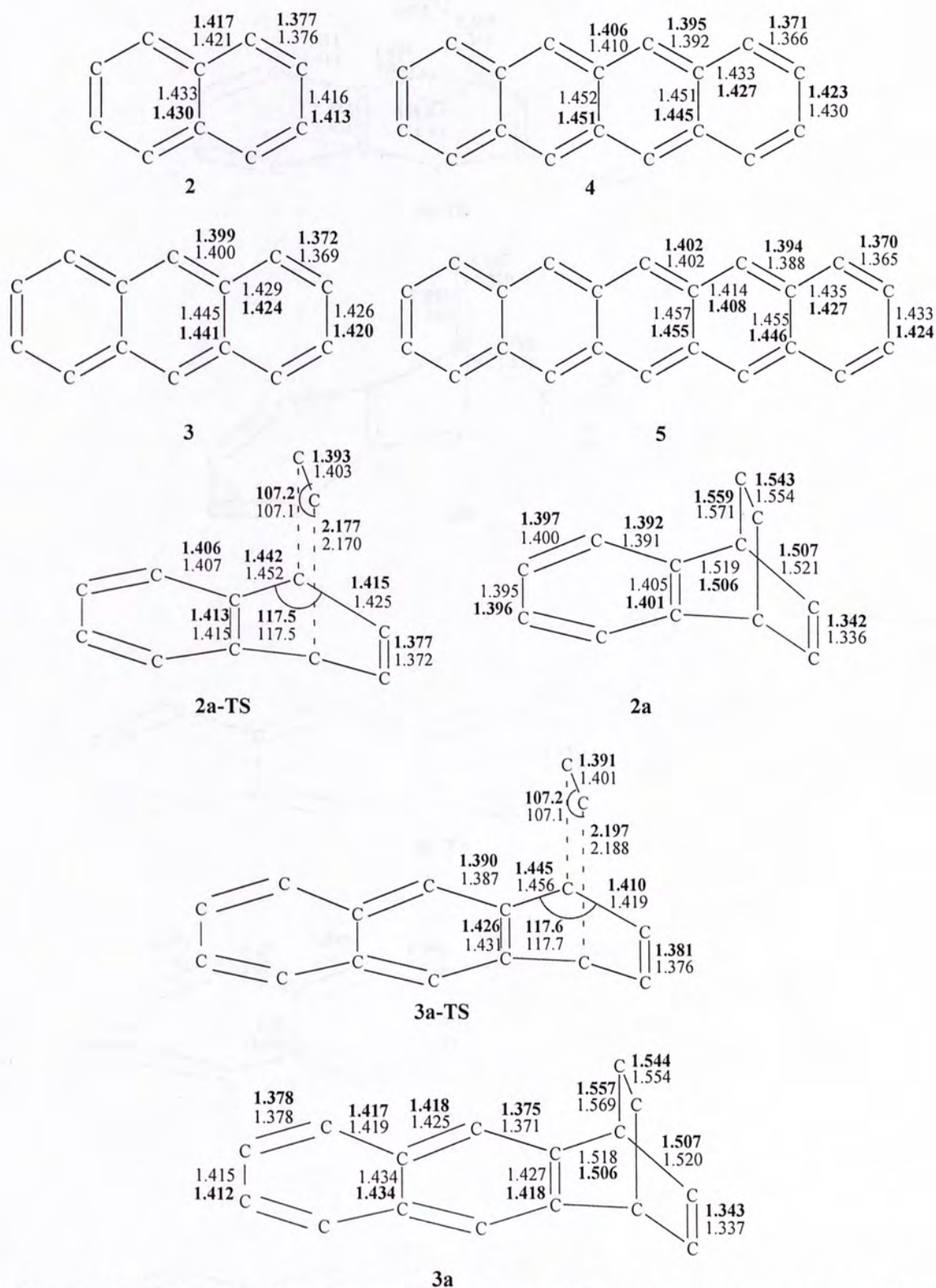**Figure 3.** Optimized products and TSs of the Diels-Alder reactions between the acenes and ethylene with selected structural parameters (in Å and degrees). The B3LYP/6-31G(d) and MP2(Full)/6-31G(d) values are given in normal type and bold font, respectively.
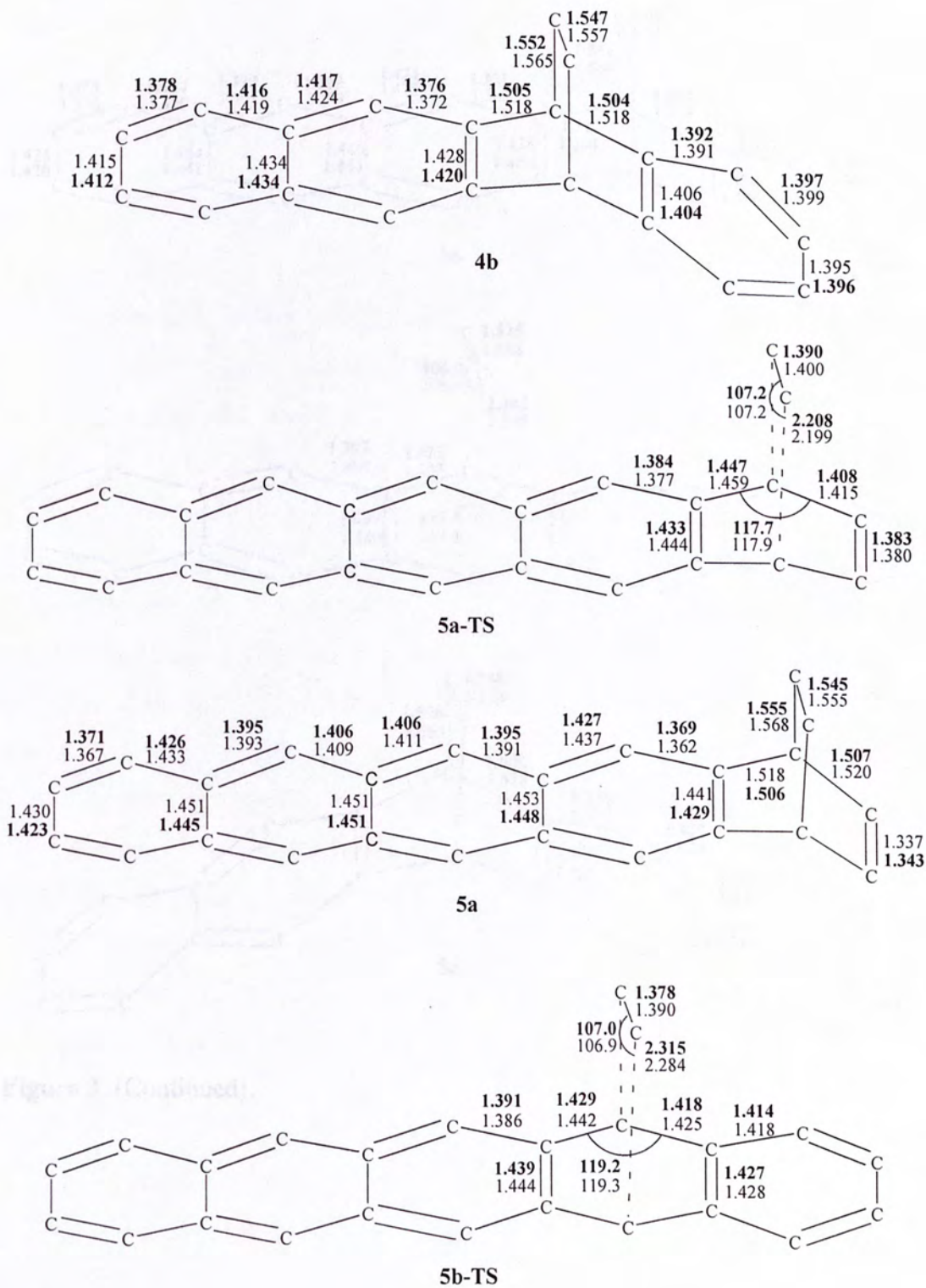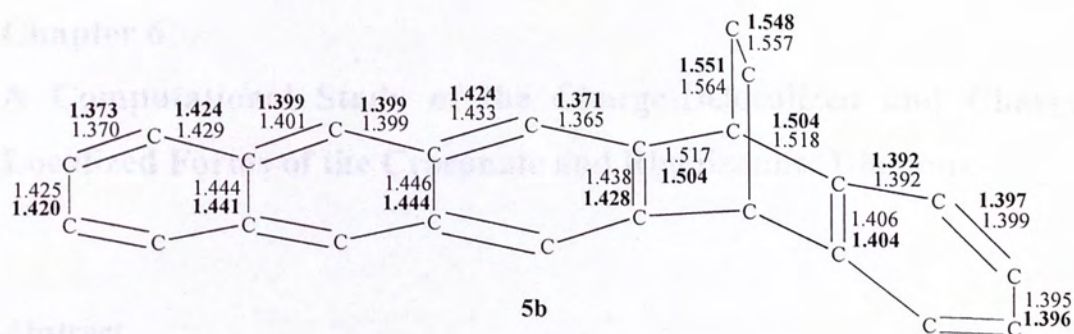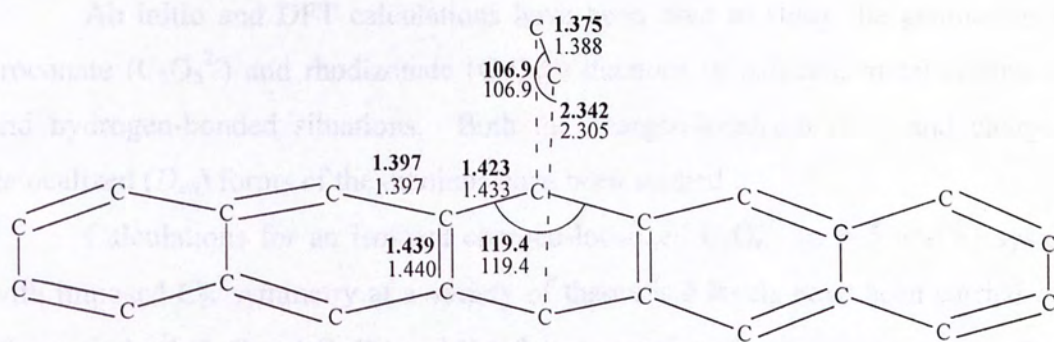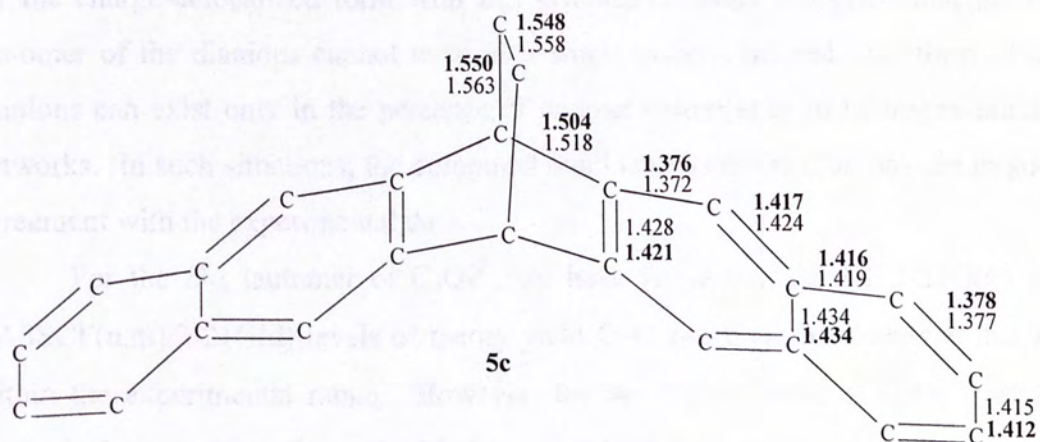
3b-TS

3b

4a-TS

4a

4b-TS

Figure 3. (Continued).

62

Figure 3. (Continued).

5b

106.9
106.9

2.342
2.305

5c-TS

5c

Figure 3. (Continued).

Chapter 6

A Computational Study of the Charge-Delocalized and Charge-Localized Forms of the Croconate and Rhodizonate Dianions

Abstract

Ab initio and DFT calculations have been used to study the geometries of croconate ($C_5O_5^{2-}$) and rhodizonate ($C_6O_6^{2-}$) dianions in isolated, metal complexes and hydrogen-bonded situations. Both the charged-localized (C_{2v}) and charged-delocalized (D_{nh}) forms of the dianions have been studied.

Calculations for an isolated charged-localized $C_nO_n^{2-}$ (n = 5 and 6) system with imposed C_{2v} symmetry at a variety of theoretical levels have been carried out. The optimized C–C and C–O bond lengths are not significantly different from those for the charge-delocalized form with D_{nh} symmetry. Thus it appears that the C_{2v} tautomer of the dianions cannot exist as a single entity. Instead, this form of the dianions can exist only in the presence of counter cation(s) or in hydrogen-bonded networks. In such situations, the computed bond lengths of the dianions are in good agreement with the experimental data.

For the D_{5h} tautomer of $C_5O_5^{2-}$, we have found that the HF/3-21G(d) and CASSCF(n,m)/3-21G(d) levels of theory yield C–C and C–O bond lengths that are within the experimental range. However, for the D_{6h} tautomer of $C_6O_6^{2-}$, all the theoretical methods we have tried led to optimized C–C bond lengths that are too long.

6.1 Introduction

In the early 1960s, West et al. suggested that monocyclic oxocarbon dianions of general formula $C_nO_n^{2-}$ should constitute a new series of "aromatic" compound.[1] Here, the "oxocarbon" designates compounds in which all, or nearly all, of the carbon atoms are attached to carbonyl or enolic oxygens or to their hydrated equivalents.[2,3] The most famous monocyclic oxocarban species are the deltate ($C_3O_3^{2-}$), squarate ($C_4O_4^{2-}$), croconate ($C_5O_5^{2-}$) and rhodizonate ($C_6O_6^{2-}$) dianions. The IR and Raman spectra, along with the deduced force constants, indicated that $C_4O_4^{2-}$ and $C_5O_5^{2-}$ have D_{nh} symmetry,[4] and this was confirmed later by X-ray

analysis.[5,6] The Urey-Bradly force fields of $C_nO_n^{2-}$ (n = 3,[7] 4 and 5[4]) were compared with those of aromatic species such as benzene, the cyclopentadienyl anion, and the cyclopropenyl cation. The C–C stretching force constants for $C_4O_4^{2-}$ and $C_5O_5^{2-}$ are greater than those for a C–C single bond and those for the $C_3O_3^{2-}$ dianion are as large as those of benzene. This indicates extensive electron delocalization over the oxocarbon rings. The large delocalization energies estimated by West and Powell[8] were consistent with this observation.

However, Dewar et al.[9,10] and Hess and Schaad[11] pointed out that delocalization energy should not be used as a measure of aromatic stabilization. Almost all conjugated systems, even very labile ones, are known to have significant delocalization energies. Delocalization energies of familiar carbocyclic systems can seldom be arranged in the experimental order of stability.[12] The present consensus is that any aromaticity index of a cyclic conjugated system must be related to some thermodynamic stability estimated relative to an appropriate olefinic reference structure. Using graph theory, Aihara[13] calculated the topological resonance energy (TRE) and diamagnetic susceptibilities of $C_nO_n^{2-}$ and also found that the degree of aromaticity decreases with increasing ring size. This conclusion was supported further by the semiempirical and ab initio results on the IR frequencies and diamagnetic anisotropies of $C_nO_n^{2-}$ reported by Ha et al.[14] Jug also reached similar conclusions using bond orders as an alternative criterion.[15] In recent years, Schleyer et al. carried out ab initio calculation on $C_nO_n^{2-}$ (n = 3-6) and also concluded that the aromaticity decrease with increasing ring size.[16] They found that $C_3O_3^{2-}$, $C_4O_4^{2-}$ and $C_5O_5^{2-}$ have symmetries of D_{3h}, D_{4h} and D_{5h}, respectively, while $C_6O_6^{2-}$ has C_2 symmetry. Note that $C_nO_n^{2-}$ have only two π electrons assigned to the carbon rings, and one would expect decreasing aromaticity with the ring size on this basis.

Recently, Mak and co-workers reported that charged-localized (C_{2v}) and charged-delocalized (D_{nh}) forms of $C_5O_5^{2-}$ and $C_6O_6^{2-}$ dianions were generated and stabilized in a hydrogen-bonded host lattice. In addition, the structures of these dianions were determined by X-ray crystallography.[17,18]

The D_{5h} tautomer of $C_5O_5^{2-}$ has a charge-delocalized form and the measured C–C and C–O bond lengths fall in the ranges of 1.451-1.465 Å and 1.241-1.254 Å, respectively. The C_{2v} tautomer of $C_5O_5^{2-}$ is a charge-localized form with four long (1.451-1.465 Å) and one short (1.444 Å) C–C bonds and three short (1.232-1.247 Å)

and two long C–O (1.251 and 1.258 Å) bonds. The D_{5h} and C_{2v} structures correspond to the non-benzenoid aromatic and enediolate forms of the dianion, respectively. The measured structures of these tautomers are shown in Figure 1. In a recent theoretical study, Schleyer et al. studied the D_{5h} form of croconate dianion at the B3LYP/6-311+G(d) level and obtained optimized C–O bond length of 1.247 Å and C–C bond length of 1.488 Å. Compared to the data shown in Figure 1, the calculated C–C bond length deviates appreciably from the experimental results.[16] In addition, there has been no theoretical report on the C_{2v} tautomer.

Experimentally, the D_{6h} tautomer of the charge-delocalized $C_6O_6^{2-}$ has C–C and C–O bond lengths in the ranges of 1.440-1.442 Å and 1.245-1.246 Å, respectively. On the other hand, the C_{2v} tautomer of the charge-localized $C_6O_6^{2-}$ has five long (1.439-1.472 Å) and one short (1.404 Å) C–C bonds and four short (1.231-1.246 Å) and two long C–O (1.265 Å) bonds. Once again, the D_{6h} and C_{2v} structures correspond to the non-benzenoid aromatic and enediolate forms of the $C_6O_6^{2-}$ dianion, respectively. Also, the C–C bond length of about 1.500 Å optimized at the B3LYP/6-311+G(d) level by Schleyer et al.[16] is not in good agreement with experimental data, also shown in Figure 1. Furthermore, there has been no theoretical report on the C_{2v} tautomer of $C_6O_6^{2-}$.

In this work, our objectives are to computationally identify the experimentally found C_{2v} structures of the $C_5O_5^{2-}$ and $C_6O_6^{2-}$ dianions. Additionally, for the D_{5h} and D_{6h} structures of the dianions, we will attempt to find a theoretical level that would yield C–C bond lengths that are in better agreement with the experimental data than the previous calculated results.

6.2 Methods of Calculation and Results

All calculations were carried out using the Gaussian 98 program.[19] The charge-delocalized structures of the croconate and rhodizonate dianions have been studied at a variety of levels including HF, MP2, B3LYP, B3PW91, QCISD and CASSCF with a range of basis sets. The largest basis sets employed included 6-31+G(2df,p) and aug-cc-pvtz.

In addition to studying the isolated species of the charge-localized forms of the croconate and rhodizonate dianions, geometry optimizations and vibrational frequency calculations of the charge-localized forms of the dianions were also carried out in the presence of counter cations, either two Na^+ cations or one Ca^{2+} cation. The theoretical levels employed included HF/6-31G(d), MP2(Full)/6-31G(d), B3LYP/6-31G(d), and B3LYP/6-311+G(d).

Furthermore, geometry optimizations and vibrational frequency calculations of the 1:1 hydrogen-bonded adduct of urea with $C_nO_n^{2-}$, with imposed C_s, C_2 or C_{2v} symmetry, were carried out at the HF, B3LYP and MP2(Full) levels with different basis sets. Only the best results, obtained at the HF level, will be shown below.

Table 1 tabulates the optimized C–C and C–O bond lengths of the charge-delocalized forms of $C_5O_5^{2-}$ (D_{5h}) and $C_6O_6^{2-}$ (D_{6h}). Table 2 shows the results of Natural bond orbital (NBO) analysis[20] of the enol tautomers $C_5O_5^{2-}$ (C_{2v}) and $C_6O_6^{2-}$ (C_2). These NBO results were obtained from the studies of the complexes $Ca^{2+}[C_5O_5^{2-}]$ (C_{2v}) and $Ca^{2+}[C_6O_6^{2-}]$ (C_2) optimized at the MP2(Full)/6-31G(d) level. In Tables 3 and 4 the optimized C–C and C–O bond lengths of the charge-localized forms of $C_5O_5^{2-}$ (C_{2v}) and $C_6O_6^{2-}$ (C_{2v}) are listed. The optimized C–C and C–O bond lengths of the charge-localized form of $C_5O_5^{2-}$ with a hydrogen-bonded urea with imposed C_s, C_2 or C_{2v} symmetry are shown in Tables 5, 6 and 7, respectively. Furthermore, the optimized C–C and C–O bond lengths of the charge-localized form of $C_6O_6^{2-}$ with a hydrogen-bonded urea with imposed C_s, C_2 or C_{2v} symmetry are shown in Tables 8, 9 and 10, respectively.

Figure 1 summarizes the experimental results of the charge-localized forms and charge-delocalized forms of $C_5O_5^{2-}$ and $C_6O_6^{2-}$. Figure 2 displays the computed results of the charge-localized form of $C_5O_5^{2-}$ (C_{2v}) with metal cation(s) at different levels. Finally, the corresponding calculated results of the charge-localized form of $C_6O_6^{2-}$ (C_{2v}) with metal cation(s) are shown in Figure 3.

6.3 Discussion

6.3.1 Charge-Localized Forms of $C_5O_5^{2-}$ (C_{2v}) and $C_6O_6^{2-}$ (C_{2v})

The geometries of the charged-localized forms of the croconate and rhodizonate dianions in isolated, metal complex and hydrogen-bonded situations have been studied in this work. We have carried out calculations with a starting

model consisting of an isolated charged-localized $C_nO_n^{2-}$ (n = 5 and 6) system with imposed C_{2v} symmetry at a variety of theoretical levels, ranging from HF/STO-3G to MP2(Full)/6-31+G(2df,p). The optimized C–C and C–O bond lengths shown in Tables 3 and 4 fall in very narrow ranges. In fact, if we take only three decimal places for these bond lengths, the optimized $C_5O_5^{2-}$ structure has D_{5h} symmetry, while the optimized $C_6O_6^{2-}$ structure has D_{6h} symmetry, or very nearly so. In other words, it appears that both C_{2v} tautomer of the croconate or rhodizonate dianions cannot exist as a single entity.

On the other hand, in the presence of either two Na^+ cations or one Ca^{2+} cation, the enol tautomer of $C_5O_5^{2-}$ with C_{2v} symmetry has been identified and their optimized structures are shown in Figure 2. The charge-localized nature of $C_5O_5^{2-}$ is best exhibited in the $Ca^{2+}[C_5O_5^{2-}]$ complex, where we clearly see four long and one short C–C bonds and three short and two long C–O bonds, in qualitative agreement with the experimental range summarized in Figure 1. From the results obtained at the B3LYP/6-311+G(d) level, the five C–C bond lengths are 1.398, 1.468 (twice) and 1.540 (twice) Å, while the C–O bond lengths are 1.202, 1.213 (twice) and 1.318 (twice) Å. At the MP2(Full)/6-31G(d) level, there is one short C–C bond at 1.418 Å, and four long C–C bonds range from 1.463 to 1.523 Å; also there are two long C–O bonds at 1.324 Å and three short C–O bonds range from 1.225 to 1.233 Å. These calculated results are in good agreement with the structural data found in the $C_5O_5^{2-}$ moiety of the aqua-(croconato-O,O')-bipyridyl-copper complex,[21] as shown in Figure 2. There are other experimentally found examples of $C_5O_5^{2-}$ with a metal cation, such as $Fe^{2+}[C_5O_5^{2-}][22]$ and $Mn^{2+}[C_5O_5^{2-}][23]$ complexes. Since the structure of the $C_5O_5^{2-}$ moiety of the Cu(II) complex[21] is in better agreement with our calculated results than the Fe(II)[22] and Mn(II)[23] complexes, we only compare our calculated structure with the experimental data of the Cu(II) complex.[21] Furthermore, since the calculated and the experimental $C_5O_5^{2-}$ dianions are in different chemical environments, even though both of them are under the influence of a divalent cation, the computationally optimized C–C and C–O bond lengths are slightly different from the experimental data. But there is no question regarding the charge-localized nature of the $C_5O_5^{2-}$ calculated. To our knowledge, this is the first time that an enediolate tautomer of the croconate dianion has been computationally identified.

In the presence of either two Na^+ cations or one Ca^{2+} cation, the enol tautomer of $C_6O_6^{2-}$ with C_{2v} and C_2 symmetries have also been identified and their optimized structures are shown in Figure 3. The enol complex minimum has C_2 symmetry, while those structures with C_{2v} symmetry are transition states or higher order saddle points. The charge-localized nature of $C_6O_6^{2-}$ is best represented in the $Ca^{2+}[C_6O_6^{2-}]$ complex, where we clearly see five long and one short C–C bonds and four short and two long C–O bonds, in qualitative agreement with the experimental range[17] summarized in Figure 1. From the results obtained at the B3LYP/6-311+G(d) level, the six C–C bond lengths are 1.405, 1.472 (twice), 1.536 (twice) and 1.542 Å, while the C–O bond lengths are 1.204 (twice), 1.215 (twice) and 1.320 (twice) Å. At the MP2(Full)/6-31G(d) level, there is one short C–C bond at 1.420 Å, and five long C–C bonds range from 1.464 to 1.522 Å; also there are two long C–O bonds at 1.327 Å and four short C–O bonds range from 1.227 to 1.236 Å. Moreover, the complexes are not exactly planar, even though they are nearly so. Since we have not found experimental data on the $C_6O_6^{2-}$ dianion having similar chemical environment as the calculated $Ca^{2+}[C_6O_6^{2-}]$ complex, we may not compare these calculated results with experimental data.

We have also carried out an NBO analysis of the MP2 density of $Ca^{2+}[C_nO_n^{2-}]$. The results shown in Table 2 indicate that bonds C^4C^5, C^1O^6, C^2O^7 and C^3O^8 in $C_5O_5^{2-}$ tautomer have double bond character, while all others are single bonds. Similarly, for the $C_6O_6^{2-}$ tautomer, bonds C^1C^2, C^3O^9, C^4O^{10}, C^5O^{11}, and C^6O^{12} have double bond character, while all others are single bonds. The interaction energy arising from the electron donation to the σ^* orbital of the C^1C^2 bond of $C_5O_5^{2-}$ and C^5C^6 bond of $C_6O_6^{2-}$ are larger than those for the other bonds. This may be the reason why the C^1C^2 and C^5C^6 bonds are the longest.

In addition being stabilized in the presence of counter metal cation(s), as shown in the previous report, the C_{2v} tautomer of the $C_nO_n^{2-}$ dianion can also gain stabilization in a hydrogen-bonded lattice, as shown in previous reports.[17,18] In our calculations on the 1:1 hydrogen-bonded aggregate of urea with $C_nO_n^{2-}$ (n = 5 and 6) having C_s, C_2 or C_{2v} symmetry, we obtained very similar optimized structures. More importantly, the $C_nO_n^{2-}$ moiety exhibits the enediolate characteristics similar to those observed in experiment,[17,18] where the the C_{2v} tautomer of the $C_5O_5^{2-}$ dianion is hydrogen-bonded to three molecules of (N,N'-dimethyl)urea and the C_{2v} tautomer of

the $C_6O_6^{2-}$ dianion forms a hydrogen-bonded lattice with (3-hydroxyphenyl)urea in a 1:2 ratio. Upon comparing our optimized bond lengths for the 1:1 hydrogen-bonded aggregate of urea with $C_nO_n^{2-}$ with the experimental data summarized in Figure 1, it is seen that the best agreement is obtained by the relatively crude HF/3-21G(d) calculations for both the dianions. Higher-level computations invariably yield bond lengths that are too long for all the C–C bonds.

Results of NBO analysis lend additional credence to the charge-localized nature of the C_{2v} tautomers. In the 1:1 hydrogen-bonded aggregate of urea with $C_5O_5^{2-}$, the pair of O atoms in the hydrogen-bonded ring carry a higher negative charge of –0.759, whereas those on the remaining three O atoms range from –0.644 to –0.671. As a comparison, in the D_{5h} tautomer of $C_5O_5^{2-}$, the charges on each O and C atom are –0.716 and +0.316, respectively. Similarly, in the 1:1 hydrogen-bonded aggregate of urea with $C_6O_6^{2-}$, the pair of O atoms in the hydrogen-bonded ring again have a higher negative charge (–0.734) than the remaining four O atoms (ranging from –0.582 to –0.623). On the other hand, in the D_{6h} tautomer of $C_6O_6^{2-}$, the charges on each O and C have are –0.656 and +0.323, respectively. There is thus theoretical evidence for the charge-localized forms of the croconate and rhodizonate dianions in a hydrogen bonding environment.

In a complementary study, the natural charges of the X-ray structure of croconate dianion bounded by three (N,N'-1,3-dimethyl)urea molecules was also studied by NBO analysis. It was found that the pair of O atoms in the hydrogen-bonded ring carry a higher negative charge of -0.790, whereas those on the remaining three O atoms of $C_5O_5^{2-}$ range from –0.618 to –0.691. Therefore, the charge-localization is more pronounced in the (N,N'-1,3-dimethyl)urea adduct than that in the urea adduct.

6.3.2 Charge-Delocalized Forms of $C_5O_5^{2-}$ (D_{5h}) and $C_6O_6^{2-}$ (D_{6h})

In Table 1, we summarize the C–C and C–O bond lengths of the D_{nh} tautomer optimized at a large number of theoretical levels. As can be seen in the results for the D_{5h} tautomer of $C_5O_5^{2-}$, many of the optimized C–C bond lengths are about 0.01 to 0.03 Å too long, compared to the experimental range summarized in Figure 1. On the other hand, the optimized C–O bond lengths range from 0.01 to 0.02 Å too short (for levels with relatively large basis sets such as 6-31G(d),

6-31+G(d), 6-311+G(d), aug-cc-pvtz, etc.) and 0.01 to 0.04 Å too long (for most of the MP2 results). Among the 30 sets of results for $C_5O_5^{2-}$ listed in Table 1, the rather primitive HF/3-21G(d) level (C–C = 1.462 Å and C–O = 1.248 Å) or the much more sophisticated CASSCF(6,4)/3-21G(d) level (C–C = 1.460 Å and C–O = 1.252 Å) agree reasonably well with the experimental measurements (C–C = 1.451-1.465 Å and C–O = 1.241-1.254 Å).[18,24] Our "best" computed C–C bond length is 1.458 Å, obtained at the CASSCF(10,8)/3-21G(d) level, which takes into consideration 10 electrons and 8 orbitals in the active space. But the C–O bond length optimized at this level is 1.261 Å, which is a bit longer than the experimental range. The active space in this case consists of the five highest occupied orbitals and the three lowest virtual orbitals.

However, for $C_6O_6^{2-}$ tautomer, it is seen that most of the computed C–C bond lengths are about 1.480 to 1.500 Å, while experimentally they are in the range of 1.440-1.442 Å. Our calculated results are in general agreement with those reported by Schleyer et al.,[16] but they are not in good agreement with the experimental data.[17] Our "best" computed C–C bond length is 1.459 Å, obtained at the CASSCF(14,8)/3-21G(d) level. This method takes into consideration 14 electrons and 8 orbitals in the active space and the active space consists of the seven highest occupied orbitals and the one lowest virtual orbital.

For both of the D_{nh} tautomers of $C_5O_5^{2-}$ and $C_6O_6^{2-}$, the NBO results obtained at the aforementioned "best" level reveal that there is little or no π electron delocalization between the carbon atoms and the π electrons are mainly localized at the C=O bonds for both dianions. We have not been able to find a theoretical level that would have π electron clouds covering the whole ring, as expected from chemical intuition.

Finally, it is mentioned that we also studied the $C_6O_6^{2-}$ complexes with two Na^+ counter cations, one on top and one below the six-member ring or one Ca^{2+} on top of the ring. It was found that the C–C bonds become even longer. The addition of the counter ion(s) fails once again to delocalize the π electrons around the ring.

6.4 Conclusion

Ab initio and DFT calculations have been applied to study the geometries of croconate and rhodizonate dianions in isolated, metal complex and hydrogen-bonded

situations. Both the charged-localized (C_{2v}) and charged-delocalized (D_{nh}) forms of the dianions have been studied.

We have carried out calculations for an isolated charged-localized $C_nO_n^{2-}$ (n = 5 and 6) system with imposed C_{2v} symmetry at a variety of theoretical levels, ranging from HF/STO-3G to MP2(Full)/6-31+G(2df,p). The optimized results are not very different from those for the delocalized tautomer with D_{nh} symmetry. Thus it appears that the C_{2v} tautomer of these two dianions cannot exist as a single entity. Instead, this form of the dianions can exist only in the presence of counter cation(s) or in hydrogen-bonded networks. In such situations, the computed bond lengths of the dianions are generally in good agreement with the experimental measurements. In addition, NBO results provide further evidence for the charge-localized nature of these tautomers.

For the D_{5h} tautomer of the croconate dianion, we have found that the HF/3-21G(d) and CASSCF(n,m)/3-21G(d) levels of theory yield C–C and C–O bond lengths that are within the experimental range. However, for the charge-delocalized form of the rhodizonate dianion, all the theoretical methods we have tried failed to yield C–C bond lengths of equal quality. In any event, our optimized D_{nh} structures for the $C_5O_5^{2-}$ and $C_6O_6^{2-}$ dianions are in agreement with the suggestion that aromaticity decreases with increasing ring size.[16] Finally, it is noted that, we have not been able to find a theoretical level that would have π electron clouds covering the whole ring. All our calculations have the π electrons mainly localized at the C=O bonds of the dianions. As a result, the optimized C–C bonds of the dianions are too long.

6.5 Publication Note

Two articles based on the results reported in this Chapter as well as those of the experimental work from Professor T.C.W. Mak's research group have been written up and will be submitted for publication: (1) Lam, C.-K.; Cheng, M.-F.; Li, C.-L.; Li, W.-K.; Mak, T.C.W., Stabilization of D_{5h} and C_{2v} valence tautomeric forms of the croconate dianion (to be submitted); (2) Cheng, M.-F.; Li, C.-L.; Li, W.-K., A computational study of the charge-delocalized and charge-localized forms of the croconate and rhodizonate dianions, *Chem. Phys. Lett.* (to be submitted).

6.6 References

(1) West, R.; Niu, H.-Y.; Powell, D. L.; Evans, M. V. *J. Am. Chem. Soc.* **1960**, *82*, 6204.

(2) West, R.; Niu, J. *Nonbenzenoid Aromatics*; Snyder, J. P., Ed.; Academic Press: New York: 1969; Vol. I.

(3) West, R., Ed. *Oxocarbons*; Academic Press: New York, 1980.

(4) Ito, M.; West, R. *J. Am. Chem. Soc.* **1963**, *85*, 2580.

(5) Baenziger, N. C.; Hegenbarth, J. J. *J. Am. Chem. Soc.* **1964**, *86*, 3250.

(6) McIntyre, W. M.; Werkema, M. S. *J. Chem. Phys.* **1964**, *42*, 3563.

(7) West, R.; Eggerding, D.; Perkins, J.; Handy, D.; Tuazon, E. C. *J. Am. Chem. Soc.* **1979**, *101*, 1710.

(8) West, R.; Powell, D. L. *J. Am. Chem. Soc.* **1963**, *85*, 2577.

(9) Dewar, M. J. S.; Gleicher, G. J. *J. Am. Chem. Soc.* **1965**, *87*, 685, 692.

(10) Dewar, M. J. S.; de Llano, C. *J. Am. Chem. Soc.* **1969**, *91*, 789.

(11) Hess, B. A., Jr.; Schaad, L. J. *J. Am. Chem. Soc.* **1971**, *93*, 305 and 2431.

(12) Schaad, L. J.; Hess, B. A., Jr. *J. Am. Chem. Soc.* **1972**, *94*, 3068.

(13) Aihara, J. *J. Am. Chem. Soc.* **1981**, *103*, 1633.

(14) Puebla, C.; Ha, T. K. *J. Mol. Struct. (Theochem)* **1986**, *137*, 171.

(15) Jug, K. *J. Org. Chem.* **1983**, *48*, 1344.

(16) Schleyer, P. v. R.; Najafian, K.; Kiran, B.; Jiao, H. *J. Org. Chem.* **2000**, *65*, 426.

(17) Lam, C.-K.; Mak, T. C. W. *Angew. Chem.* **2001**, *40*, 3453.

(18) Lam, C.-K.; Cheng, M.-F.; Li, C.-L.; Li, W.-K.; Mak, T.C.W. (to be submitted for publication).

(19) Frisch, M. J.; Trucks, G. W.; Schlegel, H. B.; Scuseria, G. E.; Robb, M. A.; Cheeseman, J. R.; Zakrzewski, V. G.; Montgogery, J. A.; Jr.; Stratmann, R.E.; Burant, J. C.; Dapprich, S.; Millam, J. M.; Daniels, A. D.; Kudin, K. N.; Strain, M. C.; Farkas, O.; Tomasi, J.; Barone, V.; Cossi, M.; Cammi, R.; Mennucci, B.; Pomelli, C.; Adamo, C.; Clifford, S.; Ochterski, J.; Petersson, G. A.; Ayala, P. Y.; Cui, Q.; Morokuma, K.; Malick, D. K.; Rabuck, A. D.; Raghavachari, K.; Foresman, J. B.; Cioslowski, J.; Ortiz, J. V.; Baboul, A. G.; Stefanov, B. B.; Liu, G.; Liashenko, A.; Piskorz, P.; Komaromi, I.; Gomperts, R.; Martin, R. L.; Fox, D. J.; Keith, T.; Al-Laham, M. A.; Peng, C. Y.; Nanayakkara, A.; Gonzalez, C.; Challacombe, M.; Gill, P. M. W.; Johnson, B.; Chen, W.; Wong, M. W.;

Andres, J. L.; Gonzalez, C.; Head-Gordon, M.; Replogle, E. S.; Pople, J. A. *GAUSSIAN 98*, Revision A.11; Gaussian, Inc., Pittsburgh, PA, 1998.

(20) Reed, A. E.; Curtiss, L. A.; Weinhold, F. *Chem. Rev.* **1988**, *88*, 899.

(21) Castro, I.; Sletten, J.; Faus, J.; Julve, M. *J. Chem. Soc., Dalton Trans.* **1992**, 2271.

(22) Sletten, J.; Daraghmeh, H.; Lloret, F.; Julve M. *Inorg. Chim. Acta* **1998**, *279*, 127

(23) Deguenon, D.; Bernardinelli, G.; Tuchagues, J.-P.; Castan P. *Inorg. Chem.* **1990**, *29*, 3031

(24) Lam C. K.; Mak, T. C. W. *Chem. Commun.* **2001**, 1568.
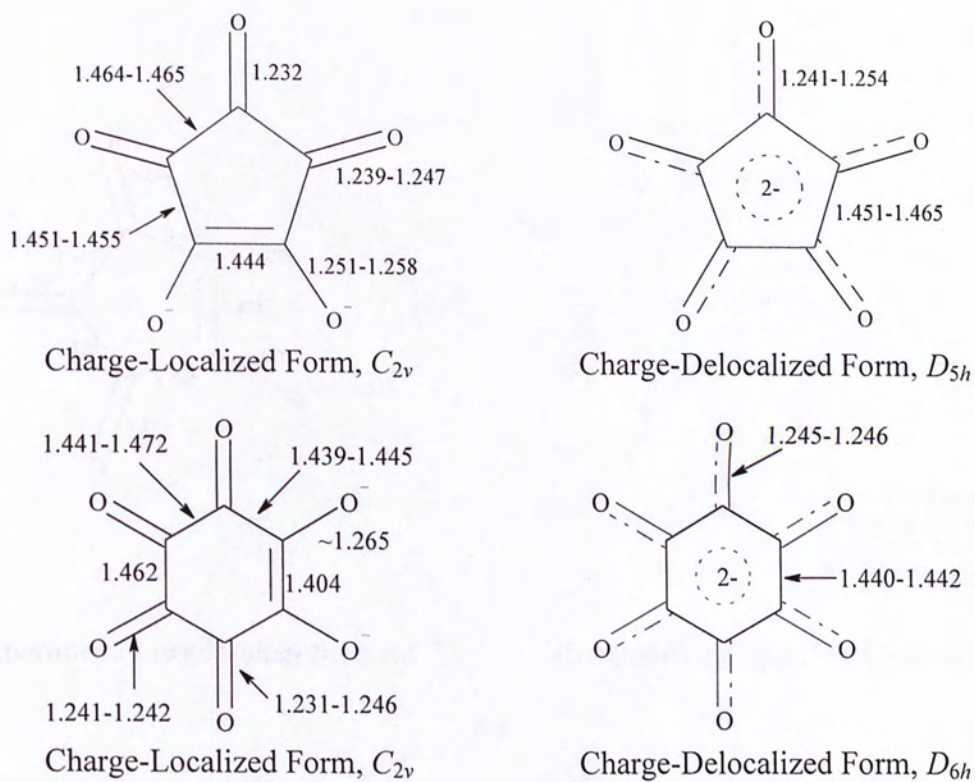
Figure 1. The experimental bond lengths of the charge-localized and charge-delocalized forms of $C_5O_5^{2-}$ and $C_6O_6^{2-}$.
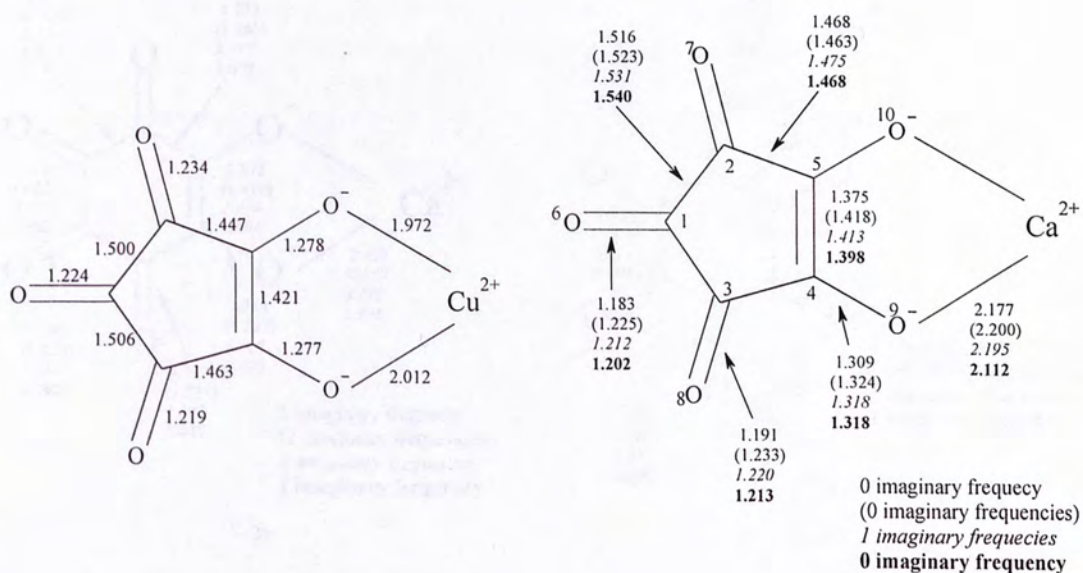
Experimental result taken from ref. 21

Computational result of CaC_5O_5, C_{2v}

0 imaginary frequecy
(0 imaginary frequencies)
1 imaginary frequecies
0 imaginary frequency

0 imaginary frequecy
(0 imaginary frequencies)
0 imaginary frequecies
0 imaginary frequency
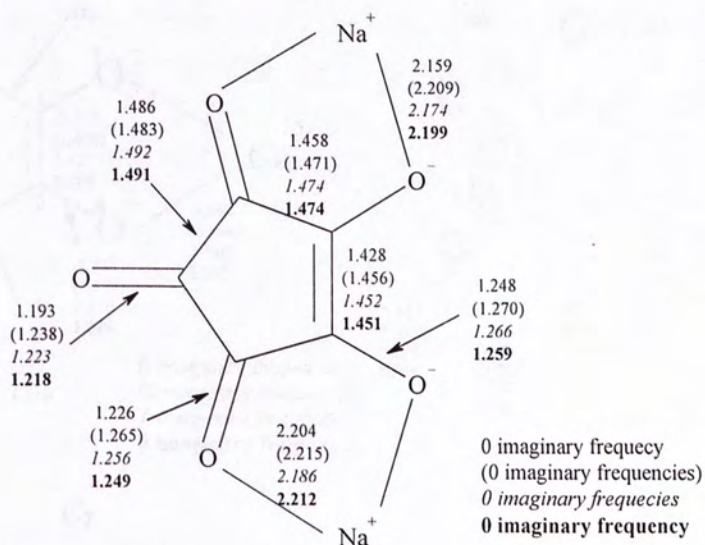
Computational result of $Na_2C_5O_5$, C_{2v}

Figure 2. The computed results of the charge-localized form of $C_5O_5^{2-}$ with C_{2v} symmetry at the levels of HF/6-31G(d) (normal font), MP2(Full)/6-31G(d) (bracketed), B3LYP/6-31G(d) (italic font) and B3LYP/6-311+G(d) (bold font).

77

Figure 3. The computed results of the charge-localized form of $C_6O_6^{2-}$ with C_{2v} and C_2 symmetry at the levels of HF/6-31G(d) (normal font), MP2(Full)/6-31G(d) (bracketed), B3LYP/6-31G(d) (italic font) and B3LYP/6-311+G(d) (bold font).

Table 1: Optimized C–C and C–O Bond Lengths of the Charge-Delocalized Forms of $C_5O_5^{2-}$ (D_{5h}) and $C_6O_6^{2-}$ (D_{6h})

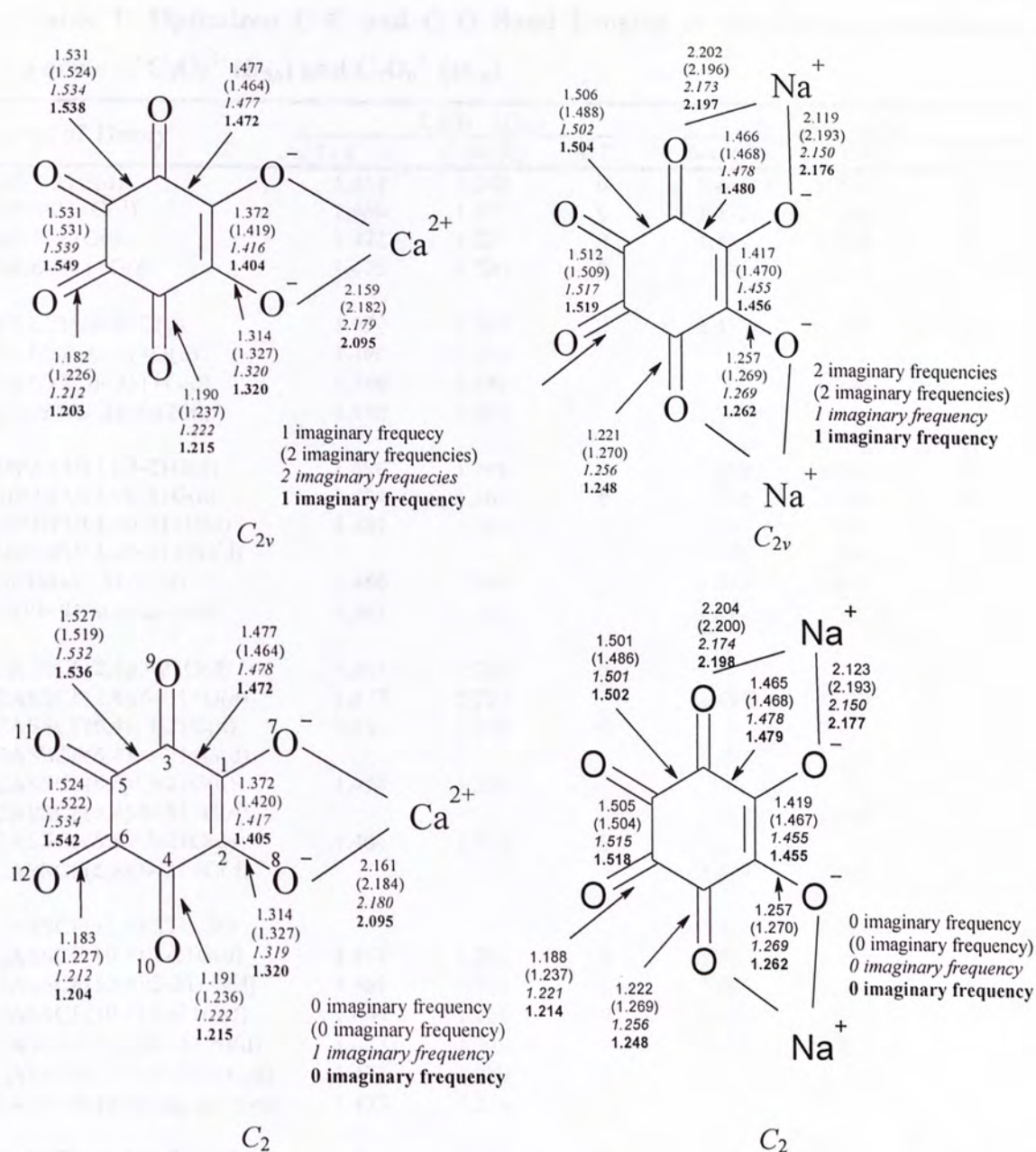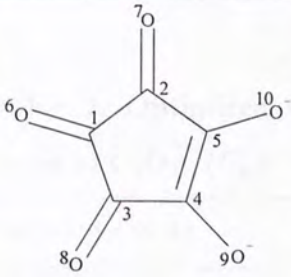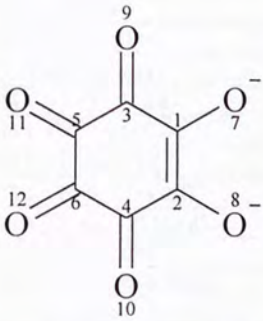| Level of Theory	$C_5O_5^{2-}$ (D_{5h})			$C_6O_6^{2-}$ (D_{6h})		
	C–C (Å)	C–O (Å)	I. F.[a]	C–C (Å)	C–O (Å)	I. F.[a]
HF/3-21G(d)	1.462	1.248	0	1.463	1.243	2
HF/3-21+G(d)	1.466	1.252	0	1.472	1.245	1
HF/6–31G(d)	1.472	1.227	0	1.483	1.218	3
HF/6–311+G(d)	1.475	1.220	0	1.491	1.210	3
B3 LYP /6–31G(d)	1.490	1.253	0	1.498	1.247	
B3 LYP /6–31+G(d)	1.490	1.253				
B3 LYP /6–311+G(d)	1.488	1.246		1.501	1.239	
B3LYP/6–31+G(2df,p)	1.488	1.247		1.500	1.240	
MP2(FULL)/3-21G(d)	1.496	1.291	0	1.489	1.294	0
MP2(FULL)/6-31G(d)	1.484	1.261	0	1.490	1.258	3
MP2(FULL)/6-31+G(d)	1.485	1.263	2	1.493	1.259	
MP2(FULL)/6-311+G(d)				1.496	1.249	
QCISD/6-31+G(d)	1.486	1.257		1.499	1.250	
B3PW91/aug–cc–pvtz	1.482	1.243		1.493	1.235	
CASSCF(2,4)/3-21G(d)	1.464	1.250	0			
CASSCF(2,4)/6–31+G(d)	1.477	1.227		1.491	1.218	
CASSCF(6,4)/ 3-21G(d)	1.460	1.252	0			
CASSCF(6,4)/6–31+G(d)				1.492	1.216	
CASSCF(6,6)/ 3-21G(d)	1.458	1.260	1			
CASSCF(6,6)/6–31+G(d)				1.488	1.220	
CASSCF(6,8)/ 3-21G(d)	1.464	1.250	0			
CASSCF(6,8)/6–31+G(d)				1.489	1.224	
CASSCF(10,8)/STO-3G				1.502	1.261	
CASSCF(10,8)/3-21G(d)	1.458	1.261	0	1.460	1.253	
CASSCF(10,8)/3-21+G(d)	1.461	1.263	0	1.463	1.260	
CASSCF(10,8)/6–31G(d)	1.469	1.235	0	1.483	1.221	
CASSCF(10,8)/6–31+G(d)	1.473	1.233		1.486	1.226	
CASSCF(10,8)/6–311+G(d)	1.471	1.229		1.491	1.210	
CASSCF(10,8)/aug–cc–pvtz	1.473	1.220				
CASSCF(12,8)/3-21G(d)	1.456	1.257	0	1.462	1.246	1
CASSCF(12,8)/3-21+G(d)	1.459	1.259	0	1.469	1.252	
CASSCF(12,8)/6–31G(d)	1.469	1.232	0	1.484	1.220	
CASSCF(12,8)/6–31+G(d)	1.471	1.231		1.489	1.218	
CASSCF(12,8)/6–311+G(d)	1.474	1.224		1.491	1.210	
CASSCF(14,8)/ STO-3G				1.499	1.265	
CASSCF(14,8)/3-21G(d)				1.459	1.251	0
CASSCF(14,8)/3-21+G(d)				1.468	1.251	
CASSCF(14,8)/6–31G(d)				1.484	1.220	
CASSCF(14,8)/6–31+G(d)				1.489	1.219	
CASSCF(14,8)/6–311+G(d)				1.489	1.213	
Experiment	1.451-1.465[b]	1.241-1.254[b]		1.440-1.442[c]	1.245-1.246[c]	

[a] Number of imaginary frequency calculated at selected levels.

[b] Values from ref. 18.

[c] Values from ref. 17.

Table 2: Results of the Second-Order Perturbation Theory Analysis of the Fock Matrix in the NBO Analysis at the MP2(Full)/6-31G(d) Level of the Enol Tautomers $C_5O_5^{2-}$ (C_{2v}) in $Ca^{2+}[C_5O_5^{2-}]$ and $C_6O_6^{2-}$ (C_2) in $Ca^{2+}[C_6O_6^{2-}]$

	Donor NBO	Acceptor NBO	ΔE^a (kcal mol^{-1})
	$BD\pi\,C^4C^5$	$BD\pi*\,C^2O^7 / C^3O^8$	40.0
	$LP\pi\,O^6$	$BD\sigma*\,C^1C^2 / C^1C^3$	26.8
	$LP\pi\,O^7/ O^8$	$BD\sigma*\,C^1C^2/ C^1C^3$	28.6
	$LP\pi\,O^7/ O^8$	$BD\sigma*\,C^2C^5/ C^3C^4$	24.7
	$LP\pi\,O^9/ O^{10}$	$BD\sigma*\,C^3C^4/ C^2C^5$	19.5
	$LP\pi\,O^9/ O^{10}$	$BD\pi*\,C^4C^5/ C^4C^5$	57.7
	$BD\pi*\,C^2O^7/ C^3O^8$	$BD\pi*\,C^1O^6$	204.0
	$BD\pi*\,C^4C^5$	$BD\pi*\,C^2O^7 / C^3O^8$	135.6
	$BD\pi\,C^1C^2$	$BD\pi*\,C^3O^9 / C^4O^{10}$	34.8
	$LP\pi\,O^7/O^8$	$BD\pi*\,C^1C^2$	56.0
	$LP\pi\,O^7/O^8$	$BD\sigma*\,C^1C^3 / C^2C^4$	17.2
	$LP\pi\,O^9/O^{10}$	$BD\sigma*\,C^1C^3 / C^2C^4$	22.5
	$LP\pi\,O^9/O^{10}$	$BD\sigma*\,C^3C^5 / C^4C^6$	26.7
	$LP\pi\,O^{11}/O^{12}$	$BD\sigma*\,C^3C^5 / C^4C^6$	24.5
	$LP\pi\,O^{11}/O^{12}$	$BD\sigma*\,C^5C^6$	25.7
	$BD\pi*\,C^1C^2$	$BD\pi*\,C^3O^9 / C^4O^{10}$	180.0
	$BD\pi*\,C^3O^9 / C^4O^{10}$	$BD\pi*\,C^5O^{11} / C^6O^{12}$	149.0

^{a} The second–order perturbation stabilization energies.

Table 3: Optimized C–C and C–O Bond Lengths* of the Charge-Localized Form of $C_5O_5^{2-}$ (C_{2v})

Level of Theory	C^2C^3 (Å)	C^3C^5 (Å)	C^5C^6 (Å)	C^1O^2 (Å)	C^3O^7 (Å)	C^5O^9 (Å)	I. F.
HF/STO-3G	1.494826	1.494909	1.494800	1.264735	1.264750	1.264682	0
HF/3-21G(d)	1.462797	1.462855	1.462812	1.248500	1.248456	1.248426	0
HF/3-21+G(d)	1.466508	1.466570	1.466516	1.252758	1.252743	1.252684	0
HF/6–31G(d)	1.472719	1.472713	1.472723	1.227288	1.227294	1.227292	0
HF/6–31+G(d)	1.476345	1.476340	1.476362	1.225849	1.225848	1.225848	2
HF/6–311+G(d)	1.475215	1.475212	1.475225	1.220894	1.220894	1.220894	0
B3 LYP /3-21G(d)	1.484892	1.484843	1.484845	1.273472	1.273252	1.273390	0
B3 LYP /3-21+G(d)	1.483551	1.483441	1.483486	1.278979	1.279090	1.279084	0
B3 LYP /6–31G(d)	1.490359	1.490331	1.490227	1.253708	1.253613	1.253712	0
B3 LYP /6–31+G(d)	1.490305	1.490215	1.490157	1.253115	1.253111	1.253178	0
B3 LYP /6–311+G(d)	1.488465	1.488487	1.488403	1.246756	1.246746	1.246744	0
MP2/6-31+G(d)	1.487339	1.487238	1.487244	1.264625	1.264550	1.264653	2
MP2(FULL)/6-31G(d)	1.484741	1.484767	1.484756	1.261331	1.261287	1.261307	0
MP2(FULL)/6-311+G(d)	1.487149	1.487072	1.487055	1.253567	1.253512	1.253602	
MP2(FULL)/ 6-31+G(2df,p)	1.478737	1.478693	1.478643	1.249415	1.249310	1.249415	
B3PW91/6-31+G(2df,p)	1.485612	1.485565	1.485360	1.244547	1.244520	1.244606	0

* The calculated bond lengths (in Å) shown here have six significant figures, instead of the usual three, after the decimal point. This is because, if we only report three significant figures after the decimal points, the optimized C_{2v} geometry cannot be distinguished from the D_{5h} geometry.
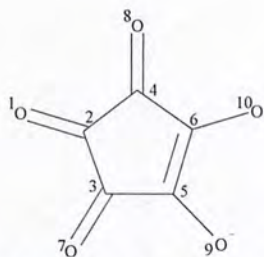
Table 4: Optimized C–C and C–O Bond Lengths* of the Charge-Localized Form of $C_6O_6^{2-}$ (C_{2v})

Level of Theory	C^1C^2 (Å)	C^1C^3 (Å)	C^3C^5 (Å)	C^5C^6 (Å)	C^1O^7 (Å)	C^3O^9 (Å)	C^5O^{11} (Å)	I. F.
HF/STO-3G	1.502643	1.502596	1.502635	1.502651	1.261288	1.261301	1.261252	0
HF/3-21G(d)	1.463138	1.463082	1.463120	1.463156	1.243254	1.243267	1.243221	2
HF/3-21+G(d)	1.473017	1.472955	1.472992	1.473026	1.245254	1.245253	1.245205	1
HF/6–31G(d)	1.483744	1.483726	1.483736	1.483748	1.218573	1.218574	1.218557	3
HF/6–31+G(d)	1.491508	1.491492	1.491502	1.491512	1.215897	1.215894	1.215880	3
HF/6–311+G(d)	1.491305	1.491291	1.491302	1.491314	1.210700	1.210696	1.210679	3
B3 LYP /3-21G(d)	1.482658	1.482614	1.482578	1.482448	1.270819	1.270887	1.270884	0
B3 LYP /3-21+G(d)	1.487283	1.487076	1.487129	1.486950	1.274976	1.275007	1.275045	0
B3 LYP /6–31G(d)	1.498288	1.498172	1.498181	1.498104	1.247298	1.247316	1.247315	3
B3 LYP /6–31+G(d)	1.501685	1.501662	1.501686	1.501494	1.246078	1.246044	1.246089	3
B3 LYP /6–311+G(d)	1.500704	1.500766	1.500767	1.500701	1.239402	1.239371	1.239402	3
MP2/6-31+G(d)	1.496055	1.496027	1.496067	1.496029	1.261030	1.261018	1.261000	
MP2(FULL)/6-31G(d)	1.490905	1.490914	1.490915	1.490925	1.258534	1.258533	1.258531	3
MP2(FULL)/6-311+G(d)	1.496672	1.496680	1.496661	1.496679	1.249759	1.249764	1.249760	
MP2(FULL)/ 6-31+G(2df,p)	1.487596	1.487758	1.487539	1.487533	1.245375	1.245365	1.245411	
B3PW91/6-31+G(2df,p)	1.496443	1.496326	1.496345	1.496251	1.237395	1.237350	1.237409	3

* The calculated bond lengths (in Å) shown here have six significant figures, instead of the usual three, after the decimal point. This is because, if we only report three significant figures after the decimal points, the optimized C_{2v} geometry cannot be distinguished from the D_{6h} geometry.
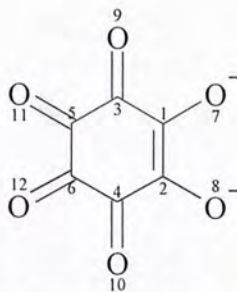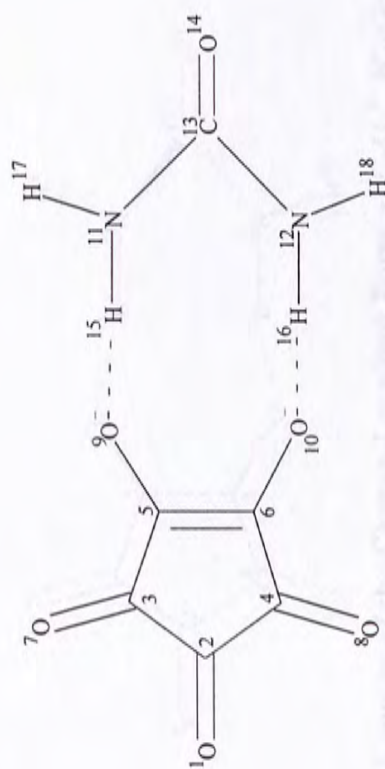
Table 5: Optimized C–C and C–O Bond Lengths of the Charge-Localized Form of $C_5O_5^{2-}$ (C_{2v}) in a 1:1 Adduct with Urea

Level of Theory	C^2C^3 (Å)	C^3C^5 (Å)	C^5C^6 (Å)	O^1C^2 (Å)	C^3O^7 (Å)	C^5O^9 (Å)	O^9H^{15} (Å)	$N^{11}H^{15}$ (Å)	$N^{11}H^{17}$ (Å)	$N^{11}C^{13}$ (Å)	$C^{13}O^{14}$ (Å)	I. F.
HF/STO-3G	1.530	1.530	1.417	1.233	1.240	1.316	1.287	1.141	1.022	1.394	1.254	4
HF/3-21G(d)	1.477	1.457	1.433	1.232	1.238	1.267	1.721	1.026	0.994	1.351	1.246	0
HF/3-21+G(d)	1.482	1.458	1.440	1.237	1.244	1.268	1.767	1.021	0.995	1.350	1.269	0
HF/6-31G(d)	1.484	1.466	1.451	1.215	1.219	1.241	1.853	1.013	0.991	1.348	1.226	2
HF/6-31+G(d)	1.487	1.469	1.454	1.214	1.219	1.239	1.877	1.012	0.992	1.347	1.230	4
HF/6-311+G(d)	1.486	1.468	1.454	1.209	1.214	1.234	1.888	1.007	0.989	1.347	1.224	3
B3 LYP /3-21G(d)	1.492	1.478	1.459	1.262	1.264	1.286	1.671	1.053	1.012	1.372	1.265	0
B3 LYP /3-21+G(d)	1.493	1.475	1.463	1.268	1.271	1.289	1.705	1.047	1.012	1.369	1.290	0
B3 LYP /6-31G(d)	1.496	1.484	1.470	1.244	1.246	1.264	1.768	1.039	1.006	1.366	1.248	2
B3 LYP /6-31+G(d)	1.498	1.483	1.471	1.244	1.247	1.262	1.788	1.037	1.007	1.363	1.255	2
B3 LYP /6-311+G(d)	1.496	1.481	1.469	1.238	1.240	1.256	1.797	1.032	1.004	1.362	1.248	2
MP2(FULL)/3-21G(d)	1.496	1.490	1.482	1.287	1.285	1.296	1.723	1.042	1.010	1.379	1.272	1
MP2(FULL)/6-31G(d)	1.487	1.479	1.472	1.256	1.256	1.268	1.790	1.035	1.006	1.362	1.251	2
MP2(FULL)/6-311+G(d)	1.492	1.481	1.474	1.247	1.249	1.260	1.811	1.027	1.003	1.361	1.248	

Table 6: Optimized C–C and C–O Bond Lengths of the Charge-Localized Form of $C_5O_5^{2-}$ (C_2) in a 1:1 Adduct with Urea

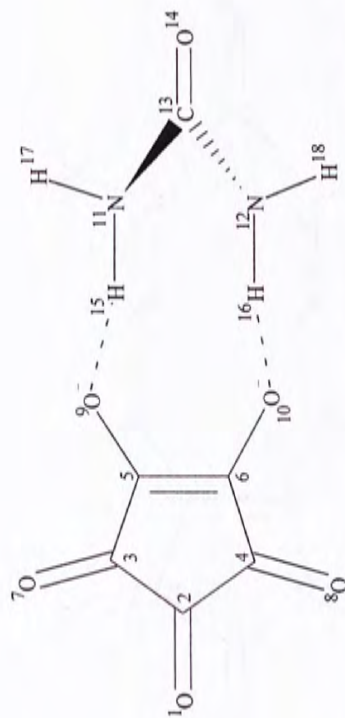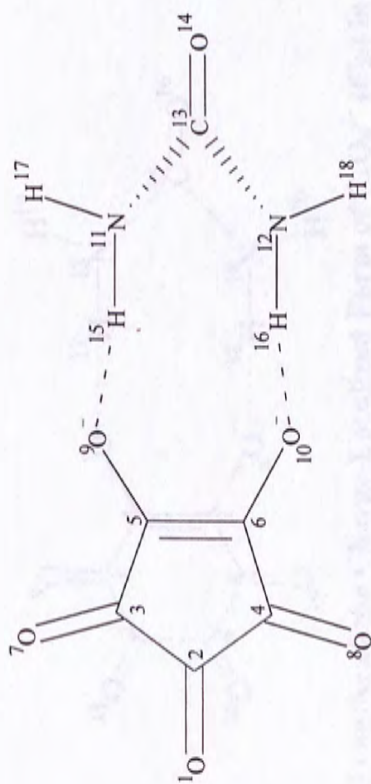| Level of Theory	C^2C^3 (Å)	C^3C^5 (Å)	C^5C^6 (Å)	O^1C^2 (Å)	C^3O^7 (Å)	C^5O^9 (Å)	O^9H^{15} (Å)	$N^{11}H^{15}$ (Å)	$N^{11}H^{17}$ (Å)	$N^{11}C^{13}$ (Å)	$C^{13}O^{14}$ (Å)	I. F.
HF/STO-3G	1.532	1.495	1.417	1.233	1.241	1.317	1.293	1.149	1.031	1.418	1.246	1
HF/3-21G(d)	1.477	1.457	1.433	1.232	1.238	1.267	1.720	1.026	0.994	1.351	1.246	0
HF/6-31G(d)	1.484	1.466	1.450	1.215	1.219	1.241	1.859	1.014	0.993	1.353	1.223	0
B3 LYP /3-21G(d)	1.492	1.478	1.459	1.262	1.264	1.286	1.670	1.053	1.012	1.372	1.265	0
B3 LYP /6-31G(d)	1.497	1.484	1.470	1.244	1.246	1.264	1.774	1.041	1.010	1.373	1.245	0
B3 LYP /6-311+G(d)	1.496	1.481	1.469	1.238	1.240	1.257	1.800	1.033	1.005	1.365	1.247	0
MP2(FULL)/3-21G(d)	1.496	1.490	1.482	1.287	1.286	1.295	1.722	1.042	1.010	1.379	1.272	0
MP2(FULL)/6-311+G(d)	1.492	1.480	1.473	1.247	1.249	1.260	1.811	1.030	1.006	1.368	1.245	

Table 7: Optimized C–C and C–O Bond Lengths of the Charge-Localized form of $C_5O_5^{2-}$ (C_s) in a 1:1 Adduct with Urea

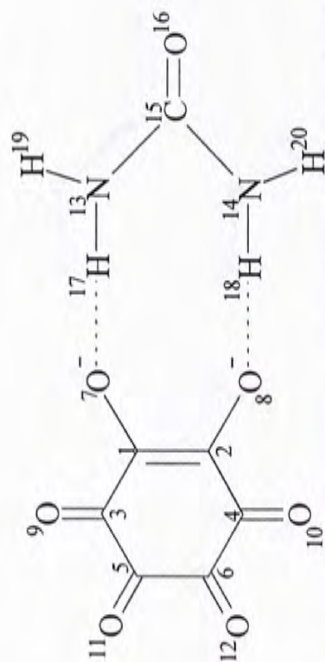| Level of Theory	C^2C^3 (Å)	C^3C^5 (Å)	C^5C^6 (Å)	O^1C^2 (Å)	C^3O^7 (Å)	C^5O^9 (Å)	O^9H^{15} (Å)	$N^{11}H^{15}$ (Å)	$N^{11}H^{17}$ (Å)	$N^{11}C^{13}$ (Å)	$C^{13}O^{14}$ (Å)	I.F.
HF/STO-3G	1.535	1.496	1.412	1.232	1.240	1.320	1.297	1.152	1.034	1.424	1.246	1
HF/3-21G(d)	1.477	1.457	1.433	1.232	1.238	1.267	1.720	1.026	0.994	1.351	1.246	0
HF/6-31G(d)	1.484	1.466	1.450	1.215	1.219	1.241	1.862	1.014	0.994	1.356	1.222	0
B3 LYP /3-21G(d)	1.492	1.478	1.459	1.262	1.264	1.286	1.669	1.053	1.011	1.372	1.265	0
B3 LYP /6–31G(d)	1.497	1.484	1.470	1.244	1.246	1.264	1.776	1.042	1.011	1.376	1.245	0
B3 LYP /6–311+G(d)	1.496	1.481	1.469	1.237	1.240	1.257	1.803	1.033	1.007	1.369	1.245	0
MP2(FULL)/3-21G(d)	1.496	1.490	1.482	1.287	1.286	1.295	1.722	1.042	1.010	1.379	1.272	1
MP2(FULL)/6-311+G(d)	1.492	1.480	1.473	1.247	1.248	1.260	1.815	1.030	1.007	1.371	1.244	

Table 8: Optimized C–C and C–O Bond Lengths of the Charge-Localized Form of $C_6O_6^{2-}$ (C_{2v}) in a 1:1 Adduct with Urea

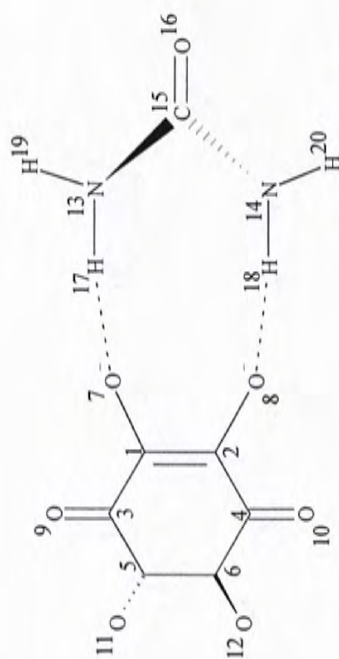| Level of Theory	C^1C^2 (Å)	C^1C^3 (Å)	C^3C^5 (Å)	C^5C^6 (Å)	C^1O^7 (Å)	C^3O^9 (Å)	C^5O^{11} (Å)	O^7H^{17} (Å)	$N^{13}H^{17}$ (Å)	$N^{13}H^{19}$ (Å)	$N^{13}C^{15}$ (Å)	$C^{15}O^{16}$ (Å)	I. F.
HF/STO-3G	1.407	1.507	1.542	1.535	1.326	1.241	1.231	1.287	1.140	1.021	1.393	1.254	6
HF/3-21G(d)	1.431	1.455	1.475	1.478	1.266	1.236	1.228	1.722	1.023	0.994	1.351	1.245	0
HF/3-21+G(d)	1.446	1.461	1.484	1.490	1.265	1.239	1.231	1.767	1.018	0.995	1.350	1.267	0
HF/6-31G(d)	1.459	1.475	1.493	1.498	1.235	1.214	1.207	1.866	1.010	0.991	1.348	1.224	5
HF/6-31+G(d)	1.468	1.482	1.499	1.504	1.231	1.212	1.206	1.892	1.009	0.992	1.347	1.228	5
HF/6-311+G(d)	1.468	1.481	1.499	1.504	1.226	1.207	1.200	1.898	1.004	0.988	1.348	1.222	5
B3 LYP /3-21G(d)	1.460	1.477	1.486	1.487	1.283	1.264	1.263	1.688	1.045	1.011	1.372	1.262	0
B3 LYP /3-21+G(d)	1.470	1.477	1.492	1.496	1.285	1.270	1.267	1.724	1.040	1.012	1.370	1.287	0
B3 LYP /6-31G(d)	1.480	1.492	1.502	1.504	1.258	1.242	1.240	1.795	1.032	1.006	1.366	1.246	5
B3 LYP /6-31+G(d)	1.484	1.494	1.506	1.508	1.256	1.242	1.239	1.812	1.031	1.007	1.364	1.253	5
B3 LYP /6-311+G(d)	1.483	1.492	1.505	1.508	1.250	1.235	1.232	1.820	1.027	1.004	1.363	1.245	5
MP2(FULL)/3-21G(d)	1.485	1.488	1.485	1.484	1.292	1.290	1.297	1.749	1.034	1.009	1.380	1.268	1
MP2(FULL)/6-31G(d)	1.483	1.488	1.490	1.489	1.261	1.255	1.257	1.819	1.029	1.006	1.363	1.248	

Table 9: Optimized C–C and C–O Bond Lengths of the Charge-Localized Form of $C_6O_6^{2-}$ (C_2) in a 1:1 Adduct with Urea

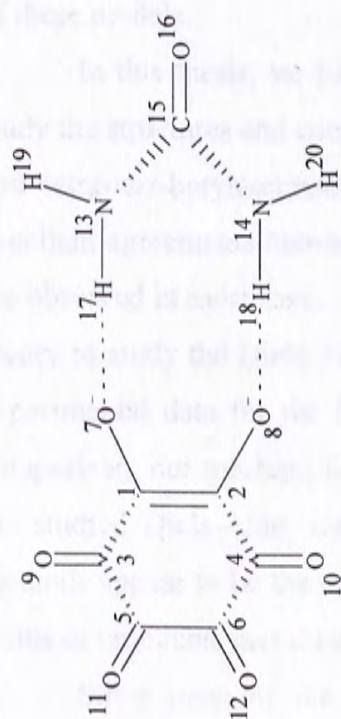| Level of Theory	C^1C^2 (Å)	C^1C^3 (Å)	C^3C^5 (Å)	C^5C^6 (Å)	C^1O^7 (Å)	C^3O^9 (Å)	C^5O^{11} (Å)	O^7H^{17} (Å)	$N^{13}H^{17}$ (Å)	$N^{13}H^{19}$ (Å)	$N^{13}C^{15}$ (Å)	$C^{15}O^{16}$ (Å)	I. F.
HF/STO-3G	1.407	1.503	1.545	1.538	1.328	1.241	1.231	1.286	1.153	1.032	1.419	1.246	1
HF/3-21G(d)	1.431	1.455	1.475	1.478	1.266	1.236	1.228	1.722	1.023	0.994	1.351	1.245	0
HF/6-31G(d)	1.457	1.473	1.488	1.491	1.236	1.214	1.208	1.879	1.011	0.993	1.354	1.222	0
B3 LYP /3-21G(d)	1.459	1.477	1.486	1.487	1.283	1.264	1.263	1.688	1.045	1.011	1.372	1.262	0
B3 LYP /6-31G(d)	1.480	1.491	1.500	1.502	1.258	1.242	1.240	1.803	1.035	1.009	1.374	1.243	0
MP2(FULL)/3-21G(d)	1.485	1.488	1.485	1.484	1.292	1.290	1.297	1.750	1.034	1.009	1.380	1.268	1
MP2(FULL)/6-31G(d)	1.480	1.485	1.488	1.488	1.263	1.255	1.256	1.827	1.032	1.010	1.372	1.245	1

Table 10: Optimized C–C and C–O Bond Lengths of the Charge-Localized Form of $C_6O_6^{2-}$ (C_s) in a 1:1 Adduct with Urea

Level of Theory	C^1C^2 (Å)	C^1C^3 (Å)	C^3C^5 (Å)	C^5C^6 (Å)	C^1O^7 (Å)	C^3O^9 (Å)	C^5O^{11} (Å)	O^7H^{17} (Å)	$N^{13}H^{17}$ (Å)	$N^{13}H^{19}$ (Å)	$N^{13}C^{15}$ (Å)	$C^{15}O^{16}$ (Å)	I. F.
HF/STO-3G	1.398	1.503	1.549	1.542	1.335	1.239	1.230	1.279	1.165	1.035	1.424	1.247	1
HF/3-21G(d)	1.431	1.455	1.475	1.479	1.266	1.236	1.228	1.721	1.022	0.994	1.351	1.245	0
HF/6-31G(d)	1.459	1.476	1.491	1.494	1.235	1.213	1.208	1.881	1.011	0.994	1.357	1.220	1
B3 LYP /3-21G(d)	1.459	1.477	1.486	1.487	1.283	1.264	1.263	1.687	1.045	1.011	1.372	1.262	0
B3 LYP /6-31G(d)	1.478	1.492	1.502	1.503	1.258	1.242	1.240	1.803	1.035	1.010	1.377	1.242	1
MP2(FULL)/3-21G(d)	1.485	1.488	1.485	1.484	1.292	1.290	1.297	1.750	1.034	1.009	1.380	1.268	1
MP2(FULL)/6-31G(d)	1.480	1.487	1.490	1.489	1.262	1.253	1.256	1.827	1.032	1.011	1.375	1.244	

Chapter 7

Conclusion

Since conclusions have been made for each project in the respective chapter, we will not, in this final chapter, specifically comment on the individual chemical systems studied in this work. On the other hand, different models of theory, Gaussian-3 (G3MP2) and Gaussian-3 (G3), as well as other high-level methods including CASSCF, QCISD(T), etc., have been employed to study the structures and energetics of several interesting systems. We will now remark on the relative merits of these models.

In this thesis, we have employed the G3 and G3(MP2) models of theory to study the structures and energetics of azine series, boron hydrides and mono-, di-, tri- and tetra-*tert*-butylmethane. Combining with the experimental results, good to excellent agreements between the G3 and G3(MP2) results and experimental values are observed in most cases. In addition, we have used the B3LYP and MP2 levels of theory to study the Diels-Alder reactivity and aromaticity of acenes. Although, few experimental data for the Diels-Alder reactions involving acenes are available for comparison, our mechanistic results shed light on the reaction pathways involved in the studied Diels-Alder reactions. Finally, it is noted that the HF and CASSCF methods appear to be the best ways to identify the charge-localized and -delocalized forms of croconate and rhodizonate dianions.

Since most of the calculated results obtained in this work are in good agreements with the available experimental data, and, based on the previous successes for the methods employed, the unexpected large discrepancies between experimental and calculated results for some quantities reported in this thesis may not be due to the failure of the theoretical model. Rather, these discrepancies suggest that the experimental results may be inaccurate and deserve re-examination. The notable exception to this general comment is the charge-delocalized form of rhodizonate dianion. We have applied more than 35 methods to optimize the structure of this species, and all of them are unable to yield a description with π electron clouds covering the whole ring. As a result, the optimized C–C bonds are too long.

Appendix A

The Gaussian-3 Theoretical Model

The mathematical detail of the Gaussian-3 (G3) methodology as well as the variant of the G3 method, G3(MP2), are presented below.

A.1 The G3 Theory

The G3 energies are the approximation of the energy calculated at the ab initio QCISD(T)/G3large level. It involves geometry optimization at the MP2(Full)/6-31G(d) level. Also, vibrational frequency calculations at the MP2(Full)/6-31G(d) level for the zero-point vibrational energy (ZPVE), thermal corrections, and a semi-empirical higher-level correction (HLC) are required. Based on the optimized geometry, several single-point energy calculations are performed, and the G3 energy are given as follow.

The G3 energy:

$$E(G3) = E_{base} + \Delta E(QCI) + \Delta E(+) + \Delta E(2df) + \Delta E(G3large) + \Delta E(SO) + 0.9661 \times ZPVE_{MP2} + HLC_{G3}, \qquad (1)$$

where $E_{base} = E[MP4SDTQ/6-31G(d)]$,

$\Delta E(QCI) = E[QCISD(T)/6-31G(d) - MP4SDTQ/6-31G(d)]$,

$\Delta E(+) = E[MP4SDTQ/6-31+G(d) - MP4SDTQ/6-31G(d)]$,

$\Delta E(2df) = E[MP4SDTQ/6-31G(2df,p) - MP4SDTQ/6-31G(d)]$,

$\Delta E(G3large) = E[MP2(full)/G3large - MP2/6-31G(2df,p) -$
$\qquad\qquad\qquad MP2/6-31+G(d) + MP2/6-31G(d)]$,

$ZPVE_{MP2} = ZPVE$ at MP2(Full)/6-31G(d),

$HLC_{G3} = -6.386\times10^{-3}n_\beta - 2.977\times10^{-3}(n_\alpha - n_\beta)$ and

$\qquad\quad -6.219\times10^{-3}n_\beta - 1.185\times10^{-3}(n_\alpha - n_\beta)$

for molecular and atomic species, respectively. Here $n_\alpha \geq n_\beta$ and n_α and n_β are the numbers of α and β valence electrons, respectively.

$\Delta E(SO)$ is spin-orbit correction for atomic species, and is taken from experiment or accurate theoretical calculations in the case where no experimental data are available.

A.2 The G3(MP2) Theory

In the G3(MP2) procedure, the basis-set-extension corrections is obtained at MP2 level, instead of the MP4 level in G3, thus eliminating the MP4 calculations: The G3(MP2) energy:

$$E(G3(MP2)) = E[QCISD(T)/6\text{-}31G(d)] + \Delta E_{MP2} + \Delta E(SO) + 0.9661 \times ZPVE_{MP2}$$
$$+ HLC_{G3MP2}, \qquad (2)$$

where $\Delta E_{MP2} = E[MP2/G3MP2large - MP2/6\text{-}31G(d)]$,

$HLC_{G3MP2} = -9.729 \times 10^{-3} n_\beta - 4.471 \times 10^{-3}(n_\alpha - n_\beta)$ and

$-9.345 \times 10^{-3} n_\beta - 2.021 \times 10^{-3}(n_\alpha - n_\beta)$ for molecular and atomic

species, respectively.

Appendix B

Calculation of Enthalpy at 298 K, H_{298}

The theoretical energies obtained with the Gaussian-n methods refer to isolated molecules at 0 K with stationary nuclei, while thermochemical measurements are carried out with vibrating molecules at finite temperature, usually 298 K. Hence, comparison of theoretical results with experimental data normally requires zero-point vibrational energy and thermal corrections. From statistical mechanics, and assuming ideal gas behavior, the difference between the enthalpy at finite temperature (H_T) and the energy at 0 K (E_0) is given by

$$H_T - E_0 = E_T{}^{\text{trans}} + E_T{}^{\text{rot}} + \Delta E_T{}^{\text{vib}} + RT$$

where $E_T{}^{\text{trans}} = (3/2)RT$,

$E_T{}^{\text{rot}} = (3/2)RT$ (for a non–linear molecule)

$E_T{}^{\text{rot}} = RT$ (for a linear molecule) or 0 (for an atom)

$\Delta E_T{}^{\text{vib}} = E_T{}^{\text{vib}} - E_0{}^{\text{vib}}$

$$= \sum_i^{3n-6} \frac{h v_i}{\exp(h v_i / kT) - 1}, \text{ where } v_i\text{'s are scaled harmonic frequencies.}$$